

Journal of Print and Media Technology Research

Scientific contributions

Ink splitting in gravure printing:
localization of the transition from dots to fingers
*Pauline Brumm, Tim Eike Weber, Hans Martin Sauer
and Edgar Dörsam*

81

Image contrast enhancement
using histogram equalization:
a bacteria colony optimization approach
*Saorabh Kumar Mondal, Arpitam Chatterjee
and Bipan Tudu*

95

Examining the uncanny valley effect
in virtual character design for digital games
Ugur Bakan and Ufuk Bakan

119

ISSN 2414-6250



9 772414 625001

Editor-in-Chief

Published by **iarigai**
www.iarigai.org

Gorazd Golob (Ljubljana)

The International Association of Research
Organizations for the Information, Media
and Graphic Arts Industries

Journal of Print and Media Technology Research

A PEER-REVIEWED QUARTERLY

PUBLISHED BY

The International Association of Research Organizations
for the Information, Media and Graphic Arts Industries
Magdalenenstrasse 2, D-64288 Darmstadt, Germany
<http://www.iarigai.org>
journal@iarigai.org

EDITORIAL BOARD

EDITOR-IN-CHIEF

Gorazd Golob (Ljubljana, Slovenia)

EDITORS

Timothy C. Claypole (Swansea, UK)
Edgar Dörsam (Darmstadt, Germany)
Nils Enlund (Helsinki, Finland)
Mladen Lovreček (Zagreb, Croatia)
Renke Wilken (Munich, Germany)
Scott Williams (Rochester, USA)

ASSOCIATE EDITOR

Markéta Držková (Pardubice, Czech Republic)

SCIENTIFIC ADVISORY BOARD

Darko Agić (Zagreb, Croatia)
Anne Blayo (Grenoble, France)
Wolfgang Faigle (Stuttgart, Germany)
Elena Fedorovskaya (Rochester, USA)
Patrick Gane (Helsinki, Finland)
Diana Gregor Svetec (Ljubljana, Slovenia)
Jon Yngve Hardeberg (Gjøvik, Norway)
Ulrike Herzau Gerhardt (Leipzig, Germany)
Gunter Hübner (Stuttgart, Germany)
Marie Kaplanová (Pardubice, Czech Republic)
John Kettle (Espoo, Finland)
Helmut Kipphan (Schwetzingen, Germany)
Björn Kruse (Linköping, Sweden)
Yuri Kuznetsov (St. Petersburg, Russian Federation)
Magnus Lestelius (Karlstad, Sweden)
Patrice Mangin (Trois Rivières, Canada)
Thomas Mejtoft (Umeå, Sweden)
Erzsébet Novotny (Budapest, Hungary)
Anastasios Politis (Athens, Greece)
Anu Seisto (Espoo, Finland)
Johan Stenberg (Stockholm, Sweden)
Philipp Urban (Darmstadt, Germany)

A mission statement

To meet the need for a high quality scientific publishing platform in its field, the International Association of Research Organizations for the Information, Media and Graphic Arts Industries is publishing a quarterly peer-reviewed research journal.

The journal is fostering multidisciplinary research and scholarly discussion on scientific and technical issues in the field of graphic arts and media communication, thereby advancing scientific research, knowledge creation, and industry development. Its aim is to be the leading international scientific journal in the field, offering publishing opportunities and serving as a forum for knowledge exchange between all those interested in contributing to or learning from research in this field.

By regularly publishing peer-reviewed, high quality research articles, position papers, surveys, and case studies as well as review articles and topical communications, the journal is promoting original research, international collaboration, and the exchange of ideas and know-how. It also provides a multidisciplinary discussion on research issues within the field and on the effects of new scientific and technical developments on society, industry, and the individual. Thus, it intends to serve the entire research community as well as the global graphic arts and media industry.

The journal is covering fundamental and applied aspects of at least, but not limited to, the following topics:

Printing technology and related processes

- ⊕ Conventional and special printing
- ⊕ Packaging
- ⊕ Fuel cells and other printed functionality
- ⊕ Printing on biomaterials
- ⊕ Textile and fabric printing
- ⊕ Printed decorations
- ⊕ Materials science
- ⊕ Process control

Premedia technology and processes

- ⊕ Colour reproduction and colour management
- ⊕ Image and reproduction quality
- ⊕ Image carriers (physical and virtual)
- ⊕ Workflow and management

Emerging media and future trends

- ⊕ Media industry developments
- ⊕ Developing media communications value systems
- ⊕ Online and mobile media development
- ⊕ Cross-media publishing

Social impact

- ⊕ Media in a sustainable society
- ⊕ Environmental issues and sustainability
- ⊕ Consumer perception and media use
- ⊕ Social trends and their impact on media

Submissions to the Journal

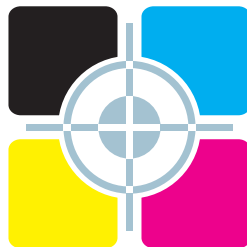
Submissions are invited at any time and, if meeting the criteria for publication, will be rapidly submitted to peer-review and carefully evaluated, selected and edited. Once accepted and edited, the papers will be published as soon as possible.

✉ Contact the Editorial office: journal@iarigai.org

Journal of Print and Media Technology Research

2-2021

June 2021



The information published in this journal is obtained from sources believed to be reliable and the sole responsibility on the contents of the published papers lies with their authors. The publishers can accept no legal liability for the contents of the papers, nor for any information contained therein, nor for conclusions drawn by any party from it.

Journal of Print and Media Technology Research is listed in:

Emerging Sources Citation Index

Scopus

Index Copernicus International

PiraBase (by Smithers Pira)

Paperbase (by Innventia and Centre Technique du Papier)

NSD – Norwegian Register for Scientific Journals, Series and Publishers

Contents

A letter from the Editor <i>Gorazd Golob</i>	79
Scientific contributions	
Ink splitting in gravure printing: localization of the transition from dots to fingers <i>Pauline Brumm, Tim Eike Weber, Hans Martin Sauer and Edgar Dörsam</i>	81
Image contrast enhancement using histogram equalization: a bacteria colony optimization approach <i>Saorabh Kumar Mondal, Arpitam Chatterjee and Bipan Tudu</i>	95
Examining the uncanny valley effect in virtual character design for digital games <i>Ugur Bakan and Ufuk Bakan</i>	119
<hr/>	
Topicalities <i>Edited by Markéta Držková</i>	
News & more	135
Bookshelf	137
Events	143



A letter from the Editor

Gorazd Golob

Editor-in-Chief

E-mail: gorazd.golob@jpmtr.org

journal@iarigai.org

The present issue is comprised of only three papers, however, all three assessed by the reviewers as original scientific papers, covering very different fields within the scope of the Journal. The first one is on the phenomena known and studied for decades, which is present in the conventional gravure printing process and recognized as dots and fingers patterns on prints. The added value is in the new classification of printed samples including the transition stage in forming fingers from dots, based on the analysis of prints retrieved with different print forms, under different conditions, and on different substrates. Added value is also a published link for download the images of all samples, available for further research.

The second paper is dealing with the methods for the improvement of digital image quality. The research was based on the comparison of well-established methods like histogram equalization and a new method based on computational intelligence algorithms mimicking the phenomena of bacteria colony optimization.

The third paper is on the study of the uncanny valley effect in virtual character design used in computer games, which may be considered as a part of a “new” digital media. The authors present a thorough overview of this psychological phenomenon and found relations between the characteristics of virtual characters in the game and the resulting effect on players – participants in the study.

The Topicalities, edited by Markéta Držková (marketa.drzkova@jpmtr.org) bring an overview of the completed projects funded under Horizon 2020, new publications available by Intergraf, and an overview of the winners of the TAGA student awards. In an interesting Bookshelf, the dominant themes are typography, design, and new materials used in functional printing, as well as two books on programming and coding in media and 3D printing.

Three theses are also presented. The first one on electromechanical modeling and control of printed electroactive polymer actuators was defended by S. Sunjai Nakshatharan at the Institute of Technology, Tartu, Estonia. Farhan Rasheed defended his thesis on modeling and physical design automation of inkjet-printed electronics at Karlsruhe Institute of Technology, Germany. The third presented successful author of the thesis is Chikwesiri Tolu Imediegwu, who was dealing with structural optimization of three-dimensional printable structures at the Imperial College London, United Kingdom. All three presented theses are from the field of functional and 3D printing, and also employ modeling to achieve the desired results, showing and confirming the trends for future research and development in printing technology.

The Events section of Topicalities is shorter again, as expected due to the adaptation of the conferences and seminars to our new reality.

The news, non-visible to the readers of the Journal, is a replacement of previously used Copyright Transfer Agreement, signed with every (corresponding) author, to a new Licencing Agreement, based on Creative Commons CC-BY-NC 4.0 copyright protection model. The main difference between the two models is in ownership of copyright, which now remains with authors and is not transferred to the publisher. With the new licensing agreement, it is also allowed to apply for indexing in the directory of open access journals (DOAJ). Papers published in the journals listed in DOAJ are in accordance with the requirements of some funding organizations and institutions, so in the future, we hope for more high-quality papers for publication in the Journal. We already applied for DOAJ, however, the procedure can last for a couple of months.

After a long-lasting pandemic and all the measures needed to bring our lives to normal condition, we are expecting the joint [iarigai](#) and IC International Research Conference in Athens, Greece. It will be a great opportunity for dissemination of knowledge and research achievements for all of us, and we also hope for a series of new papers for publication in the Journal, based on the extended and upgraded conference presentations.

Ljubljana, June 2021

JPMTR-2016
DOI 10.14622/JPMTR-2016
UDC 667.5:777-023.8

Original scientific paper | 147
Received: 2020-12-05
Accepted: 2021-04-22

Ink splitting in gravure printing: localization of the transition from dots to fingers

Pauline Brumm^{1,2}, Tim Eike Weber¹, Hans Martin Sauer^{1,2} and Edgar Dörsam^{1,2}

¹Technical University of Darmstadt, Department of Mechanical Engineering,
Institute of Printing Science and Technology,
Magdalenenstr. 2, 64289 Darmstadt, Germany

²Collaborative Research Center (CRC) 1194,
Interaction between Transport and Wetting Processes, Project C01, Germany

brumm@idd.tu-darmstadt.de
timweber@idd.tu-darmstadt.de
sauer@idd.tu-darmstadt.de
doersam@idd.tu-darmstadt.de

Abstract

For the gravure printing process, ink transfer from the printing cylinder to the substrate is studied in the parameter regime at the very border between point and lamella splitting. In this parameter regime, ink drop deposition from adjacent gravure cells is such that, by capillary and wetting forces in the nip, the drops are at the onset of mutual coalescence. This process offers the possibility to deposit an ultimately thin and closed ink film. We discuss the particular type of pattern and defect formation in the printed layer and show that these apparently stochastic patterns have reproducible features. We claim that, besides the two known regimes of point and lamella splitting, at least one additional ink transfer regime is possible, with well-controllable wetting and ink flow dynamics. A classification scheme is proposed, based on raster-scale pattern phenomenology, by which the printer can recognize and distinguish this third regime by optical inspection of the printed product. Gaining control over this regime offers novel opportunities for gravure printing in thin-film related applications such as printed electronics and package printing.

Keywords: ink transfer, viscous fingering, Saffman-Taylor instability, functional printing, print quality

1. Introduction and background

Gravure printing technique is, amongst the various printing techniques, one of the most promising technologies for future printing applications beyond graphical arts (Kumar, 2015), for example, printed electronics (Ganz, et al., 2016; Willmann, Stocker and Dörsam, 2014). Gravure is one of the backbone technologies of rapidly growing packaging markets and food technology (Siever, 2019) in numerous upcoming economies of the eastern hemisphere. In view of the present global economic and ecological challenges, recent developments in gravure technology, namely those obtained from printed electronics applications, could be useful to further reduce the quantities of printing material per area, to minimize the quantities of ecologically hazardous solvents, and to process increasingly complex functional inks. From the printer's point of view, the processing demands of extremely thin, closed layers of highly developed functional polymers or of nanoparticle colloids are not that much different from printing organic solar cells, or light emitting diodes. Both

are, admittedly, at the very high edge of present gravure technology. Nevertheless, the manufacturing of closed and smooth polymer layers of only few tens of nanometres in thickness has become a standard task in organic light emitting diode (OLED) printing (Grau, et al., 2016; Kopola, et al., 2009). Bornemann (2014) was one of the first to notice the remarkable stability of such processes. He observed that, under particular conditions, the deposition of such extreme layers was successful on elastic foils as well as on rigid and wavy glass substrates at velocities beyond 3 m/s. This was attributed to a specific dynamical and stable regime of the ink splitting or cell emptying process in the nip. The physical origin of this somewhat exceptional process and closer hydrodynamic details of ink flow remained obscure at that time. The resolution of this point was recognized much later, using high-speed video recording of the nip as done by Griesheimer (2014); Sauer, et al. (2018), and, in particular, by Schäfer, et al. (2019). Studying the hydrodynamics at a millisecond time scale on mesoscopically structured surfaces provides surprising transient cell emptying flow phenomena,

correlated on length scales of few gravure raster distances. In contrast to point and lamella splitting, there is up to now no scheme to distinguish the residuals of these transient flows in the printed pattern after leaving the nip. This is the concern of our paper.

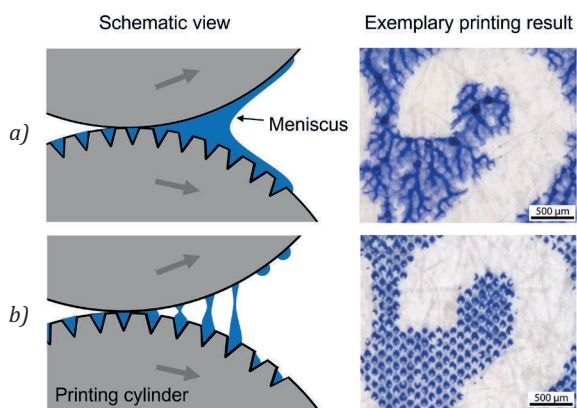


Figure 1: Schematic view of (a) lamella splitting (class 1), and (b) point splitting (class 2), in gravure printing

On the phenomenological level, according to Hübner (1991), one can distinguish two classes of ink splitting: *lamella splitting* (class 1) and *point splitting* (class 2), as shown in Figure 1. Point splitting implies that each gravure cell deposits an individual ink drop at the specific target point on the substrate. This creates the well-known raster pattern underlying a gravure printed image. Deviations from regularity are considered as defects, i. e. missing dots (Rong and Pekarovicova, 2007), or point spreading, driven by capillary and substrate imbibition forces. These effects may be also caused by gravure defects on the cylinder, however, they are not considered as the effect of ink capillarity between the diverging surfaces in the nip. The opposite case is referred to as lamella splitting. Ink drops from adjacent cells already coalesce on the printing cylinder. A continuous and highly dynamic fluid meniscus is formed in the nip, and the ink is dragged out of the cells from this meniscus and forms a closed ink layer on the substrate. Clearly, this effect spoils printing resolution. However, the positive aspect is that the considerable capillary energy of the deposited film is counteracted by the dewetting tendencies induced by the substrate. Initially, the liquid layer is metastable and delicate. Stochastic fluctuation phenomena such as *viscous fingering* or Marangoni effects may occur, and initiate e. g. a layer breakdown in the subsequent drying process. The primary goal of printing process and gravure pattern optimization, however, is to bring the liquid film across the first hurdle which is fluid transfer. Providing appropriate conditions for safe leveling of the liquid layer is a subsequent, but largely independent issue as discussed by Sauer, Braig and Dörsam (2020).

In considerable part, our understanding of ink splitting flows has developed from studies on the Hele-Shaw-Cell by Saffman and Taylor (1958) and on forward and reverse gravure roll coating (Gaskell, Savage and Summers, 1996; Benkreira and Cohu, 1998; Gaskell, Innes and Savage, 1998; Schwartz, 1999; Hewson, Kapur and Gaskell, 2006; 2009). Gravure printing is considered as the special case where cylinder and substrate surface are in synchronous motion. This view, at least for moderate printing velocities, has been supported by the work of Hopkins (1957); Kunz (1975); Hübner (1991); Voß (2002); Bornemann (2014), and, concerning flexography, by Hamblyn (2015) and Brumm, Sauer and Dörsam (2019). These studies claim that the ink splitting hydrodynamics is a unique matter of the capillary number of the ink flow in the nip, the ratio of viscous and capillary forces.

Nevertheless, there are parallel observations of ink splitting phenomena in the gravure printing process which cannot be distinguished by capillary numbers alone. Trnovec (2013) has found that pattern formation, at elevated printing velocities, systematically diverges from the expectations of former studies. This was assigned to the Bernoulli pressure under the doctor blade, which affects the filling level of the cells. However, the conclusion is that mass inertia of the ink also becomes relevant, in addition to capillarity and viscous forces. Griesheimer (2014) has demonstrated by his early high-speed video studies that, even in the nip, mass inertia takes over the fluid dynamics in the late phase of ink splitting, when liquid filaments and sheets are evolving in the ink splitting process. Gravure printing hydrodynamics becomes more ‘inkjet’-like. The observed effects depend on the Laplace or, equivalently, on the Ohnesorge number.

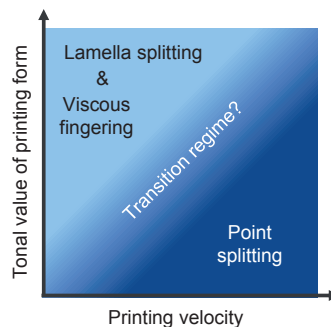


Figure 2: Qualitative concept of the transition between point splitting and lamella splitting

A first qualitative concept on transition between point and lamella splitting is depicted in Figure 2. With increasing printing velocity and decreasing raster cell volume per surface area, which equals decreasing tonal values, ink splitting dynamics will toggle between lamella and point splitting. We focus on the param-

ter regime close to this transition. We want to know if there is a transition area or a clear separation into point splitting and lamella splitting.

In a sequence of gravure printing experiments, we have elucidated the pattern formation phenomenology of the ink splitting process. After having identified the parameter ranges where the transition regime is located, our study on pattern formation was focussed on the effect of small parameter changes on pattern formation. Careful parameter variation should show that the transition may have an intermediate regime which cannot be assigned to the traditional two-class distinction.

2. Materials and methods

2.1 Printing experiments

For our experiments, we used a lab-scale sheet-fed gravure printer (GT+W Superproofer 220, Rödermark, Germany), which was also described in (Schäfer, Sauer and Dörsam, 2018; Schäfer, et al., 2019). The speciality of the setup used as shown in Figure 3 is a substrate carrier on which the substrate is mounted on the bottom side. The carrier is then accelerated by a linear motor to move the substrate into the printing nip and therefore across the gravure cylinder, with specified printing velocity (20–300 m/min). With such a setup only small amounts of ink (1–3 ml) are needed for the experiment.

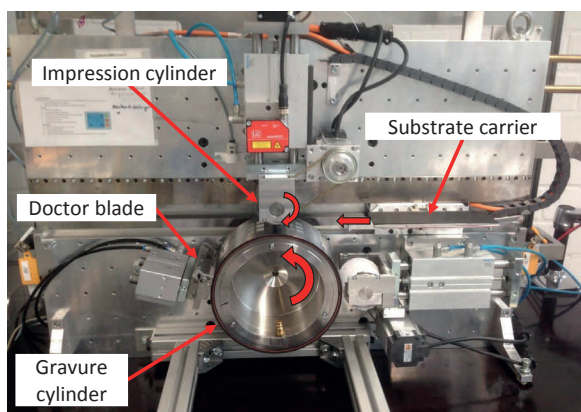


Figure 3: Gravure printing setup

Table 1 shows the parameter combinations used for the printing experiments. We used printing velocities of {20, 30, 45, 60, 75, 90, 160} m/min. As printing fluids, we utilized water-based gravure inks in a red (SunChemical R0001235761) and a blue (SunChemical B000117761) version. In addition, a diluted version of the red ink (10.14 g of printing ink with 9 g of distilled water) was tested.

Table 1: Parameter combinations used in the printing experiments (the exact names of all inks and substrates can be found in the text in Section 2.1)

Parameter combination	Printing		
	velocity in m/min	Printing fluid	Substrate
1	20	Red ink	Paper
2	30	Red ink	Paper
3	45	Red ink	Paper
4	60	Red ink	Paper
5	75	Red ink	Paper
6	90	Red ink	Paper
7	160	Red ink	Paper
8	30	Red ink	Foil
9	30	Diluted red ink	Paper
10	30	Blue ink	Paper

As substrates, we used paper (UPM Finesse matte-coated H) with a grammage of 100 g/m² and coated transparent foil (Hostaphan® GN 4660A) with a thickness of 125 µm. Substrates were cut to 200 mm × 60 mm and attached to the substrate carrier. Doctor blade pressure and angle, and also nip pressure are given in Table 2. The machine was operated in a climatized, filtered atmosphere at a temperature of 20 ± 2 °C, and a relative humidity of 33 ± 3 %.

Table 2: Process parameters that were kept constant for all printing experiments

Parameter	Value
Doctor blade pressure	0.4 N/mm
Doctor blade angle	60°
Nip pressure	16 N/mm

As printing form, an electromechanically engraved chromium-plated copper sleeve, with stylus angle 120°, raster angle 45°, diameter 220 mm and printing width 100 mm was used (engraver: Sächsische Walzengravur GmbH, Germany). Figure 4 illustrates the relevant parameters of the printing form, which can also be applied to describe the printed product. A ‘raster cell’ as shown in Figure 4a corresponds to a later printed dot (‘raster dot’) of the printed product as shown in Figure 4b. Printed dots differ a lot in shape and size. Section A-A shows a sectional view of a single pyramid-shape raster cell of a gravure printing form.

The gravure pattern on the sleeve consisted of five segments distributed over its circumference. Each segment contained two clusters of gravure fields, with specific raster frequencies for each cluster: {40, 48, 54, 60, 70, 80, 90, 100, 120, 140} lines per centimeter (L/cm). Each cluster contained 12 fields of size 13 mm × 13 mm. The tonal values of the fields within each cluster were {5, 10, 20, 30, 40, 50, 60, 70, 80, 90, 95, 100} %. For each

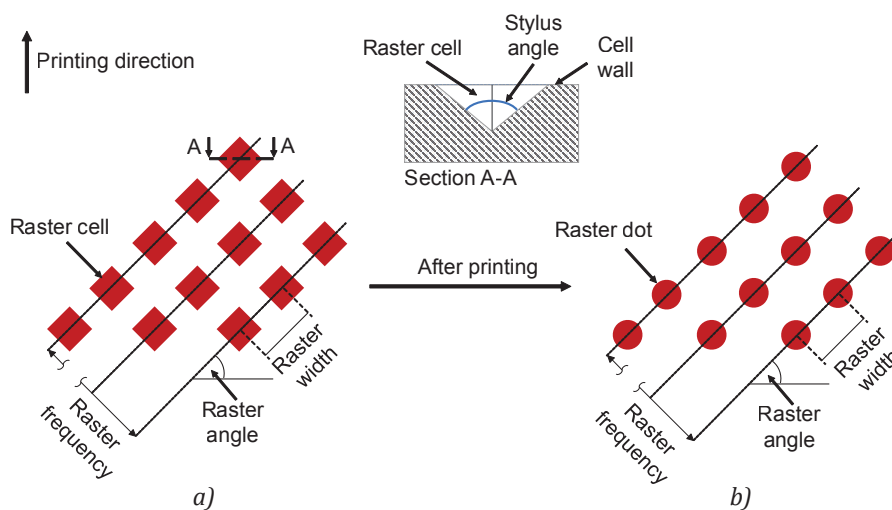


Figure 4: Illustration of (a) relevant parameters of an electromechanically engraved printing form, and (b) the corresponding printed raster pattern

parameter combination in Table 1, all five segments of the printing form were employed for printing in at least three subsequent printing runs. Printing samples from over 3 600 fields (ten parameter combinations × five segments × two clusters × twelve fields × three samples) on over 150 samples were created in this way.

2.2 Classification of the printed samples

2.2.1 Sample digitization

The printed samples were digitized using a flatbed scanner (EPSON Perfection V800 Photo) that was color-calibrated with a Kodak IT8 target once a day before each scanning series. We chose 2400 dots per inch (dpi) as the nominal scanning resolution. The actual scanning resolution was determined as 1825 dpi using an USAF-1951 resolution target. Using the profes-

sional scanning software SilverFast Ai Studio 8, unfiltered raw data in uncompressed 16 bit RGB TIFF format was created. The size of a digitized sample was about 5 800 × 18 000 pixels. Figure 5 shows such a sample with annotations. The printed fields were 13 mm × 13 mm in size, each with its tonal values in % noted below. Each cluster of 12 fields had a different raster frequency; e. g., cluster 1 had 140 L/cm, cluster 2 had 40 L/cm. The printing direction is given by an arrow. The tail of the arrow indicates areas which were printed earlier in time whereas the arrowhead points towards areas which were printed later in time. The printing parameters for Figure 5 can be looked up in the Appendix in Table A1 where a collection of printing parameters for fields used as examples in Figures 5 to 14 can be found.

All digitized printed fields can be downloaded from <<https://doi.org/10.48328/tudatalib-528.2>>.

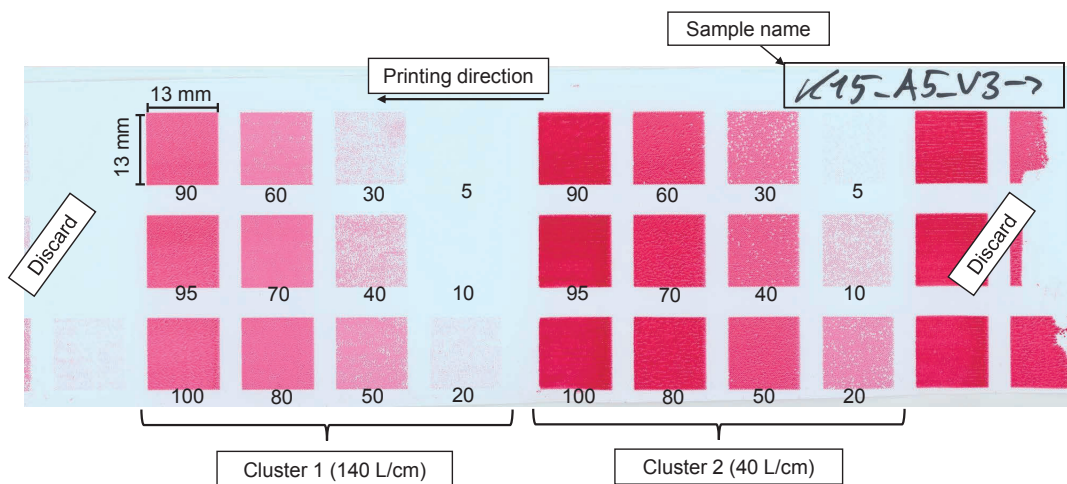


Figure 5: Exemplary digitized sample with annotations

2.2.2 Classification method

We defined criteria to classify each printed field into one of the following three classes: *Lamella splitting* (class 1), *point splitting* (class 2) and *transition regime* (class 3). The criteria for all three classes are indicated in Table 3.

Table 3: Iteratively developed ink splitting classification

Name	Type of ink splitting	Criteria
Class 1	Lamella splitting	There are only <i>fingers</i> visible on the field. They can differ in shape, size and orientation. If a form cannot be further discriminated into <i>dots</i> , it is seen as a <i>finger</i> . There is no single <i>dot</i> to be seen.
Class 2	Point splitting	There are only <i>dots</i> visible on the field. The <i>dots</i> can have different shapes (diamond-, donut-, boomerang-shape, etc.). Connections between <i>dots</i> are allowed as long as the <i>dots</i> are still discriminable. There is no single <i>finger</i> to be seen.
Class 3	Transition regime	There are <i>dots</i> as well as <i>fingers</i> visible on the field.

In order to apply Table 3, a classification scheme for *dots* and *fingers* was necessary. The graphical classification scheme for dots and fingers with corresponding

printing examples is shown in Figure 6. In the classification scheme (top), red areas represent areas wetted with printing ink. The darker the red color the higher the amount of ink. The distance between the dots equals the raster width. The printing examples (bottom) show independent dots (a1.1 to a1.3), connected but still discriminable dots (a2.1), shapes, which cannot further be discriminated into single dots and are therefore considered as fingers (b1.1 and b1.2), and fingers with a *brim* (b2.1 to b2.3). The printing parameters for the printing examples in Figure 6 can be found in the Appendix. In addition to the graphical classification scheme, we provide a textual classification scheme for *dots*, *fingers* and *brim*, as given in Table 4.

Table 4: Textual classification scheme for the terms *dot*, *finger* and *brim* as used in this research

Term	Definition
<i>Dot</i>	Isolated droplet on the printing product on a raster dot position.
<i>Finger</i>	Liquid ink bridge resulting from viscous fingering on the printed product. We assumed that the smallest finger is as long as the distance between two neighbouring raster dots. A finger may be surrounded by a brim.
<i>Brim</i>	Area, which has been in contact with ink intermediately, but now is essentially void of deposited ink, e. g. by dewetting, contact line recession or imbibition. It does not need to be restricted to a certain area but can also cover the whole background of the fingers.

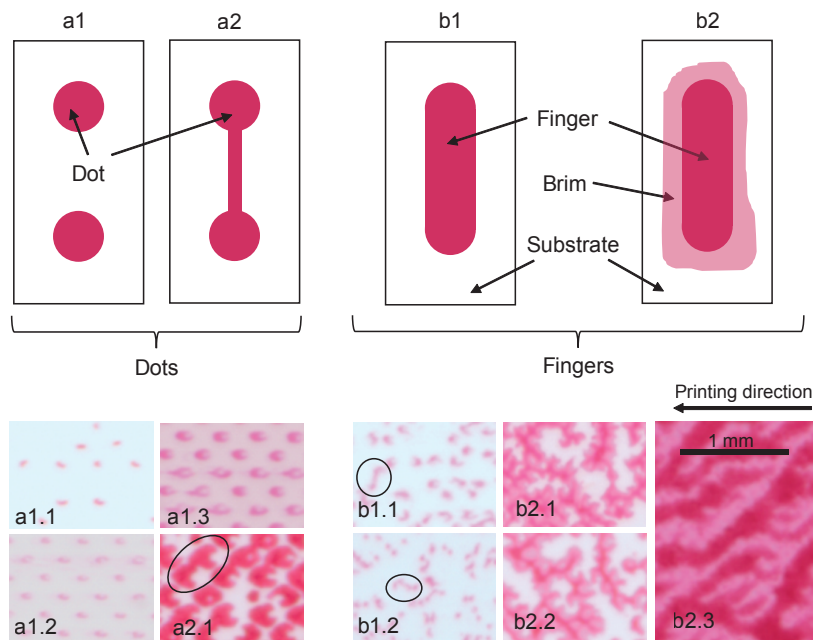


Figure 6: Graphical classification scheme for dots, fingers and brim (top) and corresponding exemplary printed samples (bottom)

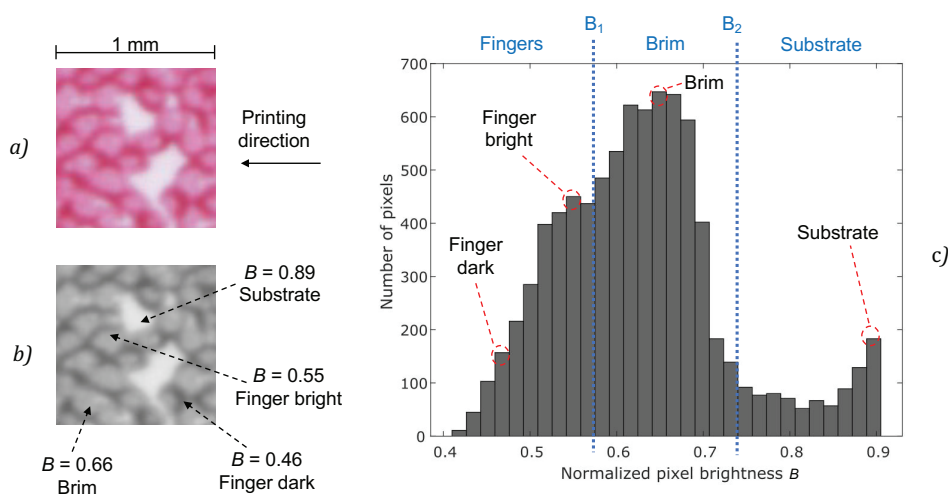


Figure 7: Possible quantitative classification approach to visualize the frequency distribution of brightness values of a sample cut-out (a), converted into grayscale (b), by using a histogram (c)

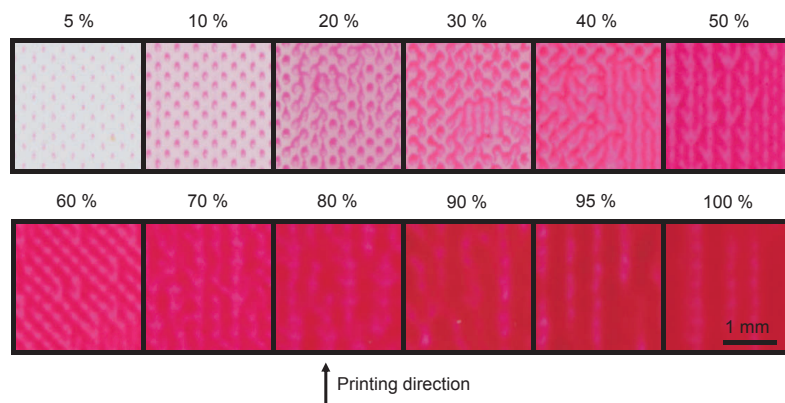


Figure 8: Change of pattern formation by altering the tonal value

In this research, the delicate distinction between dots and substrate or between finger, brim and substrate is done by a (subjective) human observer. As a future quantitative approach, we suggest distinguishing these features using a histogram which shows the frequency distribution of brightness values in a sample image. With certain defined brightness thresholds, fingers, brim and substrate could be distinguished. These brightness thresholds could be identified iteratively or using machine learning approaches for a large number of samples. The proposed quantitative approach is shown exemplarily for a cut-out of one printed field in Figure 7. The RGB sample cut-out (Figure 7a) is converted into grayscale (Figure 7b) and then a histogram with 30 bins is created (Figure 7c). The printing parameters for the printed field in Figure 7 can be found in the Appendix. By looking at the histogram we were at least able to clearly distinguish fingers and brim from the substrate. However, we were not able to easily differentiate brim and fingers since their brightness values are not clearly separated as two separate

sharp peaks in the histogram. Rather, brightness values of fingers (dark and bright) and brim merge in one single wide peak in the histogram. Nevertheless, the human observer is able to distinguish fingers and brim, although in a subjective manner. The histogram proves a possible quantitative differentiation of fingers, brim and substrate by defining suitable threshold brightness values B_1 and B_2 , which are chosen exemplarily here. There might be possible disruptive factors for a human observer, e. g. a residual lubrication film from the doctor blading process on the substrate or the phenomenon of dot gain which need to be distinguished from the expected features (dots, fingers, brim, substrate). These disruptive features have to be taken into account when developing a future objective classification approach.

Figure 8 exemplarily illustrates the transition from low to high tonal values and its resulting development of different patterns. Although each printed sample differs due to its stochastic nature, dots can be found at

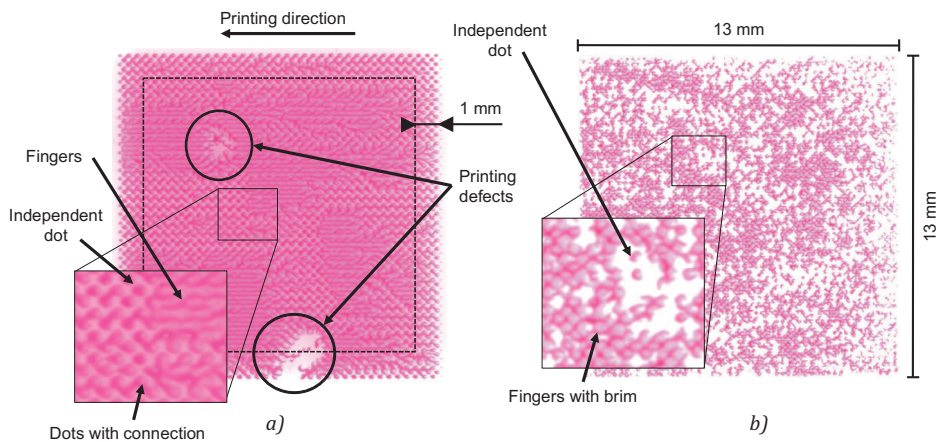


Figure 9: Transition regime, as seen on two fields (a) and (b)

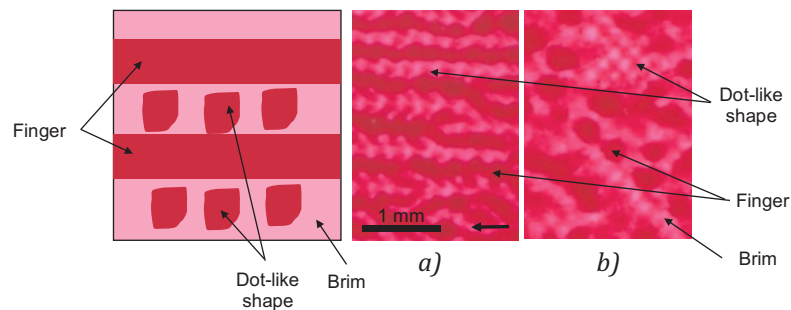


Figure 10: Dot-like shapes next to fingers as observed on two different fields (a) and (b), which are classified as lamella splitting

lower tonal values while finger patterns can be seen at higher tonal values. The transition regime in this example is located at tonal values of 20 %, 30 % and 40 %. The printing parameters used to create the various kinds of patterns in Figure 8 can be found in the Appendix.

All digitized samples with over 3600 fields were visually examined on a computer screen using adequate digital magnification. We assigned one of the three classes in Table 3 to each field. Obvious printing defects were always excluded from visual assessment as well as the rim of the fields (about 1 mm from each edge towards the center of the field), since it showed different pattern formation than the inside of the fields (Figure 9). We assume that only the inside of the fields exhibits stationary pattern formation phenomena. Figure 9 shows typical examples for the transition regime on foil (Figure 9a) and on paper (Figure 9b). In the fields classified as transition regime, dots as well as fingers appear. The printing parameters used to print the two fields in Figure 9 can be found in the Appendix.

Within the classification process, we found an especially interesting but complex type of pattern formation as seen in Figure 10 on two different fields (Figure 10a

and Figure 10b). Printing parameters can be found in the Appendix. Both fields show a pattern of dot-like shapes located on the brim next to fully developed fingers. The arrow indicates the printing direction. Since the dot-like shapes show up with a brim, they do not fall under our definition of dots. Therefore, the patterns in Figure 10 were not assigned to the class of transition regime (class 3). In fact, they were assigned to the class of lamella splitting (class 2) in this research, because there are only fingers and no dots visible on the fields, compare with Table 3. Further investigation is needed to explain the existence of dot-like shapes near to fully developed fingers. We assume that this phenomenon could be related to the absorbing properties of paper substrates, which preserves former states of forced wetting during the gravure printing process.

3. Results and discussion

Figure 11 shows classification results for red ink on paper for ten different raster frequencies: {40, 48, 54, 60, 70, 80, 90, 100, 120, 140} L/cm. On the horizontal axis, we show the printing velocity and on the vertical axis, the tonal value (left) as well as the raster frequency (right). We marked the upper and lower bor-

ders of the transition regime, by plotting the last field classified as point splitting and the first field classified as lamella splitting in a series of fields with increasing tonal values. The lines between the data points are linear interpolations. The three regimes lamella splitting, point splitting and transition regime are marked with different infill colors as shown in the legend in Figure 11. Each data point represents the combined classification result of at least three samples with the same parameter combination. For example, when we classified a field two times as transition regime and once as lamella splitting, transition regime was chosen. We expect the lamella splitting, the point splitting and the transition regime to be continuous and clearly separated. Thus, we were able to detect and exclude outliers from our data, e. g. a point splitting field in the lamella splitting regime which was caused by too little ink being transferred (obvious printing defect).

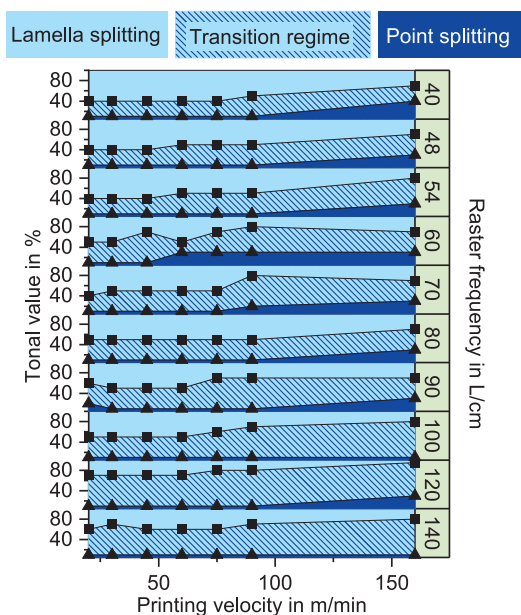


Figure 11: Classification results for the samples printed with red ink on paper

For better visualisation, the classification results shown in Figure 11 were combined in one single diagram (Figure 12) by averaging of all data points from all raster frequencies and subsequent linear interpolation to obtain the regime borders. Figure 12 shows printing velocity on the horizontal axis and tonal value on the vertical axis. It displays the regimes of printing velocity and tonal value, where lamella splitting, point splitting and an intermediate regime (the transition regime) were observed. With higher printing velocities, the transition regime shifts to higher tonal values. We observe lamella splitting at higher tonal values and point splitting at lower tonal values. This finding is in good agreement with literature, which says that the amount of ink is rather high for lamella split-

ting and rather low for point splitting (Hübner, 1991). Furthermore, we observed that for tonal values of 10 % and lower, only point splitting occurs. From Figure 12 we can derive linear trend lines for the regime borders, as marked in red dashed and dashed-dotted lines. The linear trend lines for the upper and lower regime borders are given as $y = 43.2 + 0.2x$ (red dashed line) and $y = 4.5 + 0.1x$ (red dash-dotted line), respectively, where y is the tonal value in % and x is the printing velocity in m/min.

Figure 12 shows that the size of the transition regime is unexpectedly large in comparison to the point splitting regime and even about as large as the lamella splitting regime. We assume that this has three possible reasons. First, the use of a paper substrate which causes relatively many printing defects. Second, the harsh criteria for the classification as transition regime, as chosen for this research. And third, our way of representing the regime map.

To start with the first reason, paper is a rather rough substrate (compared to foil) and thus most of the printed samples show relatively many missing dots or other printing defects. These printing defects (if not evaluated as obvious printing defects and therefore excluded by the human observer) can lead to classifying a field as transition regime since a printing defect might look like a dot in a field of fingers only.

According to the developed classification scheme from Table 3, one single dot in a field with only fingers is responsible for the classification as transition regime. This is reason two for the large transition regime. For future research, we suggest softening this relatively harsh criterion for the benefit of the robustness of our approach. For example, the existence of five dots in a field of fingers only could lead to the classification as transition regime. For the manual assessment by a human observer, a threshold of five dots would have led to an exponentially higher expenditure of time for classification which would have not been feasible. When using quantitative, automated classification approaches, e. g. image processing with deterministic algorithms or machine learning approaches, the choice of arbitrary thresholds would become feasible.

The third reason for the large transition regime is the way of representing the regime map. We chose to mark the last field that exhibits point splitting and the first field that exhibits lamella splitting in a series of increasing tonal values. Since we have discrete tonal values in 5 % or 10 % steps, the transition regime seems larger in the negative and positive y -direction up to one step. For example, when tonal values {5, 10} % are classified as point splitting, {20, 30, 40} % as transition regime and {50, 60, 70 80, 90, 95, 100} % as lamella splitting,

see Figure 8. In this case, we marked 10 % as the lower regime border and 50 % as the upper regime border in the regime map. Alternatively, we could mark the first (20 %) and the last field (40 %) that was classified as transition regime, which would lead to a transition regime that appears smaller, but this is not a useful representation when no transition regime exists.

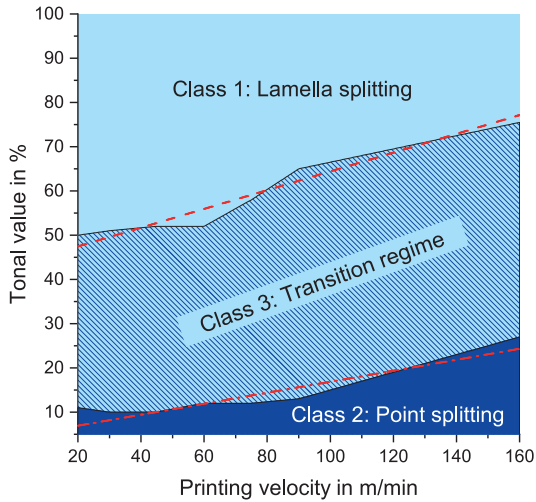


Figure 12: Location of the transition regime for the samples printed with red ink on paper

Substrate and fluid had significant influence on the visual appearance of the samples, particularly on finger shape and size, see Figure 13. Printing parameters can be found in the Appendix. The finger pattern was much less branched than on paper substrates. Finger patterns from red and blue gravure ink did not exhibit a significantly different optical appearance, except that the finger patterns were unique due to their stochastic nature (Fernandes, 2019). Diluted ink showed patterns that looked more washed-out than patterns created with non-diluted ink.

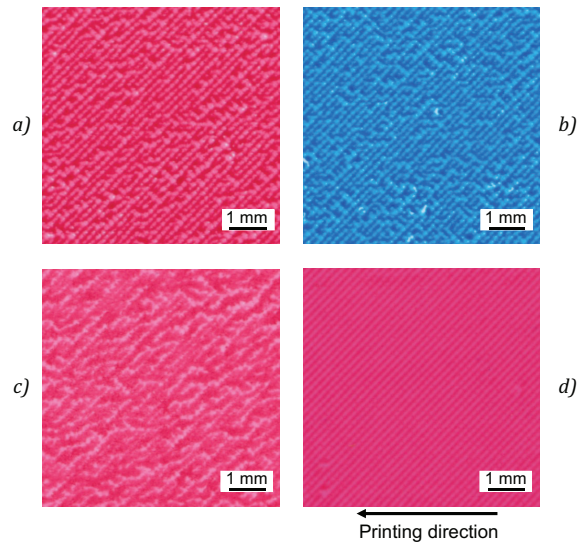
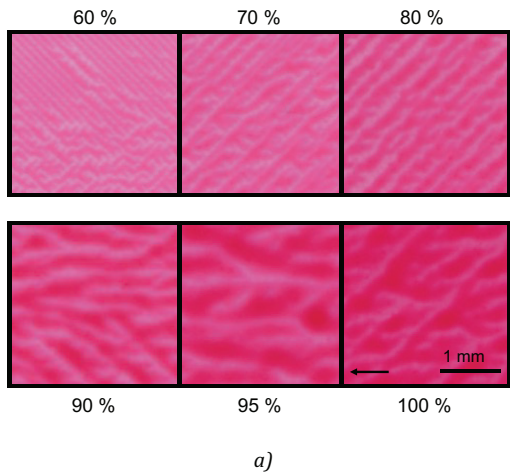


Figure 13: Comparison of pattern formation using (a) red ink on paper, (b) blue ink on paper, (c) water diluted red ink on paper and (d) red ink on foil

According to literature, viscous fingering has its predominant direction parallel to the printing direction. In this research, we also found predominant directions diagonal to the printing direction, see Figure 14. The arrows indicate the printing direction. Printing parameters can be found in the Appendix. Different predominant directions can be observed on the same sample at different tonal values (Figure 14a) or on different samples (Figures 14b to 14e). There can also be found several predominant directions in one and the same printed field, e. g. Figure 14e.

In summary, we have found evidence for the possibility of more complex types of ink splitting in the gravure process. With our classification scheme, we were able to localize the point and lamella splitting regimes as well as the transition regime. Our findings may serve

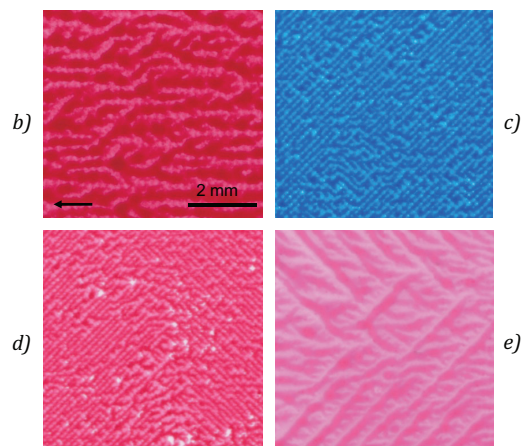


Figure 14: Various predominant directions of finger patterns, not only parallel but also diagonal to the printing direction, can be observed (a) on the same sample at different tonal values, and (b–e) on different samples

as a guideline for practical application. We emphasize that, depending on printing parameters, ink splitting in the transition regime may exhibit different types of pattern formation that we were not able to resolve here.

4. Conclusions and outlook

As shown in Sections 2 and 3 we were able to create a common basis for the classification of point and lamella splitting, and the intermediate transition regime. We were able to create a classification scheme for the three regimes, by evaluating data from over 3600 printed fields. Moreover, we were able to come up with an empirical assessment of tonal value vs. printing velocity and the impact of both on the creation of the three mentioned regimes. With this, our classification scheme sets the basis for further investigations on the transition from point to lamella splitting. However, the developed method is still at an early stage. Visual assessment and classification into dots and fingers depends on the subjective judgement of a human observer and on conditions of visual inspection. Thus, a precise classification of the morphologies is required which goes beyond the binary distinction of point and lamella splitting. Our aim here was to show that such a classification is feasible. Our findings on ink splitting contribute to known results by a refinement of the common picture. It must be noted that the distinction into the three classes as mentioned above might not capture the full spectrum of patterns and transition effects and thus is subject to further research. There is reason to suspect that even more distinctions are necessary, yielding interesting process options for novel applications of gravure printing e. g. security features or functional coating with only partial percentage of ink covering.

Optical resolution clearly is a limitation of our approach, although our definition of dots and fingers also works for higher resolutions. At high raster fre-

quencies, e. g. 140 L/cm, the printed dots were so small that scanning resolution was at its limit. At this limit of resolution, the distinction between dot and finger is rather subjective. Another limitation is the fact that we examine the printed sample after drying. This means that the sub-steps of ink relaxation and drying on the substrate, which occur after fluid transfer, have an impact on the result. Nevertheless, for this research, we assume that the printed sample is a frozen image of the moment right after fluid transfer.

For future research, in-situ experiments with high-speed imaging of ink splitting like in Schäfer, et al. (2019) are promising. In-situ experiments are elaborate, but provide more complex insight compared to our ex-situ experiments (using the printed products as samples), which are comparatively simple to implement and thus more user-friendly. For our approach, just a gravure printing machine, a high-resolution scanner, a computer for image observation and an instructed human observer are needed. For in-situ experiments, generally, expensive high-speed imaging equipment, a modified, optically accessible gravure printing machine and software for automated image analysis are needed. For future research, digital image processing, computer vision and machine learning algorithms for pattern recognition could be used in order to increase objectivity of the developed classification approach. For example, frequency-based image analysis using Fast Fourier Transformation as described in Brumm, Sauer and Dörsam (2019) could be used to determine the dominant pattern frequency and thus clearly differentiate between dominant finger frequency and known raster dot frequency. This could help in distinguishing dots and fingers. Moreover, scaling laws of finger formation can be obtained. Using more objective and automated approaches, the upscaling of gravure printing process research to industrial scale could be promoted. For future research, we plan to conduct gravure printing experiments at industrial scale and at higher printing velocities and compare the results to this research.

Acknowledgments

We kindly acknowledge the financial support by the Deutsche Forschungsgemeinschaft (DFG, German Research Foundation) – Project-ID 265191195 – SFB 1194 ‘Interaction between Transport and Wetting Processes’, project C01. Besides, we kindly thank Thorsten Euler for his help in operating the printing machine.

References

- Benkreira, H. and Cohu, O., 1998. Direct forward gravure coating on unsupported web. *Chemical Engineering Science*, 53(6), pp. 1223–1231. [https://doi.org/10.1016/S0009-2509\(97\)00446-6](https://doi.org/10.1016/S0009-2509(97)00446-6).
- Bornemann, N., 2014. *Characterization and investigation of large-area, ultra-thin gravure printed layers*. Doctoral thesis. Technische Universität Darmstadt. [online] Available at: <<https://tuprints.ulb.tu-darmstadt.de/id/eprint/3847>> [Accessed 29 November 2020].

- Brumm, P., Sauer, H.M. and Dörsam, E., 2019. Scaling behavior of pattern formation in the flexographic ink splitting process. *Colloids and Interfaces*, 3(1): 37. <https://doi.org/10.3390/colloids3010037>.
- Fernandes, F.C., 2019. *Entwicklung von gedruckten stochastischen Identifikationsmerkmalen*. Doctoral thesis. Technische Universität Darmstadt. [online] Available at: <<https://tuprints.ulb.tu-darmstadt.de/id/eprint/8795>> [Accessed 29 November 2020].
- Ganz, S., Sauer, H.M., Weißenseel, S., Zembron, J., Tone, R., Dörsam, E., Schaefer, M. and Schulz-Ruthenberg, M., 2016. Printing and Processing Techniques. In: G. Nisato, D. Lupo and S. Ganz, eds. *Organic and printed electronics: fundamentals and applications*. Singapore: Pan Stanford Publishing, pp. 47–116.
- Gaskell, P.H., Savage, M.D., and Summers, J.L., eds., 1996. *First European Coating Symposium on the Mechanics of Thin Film Coatings*. Leeds University, UK, 19–22 September 1995. Singapore: World Scientific Publishing. <https://doi.org/10.1142/3007>.
- Gaskell, P.H., Innes, G.E. and Savage, M.D., 1998. An experimental investigation of meniscus roll coating. *Journal of Fluid Mechanics*, 355, pp. 17–44. <https://doi.org/10.1017/S0022112097007398>.
- Grau, G., Cen, J., Kang, H., Kitsomboonloha, R., Scheideler, W.J. and Subramanian, V., 2016. Gravure-printed electronics: recent progress in tooling development, understanding of printing physics, and realization of printed devices. *Flexible and Printed Electronics*, 1(2): 023002. <https://doi.org/10.1088/2058-8585/1/2/023002>.
- Griesheimer, S., 2014. *Farbspaltungssphänomene von Druckfarben an strukturierten Oberflächen am Beispiel des Flexodrucks*. Doctoral thesis. Technische Universität Darmstadt. [online] Available at: <<https://tuprints.ulb.tu-darmstadt.de/id/eprint/3892>> [Accessed 29 November 2020].
- Hamblyn, A., 2015. *Effect of plate characteristics on ink transfer in flexographic printing*. Doctoral thesis. Swansea University. [online] Available at: <<https://cronfa.swan.ac.uk/Record/cronfa42827>> [Accessed 29 November 2020].
- Hewson, R.W., Kapur, N. and Gaskell, P.H., 2006. A theoretical and experimental investigation of tri-helical gravure roll coating. *Chemical Engineering Science*, 61(16), pp. 5487–5499. <https://doi.org/10.1016/j.ces.2006.04.021>.
- Hewson, R.W., Kapur, N. and Gaskell, P.H., 2009. Modelling the discrete-cell gravure roll coating process. *The European Physical Journal Special Topics*, 166, pp. 99–102. <https://doi.org/10.1140/epjst/e2009-00886-x>.
- Hopkins, M.R., 1957. Viscous flow between rotating cylinders and a sheet moving between them. *British Journal of Applied Physics*, 8(11), pp. 442–444. <https://doi.org/10.1088/0508-3443/8/11/303>.
- Hübner, G., 1991. *Ein Beitrag zum Problem der Flüssigkeitsspaltung in der Drucktechnik*. Doctoral thesis. Technische Universität Darmstadt. <https://doi.org/10.25534/tuprints-00013550>.
- Kopola, P., Tuomikoski, M., Suhonen, R. and Maaninen, A., 2009. Gravure printed organic light emitting diodes for lighting applications. *Thin Solid Films*, 517(19), pp. 5757–5762. <https://doi.org/10.1016/j.tsf.2009.03.209>.
- Kumar, S., 2015. Liquid transfer in printing processes: liquid bridges with moving contact lines. *Annual Review of Fluid Mechanics*, 47(1), pp. 67–94. <https://doi.org/10.1146/annurev-fluid-010814-014620>.
- Kunz, W., 1975. Ink transfer in gravure process. In: *TAGA Proceedings 1975: Annual meeting of the Technical Association of the Graphic Arts*. Toronto, Ontario, 1975. Rochester, NY, USA: TAGA, pp. 151–176.
- Rong, X. and Pekarovicova, A., 2007. The study of missing dots of electromechanical and laser engraved cylinders. In: *TAGA Proceedings 2007: Annual meeting of the Technical Association of the Graphic Arts*. Pittsburgh, PA, USA, 18–21 March 2007. Sewickley, PA, USA: TAGA, pp. 596–604.
- Saffman, P.G. and Taylor, G.I., 1958. The penetration of a fluid into a porous medium or Hele-Shaw cell containing a more viscous liquid. *Proceedings of the Royal Society A: Mathematical, Physical and Engineering Sciences*, 245(1242), pp. 312–329. <https://doi.org/10.1098/rspa.1958.0085>.
- Sauer, H.M., Braig, F. and Dörsam, E., 2020. Leveling and drying dynamics of printed liquid films of organic semiconductor solutions in OLED/OPV applications. *Advanced Materials Technologies*, 6(2): 2000160. <https://doi.org/10.1002/admt.202000160>.
- Sauer, H.M., Roisman, I.V., Dörsam, E. and Tropea, C., 2018. Fast liquid sheet and filament dynamics in the fluid splitting process. *Colloids and Surfaces A: Physicochemical and Engineering Aspects*, 557, pp. 20–27. <https://doi.org/10.1016/j.colsurfa.2018.05.101>.
- Schäfer, J., Sauer, H.M. and Dörsam, E., 2018. Direct observation of high-speed fluid transfer phenomena in the nip of a gravure printing machine. In: P. Gane, ed. *Advances in Printing and Media Technology Vol. XLV(V): Proceedings of the 45th International Research Conference of iarigai*, Warsaw, Poland, October 2018. Darmstadt, Germany: iarigai, pp. 72–81.
- Schäfer, J., Roisman, I.V., Sauer, H.M. and Dörsam, E., 2019. Millisecond fluid pattern formation in the nip of a gravure printing machine. *Colloids and Surfaces A: Physicochemical and Engineering Aspects*, 575, pp. 222–229. <https://doi.org/10.1016/j.colsurfa.2019.04.085>.
- Schwartz, L.W., 1999. Theoretical and numerical modelling of coating flow on simple and complex substrates including rheology, drying and Marangoni effects. In: F. Durst and H. Raszillier, eds. *European Coating Symposium: Advances in Coating and Drying of Thin Films*. Erlangen, Germany. Aachen: Shaker Verlag, pp. 105–128.
- Siever, J., 2019. Gravure market in Pakistan. *Gravure News*, 183(1), pp. 4–7.

Trnovec, B., 2013. *Experimentelle Untersuchungen zur Schichtbildung im Tiefdruck mittels hydrophobierter Druckform mit Applikationsbeispielen aus dem Bereich der gedruckten OPV*. Doctoral thesis. Technische Universität Chemnitz. [online] Available at: <<https://nbn-resolving.org/urn:nbn:de:bsz:ch1-qucosa-209748>> [Accessed 29 November 2020].

Voß, C., 2002. *Analytische Modellierung, experimentelle Untersuchungen und dreidimensionale Gitter-Boltzmann Simulation der quasistatischen und instabilen Farbspaltung*. Doctoral thesis. Bergische Universität Gesamthochschule Wuppertal. Available at: <<https://nbn-resolving.org/urn:nbn:de:hbz:468-20020367>> [Accessed 29 November 2020].

Willmann, J., Stocker, D. and Dörsam, E., 2014. Characteristics and evaluation criteria of substrate-based manufacturing. Is roll-to-roll the best solution for printed electronics? *Organic Electronics*, 15(7), pp. 1631–1640. <https://doi.org/10.1016/j.orgel.2014.04.022>.

Appendix

Printing parameters introduced in Figures 5 to 14 are shown in Table A1.

Table A1: Collection of printing parameters of printed fields used as examples in Figures 5 to 14

Figure number	Suffix	Raster frequency in L/cm	Tonal value in %	Printing velocity in m/min	Fluid	Substrate
5	–	40, 140	5–100	45	Red ink	Paper
6	a1.1	40	5	20	Red ink	Paper
	a1.2	40	5	30	Red ink	Foil
	a1.3	40	10	30	Red ink	Foil
	a2.1	40	40	160	Red ink	Paper
	b1.1	54	20	30	Red ink	Paper
	b1.2	140	20	60	Red ink	Paper
	b2.1	70	30	30	Red ink	Paper
	b2.2	90	50	60	Red ink	Paper
	b2.3	120	95	45	Red ink	Paper
7	–	60	40	30	Red ink	Paper
8	–	40	5–100	30	Red ink	Foil
9	a	40	40	30	Red ink	Foil
	b	60	40	30	Red ink	Paper
10	a	48	95	20	Red ink	Paper
	b	48	90	20	Red ink	Paper
13	a	60	70	30	Red ink	Paper
	b	60	70	30	Blue ink	Paper
	c	60	70	30	Diluted red ink	Paper
	d	60	70	30	Red ink	Foil
14	a	90	60–100	30	Red ink	Foil
	b	54	100	20	Red ink	Paper
	c	48	80	30	Blue ink	Paper
	d	54	60	60	Red ink	Paper
	e	120	90	30	Red ink	Foil



JPMTR-2103
DOI 10.14622/JPMTR-2103
UDC 004.93|51-3

Original scientific paper | 148
Received: 2021-03-22
Accepted: 2021-05-31

Image contrast enhancement using histogram equalization: a bacteria colony optimization approach

Saorabh Kumar Mondal¹, Arpitam Chatterjee² and Bipan Tudu³

¹Department of Instrumentation and Control Engineering,
Haldia Institute of Technology, Haldia, India

arpitam.chatterjee@jadavpuruniversity.in

²Department of Printing Engineering, Jadavpur University, Kolkata, India

³Department of Instrumentation and Electronics Engineering, Jadavpur University, Kolkata, India

Abstract

Histogram equalization (HE) is a popular method for image contrast enhancement that probabilistically maps the existing tonal levels of image to a new set of intensity levels. Despite simplicity, conventional global HE (GHE) has several limitations including visually disturbing false contouring, loss of original image features and wrong color representation in case of color images. Further modifications of GHE method have shown considerable improvement but many such techniques lack retention of original image characteristics. Computational intelligence algorithms can be a potential paradigm to address those limitations. This paper explores the scope of bacteria colony optimization (BCO) to obtain contrast enhancement while maintaining the original image characteristics. The fitness function has been formulated in frequency domain upon rigorous analysis in comparison with the results of existing contrast enhancement techniques. The paper includes implementation results with standard databases and the comparative evaluations. The comparative visual and objective evaluations confirm potential of BCO for improved performance.

Keywords: computational intelligence, Fourier analysis of contrast enhancement, image enhancement algorithm, image quality assessment

1. Introduction

Image contrast is an important characteristic of image that largely contributes towards perceived image quality. In general image contrast is the ratio between darkest and lightest part of the image. Contrast sensitivity has two major interpretations namely absolute and perceived contrast sensitivity. The former one is the minimum difference in luminance required for distinguishing between two intensities. The human eyes are not very sensitive to this and as a result very small difference may not be visible. The second one is more important as this is to which human eyes are sensitive. For instance, a bright object is more visible in a dark background than a bright one since the contrast between bright object and bright background is not enough for human eyes to distinguish. This phenomenon is mathematically modeled using contrast sensitivity function. There are interpretations called global and local contrast as well. The global contrast is an overall ratio between luminance of dark and light region of entire image while local contrast is the distin-

guishability of different image regions in reference to the luminance of its local surrounding pixels. Contrast enhancement techniques focus on perceived and local contrast. Due to many reasons, such as insufficient illumination, noise during image acquisition, information loss during image transmission and limitation in sensing capability of the optical sensors, low contrast images are resulted. Low contrast not only results in visual unpleasantness but also limits performance of different image analysis tasks like edge extraction, feature extraction and object recognition. Image contrast enhancement therefore is a key research area (Jayaraman, Esakkirajan and Veerakumar, 2011; Maini and Aggarwal, 2010).

The goal of image contrast enhancement is to reconstruct the low contrast input image with new intensity levels that keep informational symmetry with the original image. In the digital era histogram has evolved as a potential alternative to the gradation curves and differential operators of analog era. Histogram has several advantages as it provides intensity distribu-

tion across the available intensity levels as a numeric array. Different statistical information of the images can thus be derived from histograms that are widely used for many image processing and transformation operations like image compression, segmentation, etc. It provides better control over different visual regions in the images, i.e. shadow, mid-tone and highlight since it is a numerical array that provides clear brightness distribution across the local regions of the images. For instance, a narrow histogram conveys the low contrast since the pixel values can vary only within few intensities and rest of the intensity levels remain unutilized. Histogram can provide better insight of the image information particularly using the probability density function (*PDF*) which can also convey the gradient curve information when taken in the cumulative manner as cumulative *PDF* (*CPDF*). Being powerful and simple, histogram has become the obvious choice for many real-time applications of image reproduction and representation systems. Histogram equalization (HE) widens up the histogram of the input image across the available intensity levels since the histogram of low contrast images is found with narrow distribution.

The two broad categories of approaches towards contrast improvement are spatial intensity based and frequency-based approaches. Global histogram equalization (GHE) (Arici, Dikbas and Altunbasak, 2009) is one of the classical techniques under former class that maps the existing intensity levels to new levels that are more apart from each other resulting in better contrast. In GHE this is achieved probabilistically based on the *CPDF* of the image. The results of GHE frequently suffer from false contouring and artificial appearance. Many algorithms were proposed towards improvement over the conventional algorithm, for example brightness preserving bi-histogram equalization (BBHE) (Kim, 1997), dual sub-image histogram equalization (DSIHE) (Wang, Chen and Zhang, 1999), dynamic histogram equalization (DHE) (Abdullahal-Wadud, et al., 2007), exact histogram specification (EHS) (Coltuc, Bolon and Chassery, 2006), etc.

Adaptive histogram equalization (AHE) is another paradigm reported in this domain which can result in better enhancement in case of unevenly illuminated low-contrast images. Contrast limited adaptive histogram equalization (CLAHE) (Reza, 2004), overlapped sub-blocks and local histogram projection (NOSH) (Bovik, 2009), and fast local histogram specification (FLHS) (Liu, et al., 2014) are some of the examples of AHE. However, AHE can also cause artificial appearance in the enhanced images due to amplification of noise. Works have been reported towards suppression of noise which include a multi-level histogram segmentation based algorithm that can also achieve improvement in terms of noise suppression (Tohl and

Li, 2019) and pre-specified threshold based noise control in gain-controllable clipped histogram equalization (GC-CHE) (Kim and Paik, 2008). These algorithms involve contextual partitioning of the image prior to HE which provides a better sense of local mapping of the input gray levels.

In case of the approaches under the second group the images are converted to its frequency domain representations using appropriate transforms and then the contrast enhancement is performed in different frequency bands. Some of the examples in this category are logarithmic transform histogram matching (LTHM), logarithmic transform histogram shifting (LTHS), logarithmic transform histogram shaping using Gaussian distributions (LTHSG) (Cao, et al., 2018; Lin, et al., 2015; Agaian, Silver and Panetta, 2007), spatial entropy-based contrast enhancement (SECE) and spatial entropy-based contrast enhancement by discrete cosine transform (SECEDCT) (Celik, 2014). Residual spatial entropy-based contrast enhancement (RSECE) and its extension to discrete cosine domain (RSECEDCT) have been reported as an improvement over SECE (Celik and Li, 2016). Spatial mutual information rank (SMIRANK) is another algorithm proposed in recent years where the gray levels in images are considered as nodes that are subjected to PageRank algorithm for mapping and can achieve both local and global contrast enhancement simultaneously (Celik, 2016).

Retinex, a model that removes bias of source lighting from the image, has been adopted for contrast enhancement as well. It includes single scale, multi scale retinex (MSR) (Jobson, Rahman and Woodell, 1997) and adaptive MSR (AMSR) (Lee, et al., 2013) models. The application of camera response model has been reported in literature for contrast enhancement where exposure ratio map estimation is proposed towards assessment of the image under consideration as low-light image enhancement algorithm (LLIEA) (Ying, et al., 2017). The HE algorithms for image enhancement in specific applications have been developed as well. Improvement of infrared thermal image contrast based on the adaptive double plateaus HE (Li, et al., 2018), particle swarm optimization based infrared image contrast enhancement (Wan, et al., 2018), improvement of face images suffering from non-uniform illumination (Shakeri, et al., 2017) and dynamic contrast enhancement of magnetic resonance imaging (DCE-MRI) (Padhani, 2002) are few examples of application specific developments of HE.

In recent years computational intelligence (CI) algorithms have also been used to achieve contrast enhancement (Ritika and Kaur, 2013) where the mathematical formulations are used as an evaluation function, conventionally called fitness function (Osareh,

Shadgar and Markham, 2009; Zhang, et al., 2009). In this context application of artificial bee colony (ABC) has been reported where image contrast enhancement is modeled as a transfer function using incomplete beta function (IBF) (Chen, Li and Yu, 2016). Different applications of genetic algorithm (GA) for contrast enhancement can also be found (Tang, 2014) where the fitness function is developed using image intensity and edge information.

The application of hybrid approach involving ant colony algorithm, GA and simulated annealing to optimize the fitness function consisting of edge, intensity and entropy information has been reported as well (Hoseini and Shayesteh, 2010). Dynamic fuzzy histogram equalization (DFHE) technique has presented the application of fuzzy algorithms in this context (Sheet, et al., 2010). One of the attractive reasons of applying CI algorithms is their adaptive nature that has been proven advantageous over conventional methods in solving many critical engineering problems (Konar, 2006).

Bacteria colony optimization (BCO) is a popular CI algorithm (Passino, 2010; Chen, et al., 2014) that performs optimization using behavioral pattern on motile bacteria such as *Escherichia coli* (*E. coli*), *Salmonella* and *Myxococcus xanthus* (*M. xanthus*). In case of BCO the chemotaxis behavior of bacteria for surviving in the environment (such as nutrients) and their movement towards or away from a specific location is employed (Niu, et al., 2013). The rationale behind selecting BCO is its advantage of not largely being affected by the size and non-linearity of the problem. This algorithm also has advantages such as less computational time requirement and can handle higher number of objective functions when compared to the other evolutionary algorithms (Majumder, Laha and Suganthan, 2019). Yet this algorithm has not been applied for contrast enhancement to the best of our knowledge.

The contribution of this work is two-fold: mathematical formulation of a new objective function in frequency domain instead of using image quality evaluation metrics and optimizing the same using BCO. It is a tradeoff of spatial and frequency domain approaches since the objective function is formulated in spatial domain but the fitness evaluation is performed in frequency domain. A considerable number of test images, both grayscale and color ones, have been tested with the presented method. The performance comparison of the presented method is portrayed using subjective and objective evaluation measures. The subjective evaluation is supported by observations in frequency domain analysis. The objective evaluation is presented using different standard image quality assessment (IQA) metrics of both full reference (FR) and no-reference (NR) types.

2. Histogram equalization using bacteria colony optimization

2.1 Fitness function formulation

Histogram equalization in grayscale image is based on *CPDF* calculated from the image intensity values in spatial domain. In case of color images application of HE remains same however a conversion from the native RGB color space to a perceptual color space such as Hue, Saturation and Value (HSV) (Saravanan, Yamuna and Nandhini, 2016; Chien and Tseng, 2011) is needed. Applying the HE individually to the three channels of RGB can cause erroneous results because post HE mixing between the color channels can result in a totally different perceived color at output image. Hence conversion to a device independent color space like HSV is required prior to HE. After conversion the HE can be applied only to the Value (V) channel followed by combining the equalized V channel to the other two channels which remain unaltered. Finally image is reverted to RGB color space.

In this section a Fourier domain analysis on the results of histogram equalization techniques is presented towards development of fitness function. In this analysis the results of conventional and state-of-art techniques, namely, GHE, BBHE, DSIHE, CLAHE, AMSR and LLIEA have been included. These techniques represent different classes of algorithms as mentioned in previous section. The study can be described with the help of Figures 1 and 2 where the results of said algorithms, corresponding difference fast Fourier transform (FFT) spectra (original spectrum subtracted from the enhanced image spectrum) and projection plots (horizontal and vertical) of the FFT spectra have been included. It may be noted that the Fourier spectra have been processed to obtain a clear view of resulting changes. The processing here involves binarization of log-transformed FFT spectrum followed by morphological operation.

Figure 1 shows that most of the conventional techniques fail to retain the background of the test image while the advanced algorithms namely, CLAHE, AMSR and LLIEA can successfully retain that. The difference FFT spectra along with the projection plots can be a possible tool to analyze the results. In frequency domain the contrast enhancement is expected to introduce more frequency components and an expansion of the Fourier spectrum is desired for better results. But the expansion in Fourier spectrum should not be random. The contrast enhanced image is expected to generate the Fourier spectrum which will be an expanded or stretched version of the original image spectrum keeping parity to its shape of original image spectrum. Any HE algorithm that results in expansion of spectrum without keeping

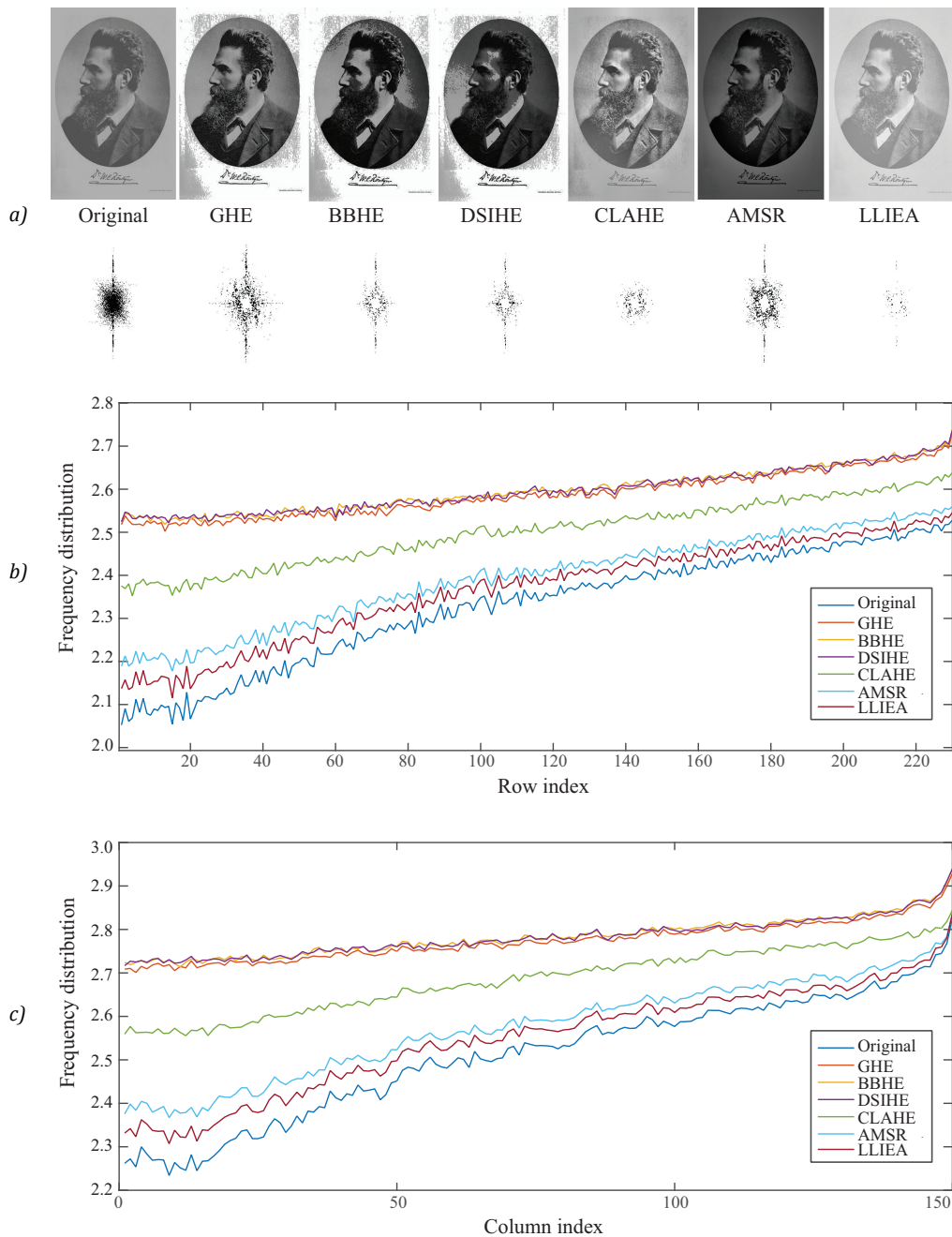


Figure 1: Fourier spectrum analysis of grayscale test image 'Man'; (a) results of different HE techniques and corresponding FFT spectra, (b) horizontal projection plots, and (c) vertical projection plots for different techniques

similarity to the shape of original spectrum will also show improvement but may not retain the important characteristics of the original image. As it can be seen in Figure 1, all classical HE enhancements result in contrast enhancement as reflected in their difference-spectrum by the resulted expansion. But at the same time expanded results are not well conforming to the shape of the original spectrum which results in loss of information as can be seen comparing the background gray region of original and modified images.

Hence, the algorithms can enhance image contrast or quality undoubtedly but there is noticeable lack in preserving the image characteristics. The projection plots can be possibly used to assess the shape conformance. The projection plots show that GHE, BBHE and DSIHE plots escalate through y axis keeping low adherence to the plot nature of original image. The plots for CLAHE shows comparatively better adherence while AMSR and LLIEA techniques are showing visibly improved adherence. These adherence results in better reten-

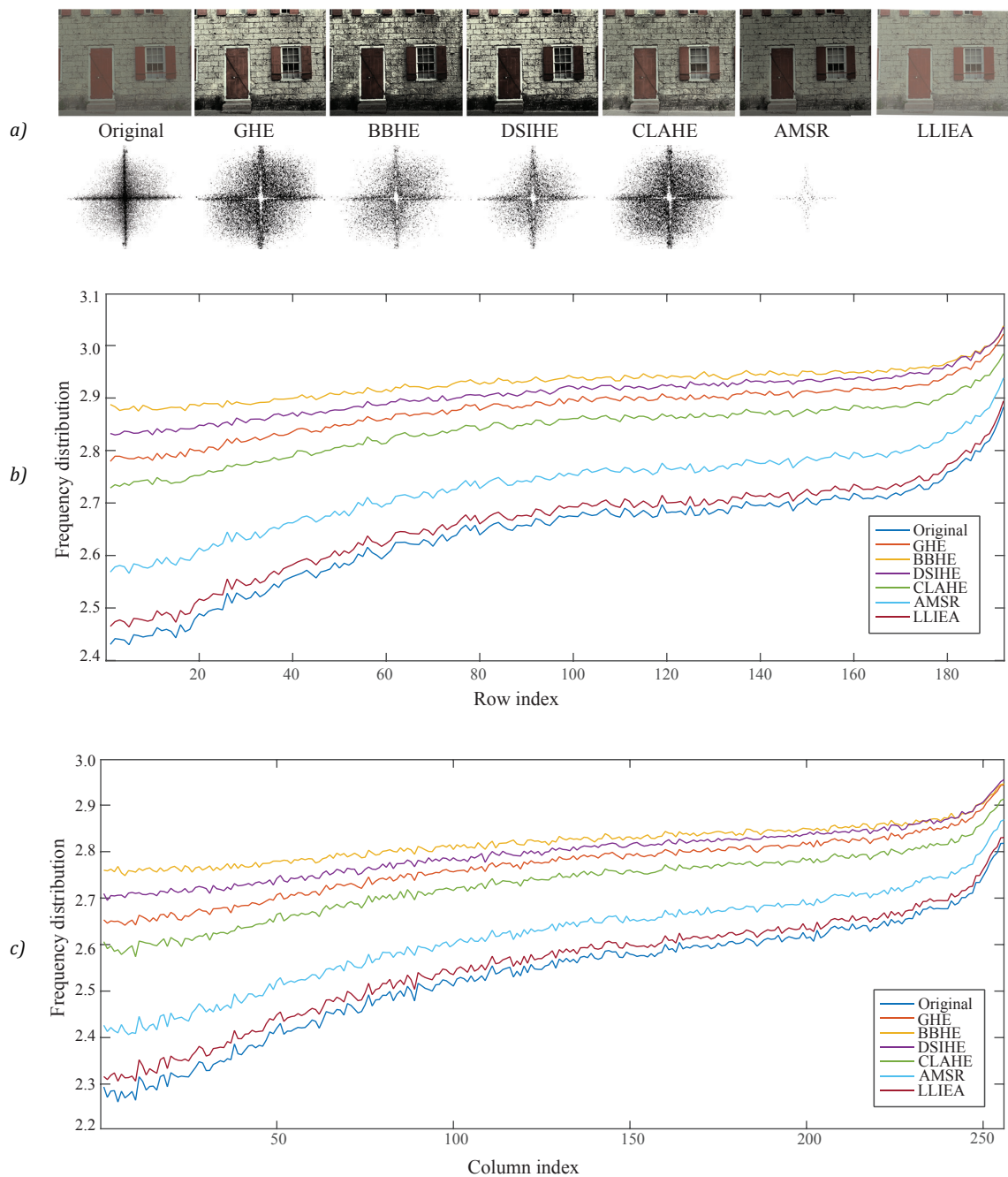


Figure 2: Fourier spectrum analysis of color test image 'House'; (a) results of different HE techniques and corresponding FFT spectra, (b) horizontal projection plots, and (c) vertical projection plots for different techniques

tion of original image features which can be seen by the retention of background grayness in their results. Nevertheless, the scope of improvements is still open. The same explanation may be drawn with color images as shown in Figure 2 where LLIEA does not show any visible expansion over the original image FFT spectra but it shows high degree of conformity to the shape of original image spectra as shown in projection plots of Figure 2. The classical techniques GHE, BBHE and DSIHE are more prone towards expansion of spectra

while less conforming to shape. The CLAHE method makes a balance between the expansion and shape conformity but a bit higher inclination towards spectra expansion while AMSR shows smaller expansion and better conformation to the shape.

From the presented images and the Fourier domain analysis it can be observed that the classical techniques are more towards the magnitude expansion than shape adherence while the advanced techniques attempt to

reach the balance between those two parameters but room of improvement is visible. The under- and over-enhancements can also be correlated to the magnitude expansion and shape adherence. Concretely, this work aims to achieve an optimum balance using BCO which can be a possible way to ensure avoidance of under- and over-enhancement problems that are visible in most of the classical as well as lately reported techniques. This leads to developing the optimization fitness function as a frequency domain parameter that will consider expansion and adherence to the shape of the original input spectrum. To use these parameters as fitness function the representative mathematical expression has been formulated as Equation [1].

$$\varphi = w_1 M \cdot w_2 S \quad [1]$$

where φ is the fitness function, M is the magnitude function and S is the shape parameter. The weight parameters w_1 and w_2 are tunable. The tuning of w_1 and w_2 is end-user requirement dependent; in the cases where retention of original image feature is of higher importance, such as in case of computer vision application, w_2 can be assigned with a higher value. In cases where the visual appearance is more important and loss of features may be compromised, for example, for reproduction operations like printing, w_1 can be assigned with a higher value. However, their sum must be equal to unity. Here, considering more general requirement, both visual appearance and feature retention have been given equal importance, i.e. $w_1 = w_2 = 0.5$.

In Equation [1], the magnitude function M can be calculated as the sum of the differences between processed FFT spectrum of original and enhanced image. It is important to note here that the expectation is towards expansion the magnitude function M not the contraction of the FFT spectrum. In the case of contraction the sum of the processed difference spectra becomes negative where the sum calculated from the binary difference image may be magnitude wise higher but with a negative difference value. This is not the desired case hence even if the value is higher this needs to have a measure of retreatment so that they are not favored over the case where a smaller positive value gets lower merit. To facilitate such cases the logarithmic value of sum is taken. Logarithmic transform can help in two ways: the range of the magnitude is reduced which gives ease of interpretation and also the contraction cases result in an imaginary value. In such cases the real value is divided by the imaginary value to get the final M value. The calculation of M value may be expressed as Equation [2].

$$M = \log(\sum D) \text{ where } D = HE_{FFT} - I_{FFT} \quad [2]$$

if $Im(M) \neq 0 : M = Re(M)/Im(M)$

where HE_{FFT} and I_{FFT} indicates the binary FFT spectra of histogram equalized image and original image, respectively. In Equation [2], Re and Im correspond to real and imaginary parts, respectively.

The shape parameter S in Equation [1] can be calculated from the projection plots shown in Figures 1 and 2 using the pair-wise Euclidian distance between the observations. Lower distance between observations interprets better adherence. The reciprocal combination of pair-wise distance in horizontal and vertical projections is considered in this work as shown in Equation [3]. The reason of taking reciprocal is to bring both S and M into same interpretability, i.e. for both of those parameters higher values indicate better results.

$$S = \frac{1}{pair_dist(I_{hor}, HE_{hor}) \cdot pair_dist(I_{ver}, HE_{ver})} \quad [3]$$

where, I_{hor} and HE_{hor} indicate the horizontal projections of original image and histogram equalized image, respectively. Similarly, I_{ver} and HE_{ver} represents the vertical projections. The higher value of M and S will cause a higher fitness value of φ which is considered as better fitness while performing the optimization.

2.2 Bacteria colony optimization

In BCO the bacterial behavior is mimicked. Like many other agent based search algorithms BCO also follows the dynamics of bacterial foraging to find an optimum solution of complex problem. Bacteria generally gather to the high nutrient areas by propelling themselves through rotation of the flagella maintaining an activity called chemotaxis (Chen, et al., 2014). The flagella rotate counter clockwise for forward movement; it is called that the organism “swims” or “runs”. When the flagella rotate clockwise, it causes the bacterium to “tumble” itself randomly and then it starts to swim again in a new direction. These *swim* and *tumble* activities help the bacterium for searching nutrients in random directions. Swimming and tumbling occurs more frequently for approaching a nutrient gradient by bacterium and to move away from some food for searching more foods. Bacterial chemotaxis is a complex combination of swimming and tumbling for placing the bacteria to a higher concentration of nutrients. Schematically BCO can be represented as an algorithm in Figure 3. The different mechanisms of BCO are described in following sections.

2.2.1 Chemotaxis

Chemotaxis mechanism works on the principle of *tumble* and *run* process. The movement of the i^{th} bacterium for every step of chemotactic process is expressed as Equation [4] (Niu, et al. 2013) considering $\theta^i(j, k, l)$

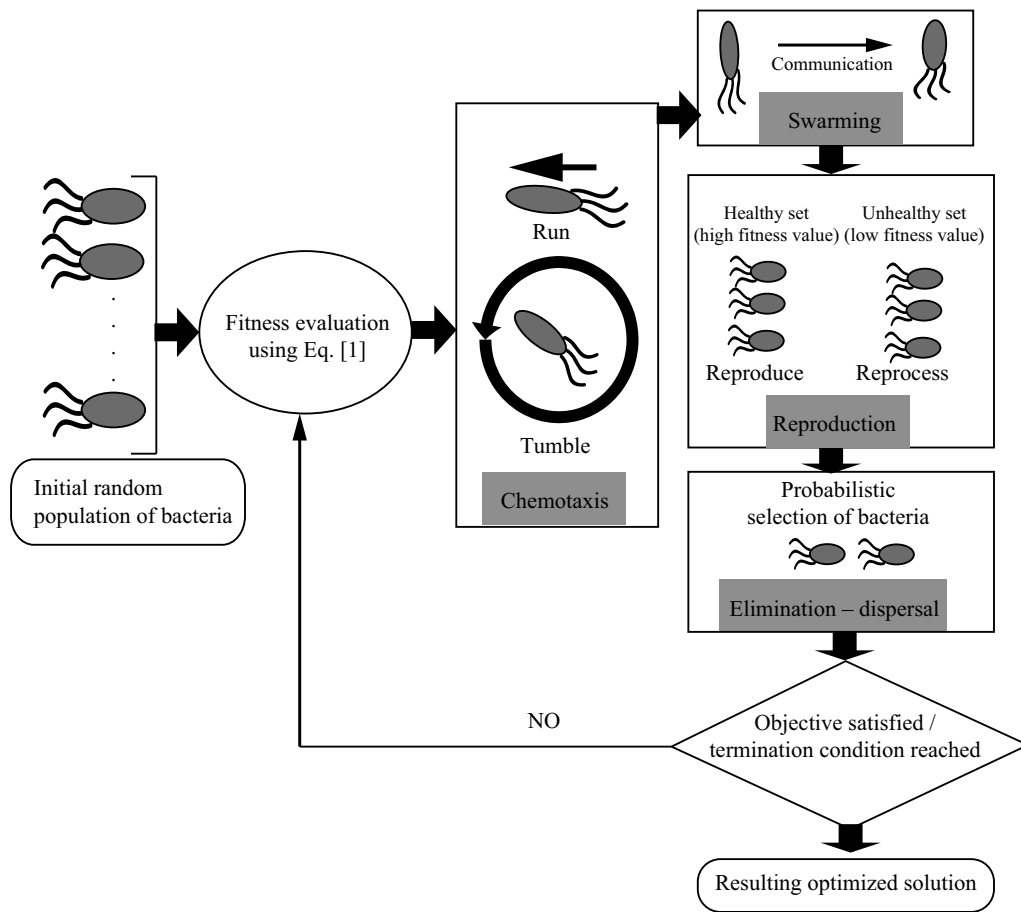


Figure 3: Schematic representation of BCO algorithm

denotes the position of i^{th} bacterium at j^{th} chemotactic, k^{th} reproductive, and l^{th} elimination-dispersal step. Further, $R(i)$ represents the step size of the chemotaxis for this bacterium at the time of every run or tumble (run-length unit).

$$\theta^i(j + 1, k, l) = \theta^i(j, k, l) + R(i) \frac{\Delta(i)}{\sqrt{\Delta^T(i) \cdot \Delta(i)}} \quad [4]$$

where $\Delta(i)$ is the j^{th} chemotactic step direction vector. At the time of run movement, $\Delta(i)$ is maintained the same with the last chemotactic step; otherwise, $\Delta(i)$ is a random vector whose elements are in the range of $[-1,1]$. Finally for each bacterium, a step fitness denoted by $J(i, j, k, l)$ is evaluated from the activity of run or tumble taken at each step of the chemotaxis process.

2.2.2 Swarming

Swarming mechanism as expressed in Equation [5] (Niu, et al., 2013) represents the the cell-to-cell communication process as each bacterium is capable of actuating, sensing, and decision-making mechanism. During the time of bacterium movement, it releases attractant

to provide indication of other bacteria to swarm that direction. In the meantime, every bacterium releases repellent to inform other bacteria to maintain a safe distance from it.

$$J_{cc}(\theta, P(j, k, l)) = \sum_{i=1}^{S_b} J_{cc}^i(\theta, \theta^i(j, k, l))$$

$$= \sum_{i=1}^{S_b} \left[-d_{attract} \exp \left(-w_{attract} \sum_{m=1}^{P_b} (\theta_m - \theta_m^i)^i \right) \right] \quad [5]$$

$$+ \sum_{i=1}^{S_b} \left[-h_{repellent} \exp \left(-w_{repellent} \sum_{m=1}^{P_b} (\theta_m - \theta_m^i)^2 \right) \right]$$

where, $J_{cc}(\theta, P(j, k, l))$ is the fitness function value with the addition of the actual fitness function for minimizing a presented time varying fitness function. The total bacteria number is denoted by S_b .

The number of parameters present in each bacterium to be optimized is denoted by P_b ; $w_{attract}$, $w_{repellent}$, $d_{attract}$ and $h_{repellent}$ are various optimization coefficients.

2.2.3 Reproduction

The reproduction mechanism maintains the good individual bacteria and eliminates bad ones based on the health condition of every bacterium. This is calculated by the sum of the step fitness during its life,

$$\text{i.e., } \sum_{j=1}^{N_c} J(i, j, k, l),$$

where N_c denotes the maximum number of steps in a chemotaxis process (Niu, et al., 2013). The fitness values of all bacteria are sorted in the order of good health status. In the production step, only the first half of total bacteria stay and second half of bacteria with poor health status are deleted. Each bacterium from the first half divides into two identical ones which are placed then in the same location to maintain the number of bacteria constant.

2.2.4 Elimination and dispersal

According to the change of environmental conditions, bacteria are greatly affected. In BCO model, when a certain number of reproduction processes happens, the dispersion processes occur. According to a fixed probability P_{ed} , some bacteria are to be selected for elimination and shift to another location within the environment. Simultaneously, the new ones are generated according to reproduction process.

2.3 Implementation of bacteria colony optimization in histogram equalization

This section presents the process of HE using BCO (HEBCO). To apply the BCO for color images first the image was converted to HSV color space from its native RGB color space. The V channel was separated and subjected to the BCO algorithm. The BCO was initiated with predefined numbers of solutions which are some randomly generated intensity levels in our case. Since the V channel values can vary from 0–255 in an 8-bit system the dimension of the space here is 256. The optimization has been performed towards maximization of the fitness function as described in section 2.1. Like all the meta-heuristics, BCO also is iterative in nature and the best solution at the end of each iteration is found using an objective function. This objective function can be kept same as fitness function but in our case an IQA based objective function has been used.

Considering our goal of retaining the original image features in enhanced image, brightness preservation is an important criteria and it can be measured using absolute mean brightness error (AMBE) (Raju, Dwarakish and Reddy, 2013) metric as expressed in Equation [6]. Apart from brightness, the optimization is driven to maintain information fidelity in terms

of image entropy (Wang and Ye, 2005) calculated as given in Equation [7] and structural similarity using structural similarity index measure (SSIM) (Horé and Ziou, 2010) calculated according to Equation [8].

$$AMBE(X, Y) = |E(X) - E(Y)| \quad [6]$$

where, X and Y denote the input image and output image, respectively, and E denotes the expected value of statistical mean. Lower AMBE indicates the better brightness preservation of the image.

$$ENT[P] = - \sum_k P_k \log(P_k) \quad [7]$$

where ENT denotes entropy and P is indicating the probability, which is the difference between two adjacent pixels of the image. Higher values of entropy indicate the richness of the image quality.

$$SSIM(X, Y) = l(X, Y) \cdot c(X, Y) \cdot s(X, Y) \quad [8]$$

where X and Y denote the input image and output image, respectively, and l denotes the luminance comparison of input and output image. Similarly, c and s denote the contrast and structural comparison between input and output image, respectively. Higher value of SSIM indicates better quality of output images. Using the above three parameters the objective function has been formulated as Equation [9]. The pseudo code of the HEBCO is presented in Table 1.

$$\emptyset = \frac{(ENT(I) + SSIM(I, O))}{AMBE(I, O)} \quad [9]$$

where I and O represent the enhanced image and original image, respectively. The \emptyset has been formulated such a way that a higher value will indicate better result. Thus, the objective of optimization is towards maximization. The algorithm performs iteratively with predefined termination condition. In this case the condition is either exhausting specified number of iterations or not showing any improvement for 10 consecutive iterations.

Table 1: Pseudo code of HEBCO

```

/* Assignment */
Load the low contrast image as input.
Initialize BCO parameters
  d: Dimension of the search space
  B: Number of bacteria
  Sc: Chemotaxis steps
  Ss: Swim steps
  Sre: Reproductive steps
  Sed: Elimination and dispersal steps
  Ped: Probability of elimination
  Rt: The run-length units during each run or tumble
Initialize random solutions based on input image histogram.

```

/* Update */

Compute the fitness value of these solutions using Equation [1].

Compute a new solution with improved fitness using the process of chemotaxis loop.

Store the fitness value for finding better value by run process of BCO operation.

Generate a number of random solutions based on the number of eliminating solutions by fitness value according to the process of reproduction loop and elimination–dispersal loop.

Compute the fitness of these randomly generated solutions.

Check the fitness value, whether it is better with respect to the previously selected solutions.

Store the fitness value and select the most-fit solutions.

Find the objective function value resulting from the most-fit solution at each iteration using Equation [9].

Terminate the loop while meeting the termination condition.

/* Enhancement */

Reconstruct the V channel with the best solution found using BCO.

Replace the original image V channel with the optimized V channel.

Convert the image back to RGB color space for visual presentation.

3. Results

The presented HEBCO was tested with different images from standard databases, namely, SIPI, TID2008 (TID), and LIVE (SIPI, n.d.; Ponomarenko, et al., 2009; Ghadiyaram and Bovik, 2015). The algorithms have been implemented using Matlab® software in Windows personal computer. All the images have been reproduced at 300 dpi resolution.

The experimental setup for the tunable parameters was arrived at using training–validation–testing method. To decide the parameter values a set of 100 images from different datasets was maintained. Images with all possible variations from the database were included in this dataset ranging from grayscale to color, different degree of low contrast and different illumination distortions. This dataset was partitioned in train, validation and test set with 60:20:20 proportions. The tunable parameters were varied within the ranges of values as commonly practiced in BCO. The combination that gave best fitness was considered for validation set. In validation set even lower range of variation with a smaller step size was used to finalize the parameter values. The final values arrived with the validation set are presented in Table 2 and were used for testing set as well as results presented in this paper.

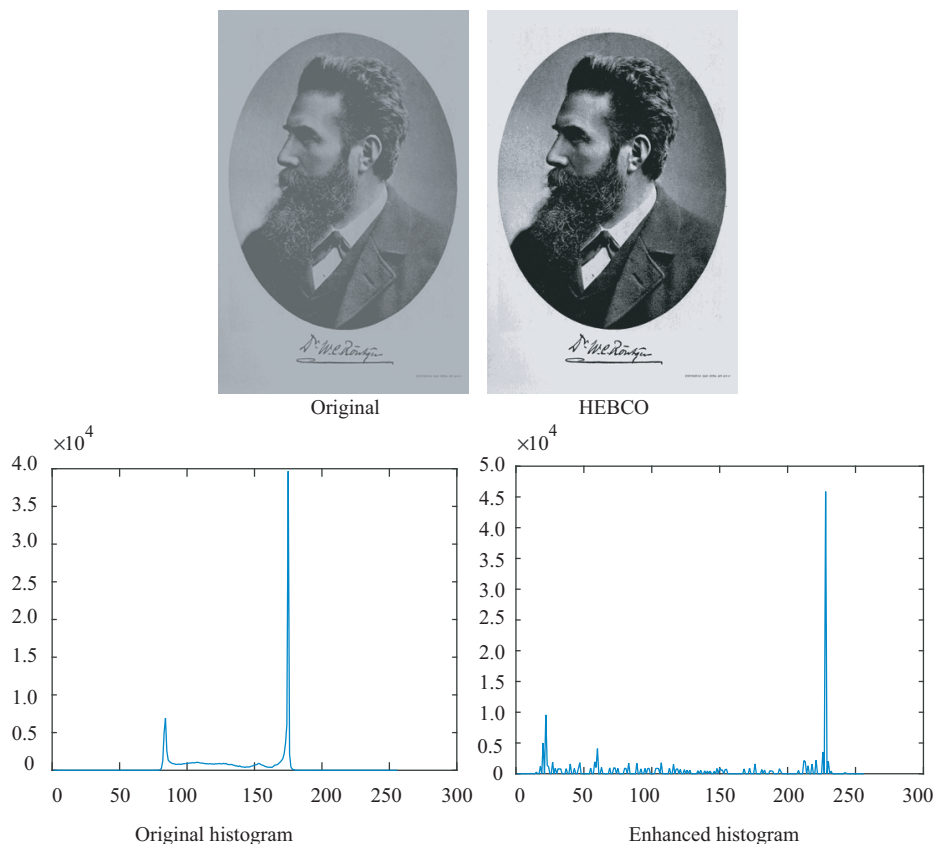


Figure 4: Result of HEBCO technique for grayscale test image 'Man'

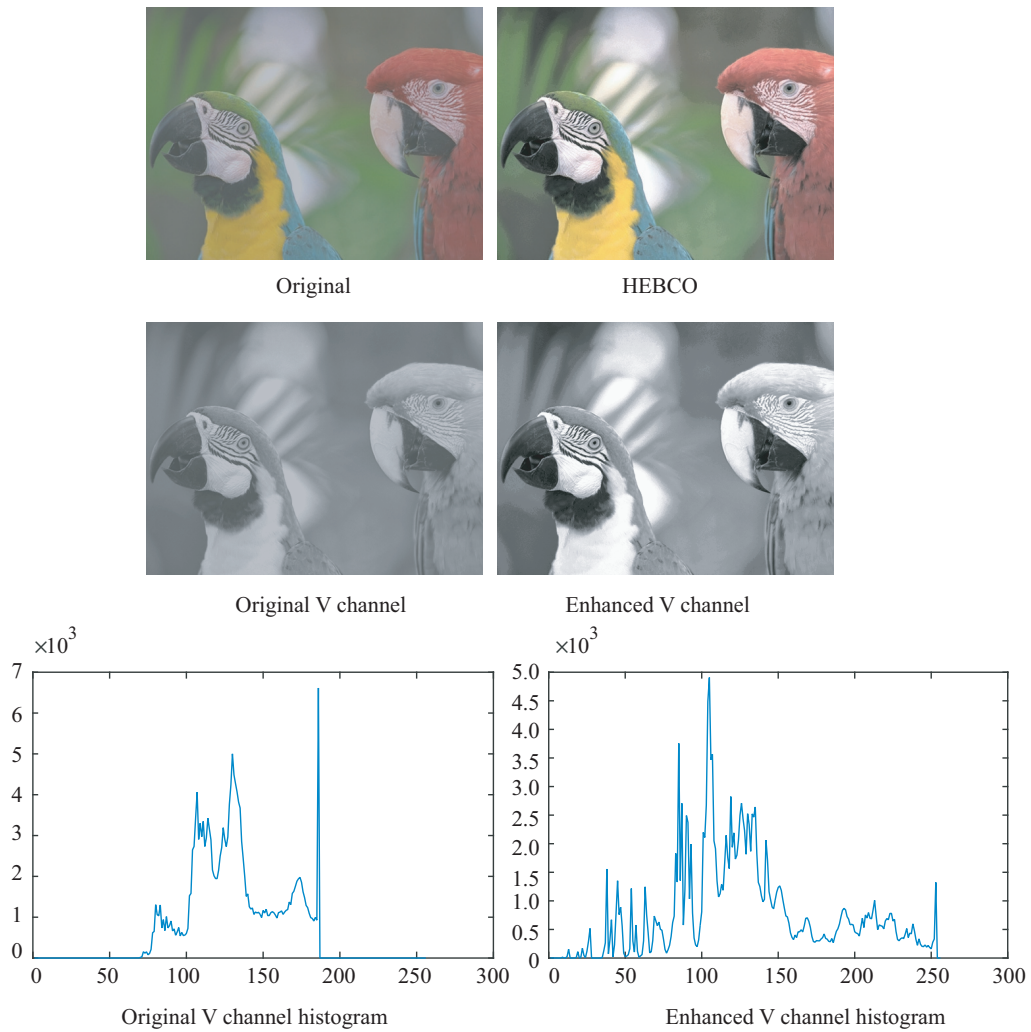


Figure 5: Result of HEBCO technique for color test image ‘Bird’

Table 2: HEBCO parameter setting

d : Dimension of the search space	256
B : Number of bacteria	10
S_c : Chemotaxis steps	50
S_{re} : Reproductive steps	8
S_{ed} : Elimination and dispersal steps	5
P_{ed} : Probability of elimination	0.20
R_l : The run-length units during each run/tumble	0.1

The results of HEBCO have been presented with two examples in Figures 4 and 5 for grayscale and color images, respectively. In both the cases histograms are included for understanding the contrast enhancement.

In Figure 4 it can be seen that HEBCO can retain the original image characteristics. The background grayness which many of the conventional as well as later developed HE techniques could not retain (as shown in Figure 1) has been well retained by HEBCO. There are

no visible false contouring and artificial patches in the HEBCO result. Also the balance between the dark and highlight regions is visually pleasant. The result also does not show occurrences of over- or under-exposure since the result is not inclined to white or black regions of intensity range. The corresponding histograms also convey the balanced enhancement. Another important observation in terms of histogram is retaining the peak information of original histogram.

Figure 5 shows the result with one of the color test images. In this case the corresponding V channels have also been included. It can be clearly seen that the contrast in the V channel has been significantly improved. That in turn results in improved visual appearance of enhanced image. The histograms of V channel convey that the HEBCO can result in stretching the original narrow histogram across the available intensity levels while maintaining the characteristics of original image histogram.

4. Discussions

This section presents the comparative assessment of HEBCO with the established reported techniques. Among different techniques, 10 have been considered in this paper. These techniques cover different paradigms of algorithms in both spatial and frequency domains.

Figure 6 shows the performance of different algorithms on a grayscale image. The enhancement capability of HEBCO is visibly better than the other techniques under consideration. The result of CLAHE is having higher sharpness while AGCWD provides higher smoothness and whiteness. Similarly, the AMSR and LLIEA results are under- and over-enhanced, respectively. The CI techniques based algorithms, except ABCHE, result in comparatively balanced enhancement.

Figures 7 to 9 are the examples of results with different algorithms on color test images. The visual appearances of HEBCO results clearly show the attainment of contrast improvement while retaining the original image characteristics in case of color images. In Figure 7 most of the conventional techniques fail to retain the color information of input image which is visible in case of leaves that are appearing almost black in the output

of most of the conventional techniques. While AMSR and DFHE results are showing the biasness of the level distribution towards dark intensities which causes under-enhancement, LLIEA and ABCHE show tendency of increasing overall whiteness which causes over-enhancement. The results of CLAHE, AGCWD, GAHE and HEBCO are more appealing but HEBCO shows better visual balance as tendency to increase whiteness and darkness can be seen in the results of AGCWD and GAHE, respectively. The observations drawn with Figure 7 remain true for Figure 8 as well but CLAHE shows a higher tendency of over-sharpening the image. In Figure 9 apart from previous observations one more important observation is the retention ability of patterns, particularly gradient. It can be seen that most of the techniques fail to retain the blue gradient pattern. In most of the cases the gradient is flattened down while HEBCO can retain that visibly.

Figures 10 and 11 are results from LIVE database images which consist of images captured by mobile devices in different lighting conditions and enhancement of contrast is challenging. It can be seen that all the CI algorithms perform well in this type of images. Conventional techniques like GHE, BBHE and DSIHE performs poorly in these cases and they tend to flatten down the images in either side of the intensity scale



Figure 6: Results of different HE techniques for grayscale test image 'Cat'; (top row from left to right) original (input) image, GHE, BBHE, DSIHE, (middle row left to right) CLAHE, AGCWD, AMSR, LLIEA, (bottom row left to right) DFHE, GAHE, ABCHE, and presented HEBCO

which causes patches, loss of details and poor visual appearance. The CLAHE, AGCWD, AMSR and LLIEA techniques can overcome those limitations but they also show under- or over-enhancement that can be seen as whitish appearance of LLIEA result or loss of desired brightness in AMSR result. The HEBCO result is comparatively better in terms of appearance since

there are no such patches or false contouring and also better retention of details as can be seen in the ‘denim’ hanging in the picture. In the results of conventional techniques the ‘denim’ pattern is almost turned into dark patches while CLAHE and HEBCO gives a much natural appearance along with contrast enhancement in the resulting image.



Figure 7: Results of different HE techniques for color test image ‘Flower’; (top row from left to right) original (input) image, GHE, BBHE, DSIHE, (middle row left to right) CLAHE, AGCWD, AMSR, LLIEA, (bottom row left to right) DFHE, GAHE, ABCHE, and presented HEBCO

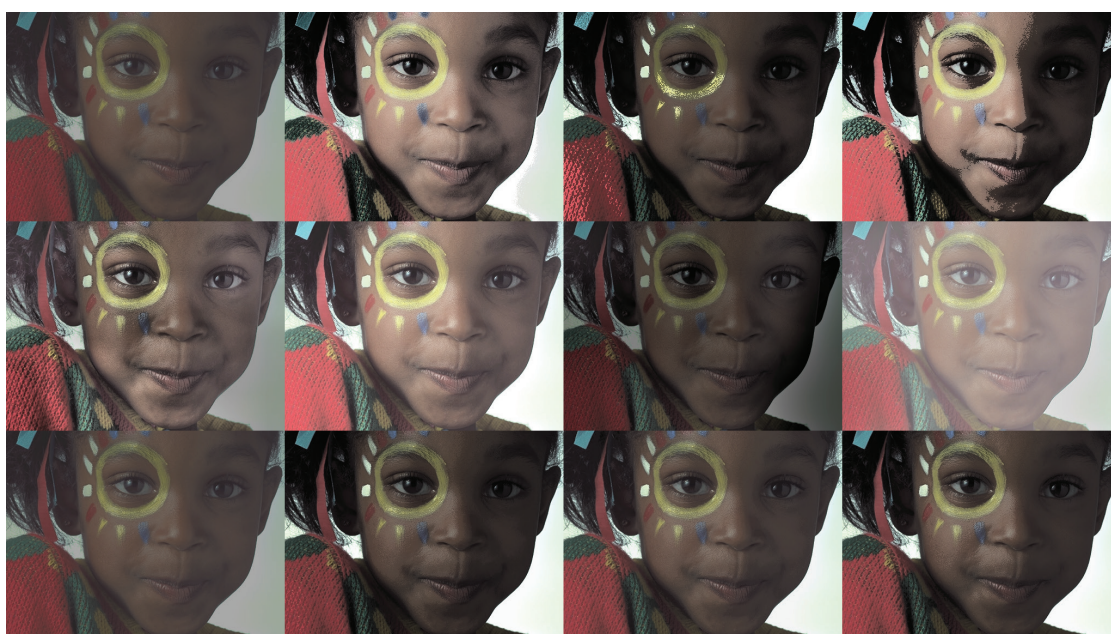


Figure 8: Results of different HE techniques for color test image ‘Girl’; (top row from left to right) original (input) image, GHE, BBHE, DSIHE, (middle row left to right) CLAHE, AGCWD, AMSR, LLIEA, (bottom row left to right) DFHE, GAHE, ABCHE, and presented HEBCO

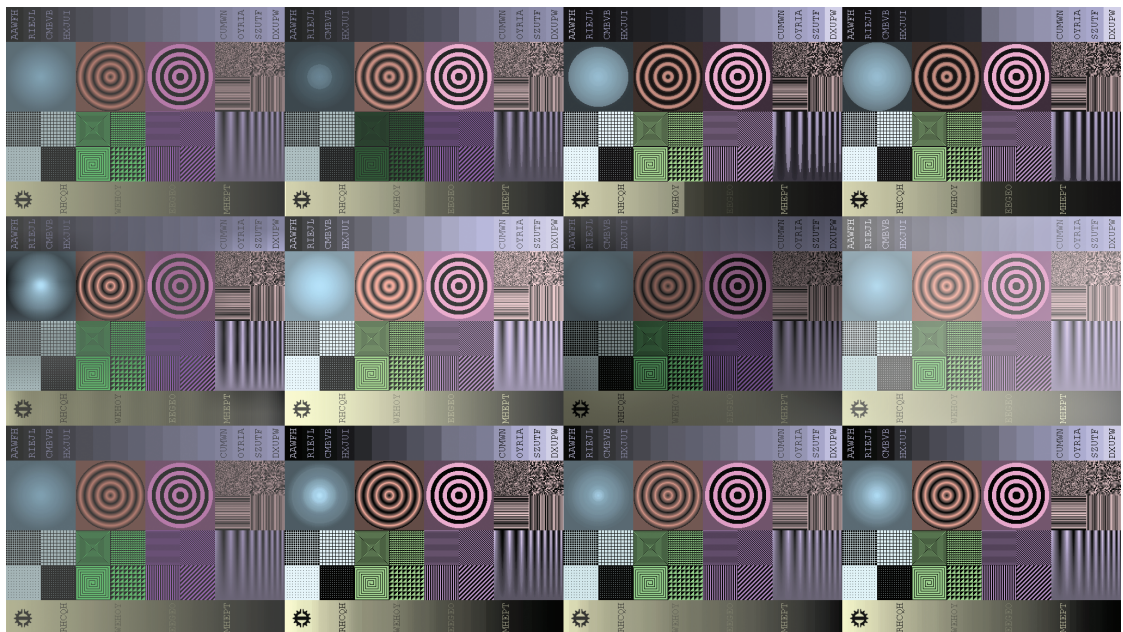


Figure 9: Results of different HE techniques for color test image 'Pattern'; (top row from left to right) original (input) image, GHE, BBHE, DSIHE, (middle row left to right) CLAHE, AGCWD, AMSR, LLIEA, (bottom row left to right) DFHE, GAHE, ABCHE, and presented HEBCO



Figure 10: Results of different HE techniques for color test image from LIVE database; (top row from left to right) original (input) image, GHE, BBHE, DSIHE, (middle row left to right) CLAHE, AGCWD, AMSR, LLIEA, (bottom row left to right) DFHE, GAHE, ABCHE, and presented HEBCO

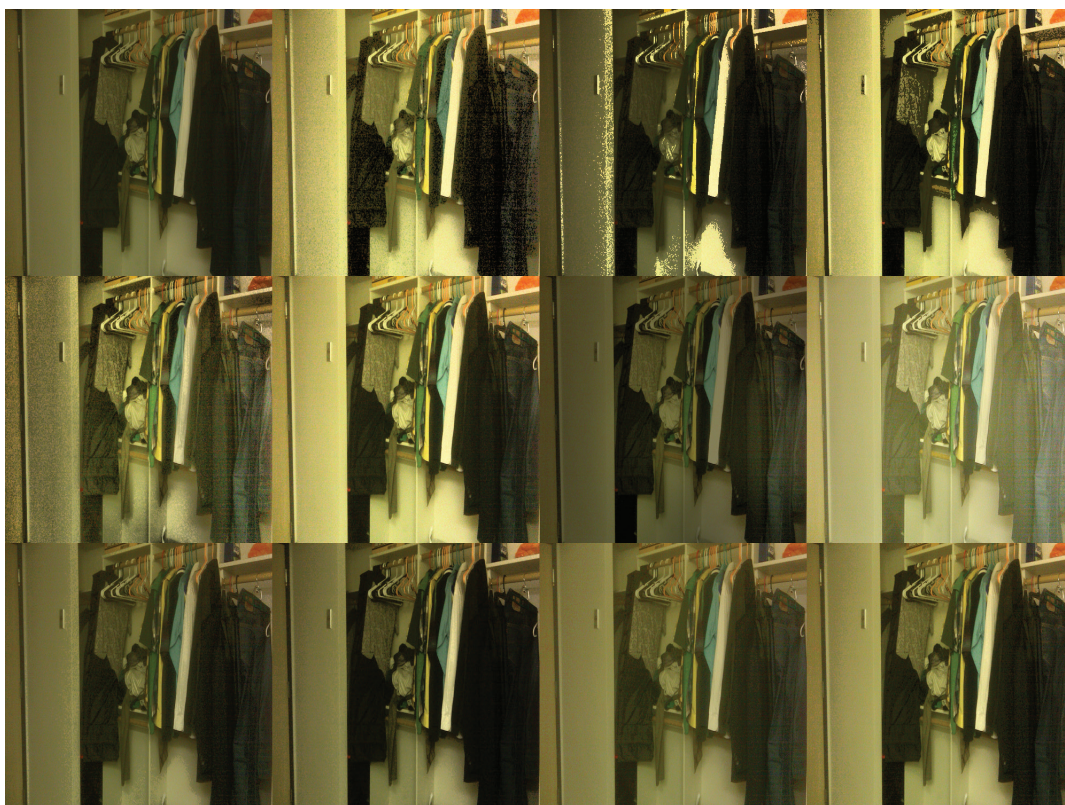


Figure 11: Results of different HE techniques for color test image from LIVE database; (top row from left to right) original (input) image, GHE, BBHE, DSIHE, (middle row left to right) CLAHE, AGCWD, AMSR, LLIEA, (bottom row left to right) DFHE, GAHE, ABCHE, and presented HEBCO

On an overall visual assessment it can be stated that CLAHE, AGCWD, AMSR and LLIEA techniques are superior to conventional HE techniques. But they also show limitations like over- or under-enhancement, unwanted sharpness or smoothness and loss of original image features. Such limitations can result in loss of naturalness in the enhanced images. The CI techniques show promising improvement on those parameters and HEBCO shows considerable potential by visually equivalent or better results in all the cases. The limitations can be further studied using the magnitude and shape parameters presented in this paper. A comparative presentation of the differential Fourier spectrum and projection plots with different techniques is presented in Figures 12 and 13. In those figures the algorithms have been classified into three groups for better visualization. The green lines present the algorithms that are based on histogram segmentation and statistical partitioning which include GHE, BBHE, DSIHE, CLAHE and AGCWD. The magenta lines plot model based algorithms that include AMSR and LLIEA. The blue lines indicate the CI based algorithms. To distinguish the original and the result of presented HEBCO, they have been represented using red and black color, respectively.

Figures 12 and 13 reveal interesting facts about the enhancement by different techniques. The DSIHE shows considerable magnitude expansion in spectra but like other histogram partitioning approaches it does not conform much to the original image brightness distribution pattern which can be seen in the green projections plots. The CLAHE and AGCWD are showing much better expansion in FFT spectra and conformity to the plots of original image including an escalation in the y -axis of the projection plots. The CLAHE and AGCWD plots are the plots coming in the region where the black, blue and magenta plots are coming. On the other hand AMSR and LLIEA results are showing good adherence to the original image features in the projection plots as the magenta plots are closely following the plot of original image and a reasonable escalation in the y -axis. All the CI based techniques show their potential to enhance the image contrast but HEBCO result shows visible adherence to the original image characteristics while improving the contrast. The difference FFT spectra are closely matching to the shape of original image spectra while in terms of projection plot it is neither going very high in the y -axis of the projection plots nor losing similarity to the original image plot. This confirms the potential

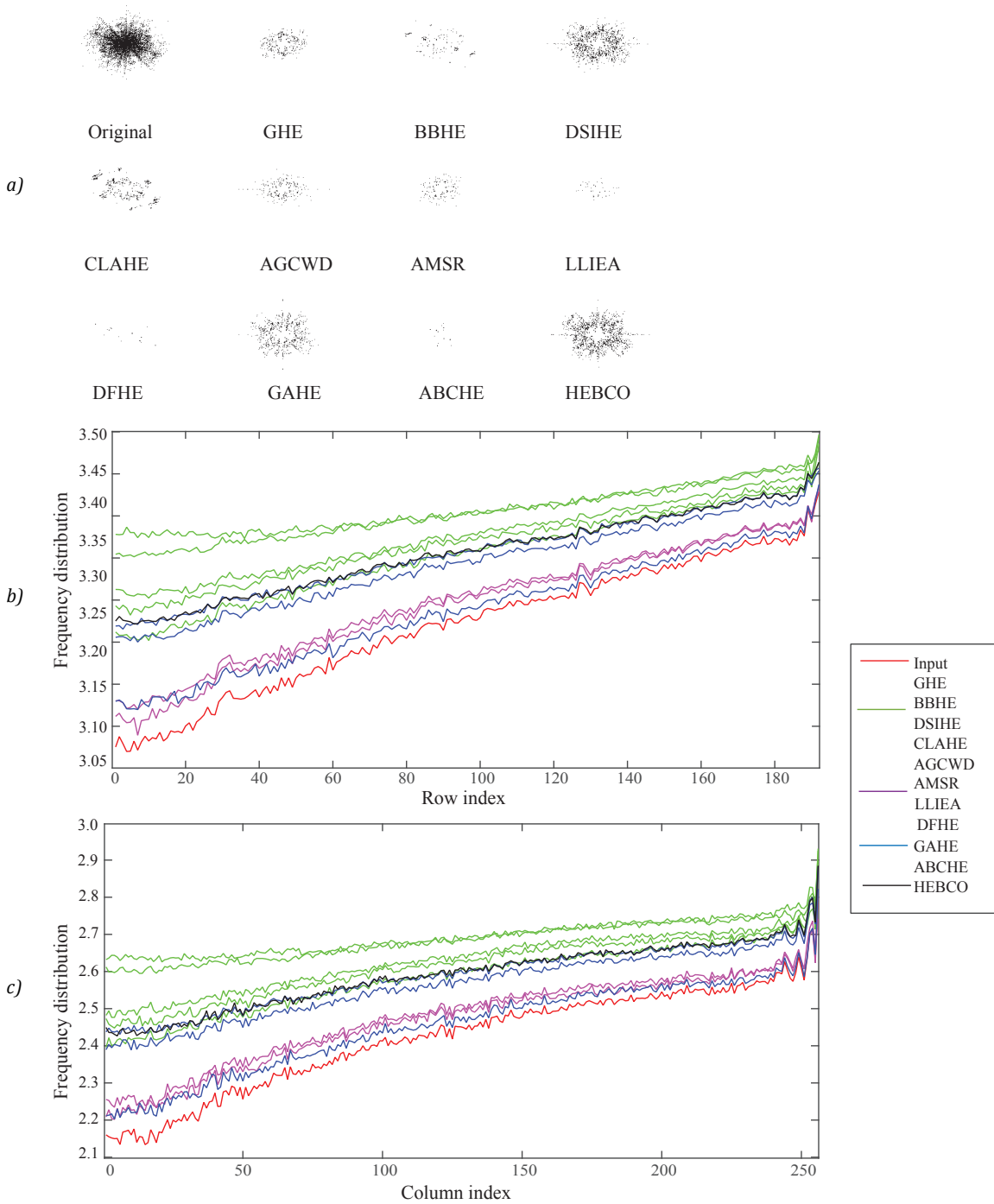


Figure 12: Adherence to the original image characteristics analysis for test image 'Girl' (a) differential magnitude spectra, (b) horizontal projection plots, and (c) vertical projection plots

of HEBCO to avoid over- or under-enhancements. The conventional GHE and BBHE in all the cases majorly increase the contrast keeping fewer adherences to the original image features as can be seen by the green plots appearing at the top, far away from the plot of original image, in the projection plots.

The visual analyses have further been extended to the objective evaluations against the IQA metrics. Among many IQA metrics in this work two FR and two NR metrics have been considered in this presentation. The FR (Larson and Chandler, 2010) metrics include the ground truth images for evaluation and in this paper

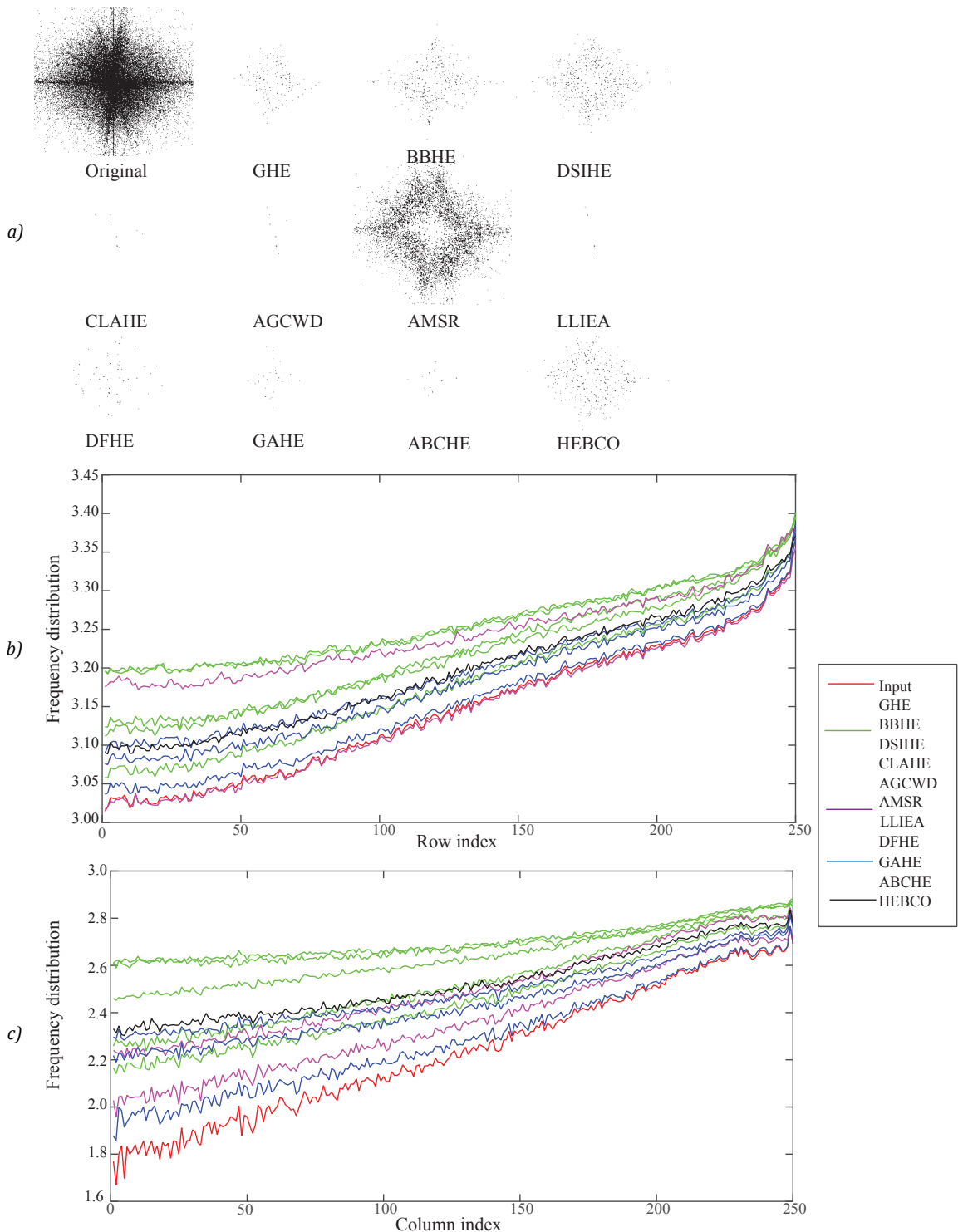


Figure 13: Adherence to the original image characteristics analysis for test image from LIVE database shown in Figure 11; (a) differential magnitude spectra, (b) horizontal projection plots, and (c) vertical projection plots semilogx scale

patch-based contrast quality index (PCQI) (Wang, et al., 2015) and feature similarity index measure (FSIM) (Zhang, et al., 2011) metrics have been used. The PCQI can be a good indicator of contrast enhancement and

local distortion measure while FSIM can be good measure for feature retention in enhanced images. Despite being FR metrics, both PCQI and FSIM consider the human perceptual characteristics in evaluation. The NR

(Mittal, Soundararajan and Bovik, 2012a) metrics do not include the ground truth for evaluation but they measure overall naturalness in enhanced images and a higher degree of naturalness is desired to avoid over- and under-enhancement causing artificial appearance in the enhanced images. The BRISQUE (Mittal, Moorthy and Bovik, 2011) and NIQE (Mittal, Soundararajan and Bovik, 2012b) are considered here as NR metrics for this purpose.

The PCQI is a metric popular in contrast enhancement evaluation. Instead of global enhancement it performs local patch based evaluation. It is based on signal decomposition philosophy and mathematically represented by variations in signal strength and signal structure as presented in Equation [10]. The outcome of PCQI can be interpreted in two ways; the PCQI map which is a graphical representation of contrast enhancement and a mean PCQI value which indicates improvement by higher values. The white and bright patches show improvement while the dark and black patches show degradation. For easier understanding PCQI map is often binarized setting patches with $PCQI < 1$ to 0 and rest to 1. There may be areas in output image which appear with high contrast and brightness but if that comes as a black patch in the binarized PCQI then it is showing under- or over-enhancement which results in distortions. Therefore, binarized PCQI map with lesser black patches indicates better enhancement. Similarly, calculating the mean value of patches as shown in Equation [10] the mean PCQI value is obtained which also has higher values for better enhancement. The binarized PCQI maps for two test images are shown in Figures 14 and 15.

$$PCQI(x, y) = q_i(x, y) \cdot q_c(x, y) \cdot q_s(x, y) \quad [10]$$

where, x and y are co-located patches in the reference image X and enhanced image Y , respectively, $q_i(x, y)$ is the difference estimation in terms of mean intensity, $q_c(x, y)$ is the parameter that corresponds to contrast change and for a better contrast image $q_c(x, y) > 1$. Finally, $q_s(x, y)$ corresponds to the structural distortion. If there are total N patches then mean PCQI is calculated as Equation [11].

$$PCQI(X, Y) = \frac{1}{N} \sum_{j=1}^N PCQI(x_j, y_j) \quad [11]$$

The PCQI maps shown in Figures 14 and 15 portray the potential of different algorithms towards enhancement and causing degradation in the resulting enhanced images. Figure 14 shows that BBHE, DSIHE and Ying et al. resulting considerable amount of distortion which we observed in terms of under-enhancement in our FFT spectrum and projection plot based analysis.

The distortions obtained in GHE, AGCWD and AMSR are comparable but they show higher degree of distortion than the DFHE, GAHE and ABCHE. The results of CLAHE and presented HEBCO are showing least degree of distortions in comparison to all other techniques. The results of PCQI in Figure 15 show that GHE produced higher degree of distortion like BBHE and DSIHE while DFHE produced lesser distortions. However, results of CLAHE and HEBCO are consistently maintaining visibly lesser amount of distortion. The AMSR and AGCWD show lesser distortion than LLIEA and all the CI techniques performed better. Experimental results have shown that CI algorithms work comparatively better in case of uneven illumination for the images from LIVE database.

The FSIM is a metric which can represent the feature similarity between reference/original and enhanced image. This can be calculated as Equation [12]. The higher values of FSIM indicate better results, i.e. better retention of original image features. It is based on phase congruency (PC) and gradient magnitude (GM) feature maps extracted between reference and enhanced images. The human perceptual nature is included in this metric in terms of phase congruent structure to which human eyes are sensitive. Feature retention can be important for computer vision applications of HE for example medical imaging.

$$FSIM = \frac{\sum_{x \in \Omega} S_L(x) \cdot PC_m(x)}{\sum_{x \in \Omega} PC_m(x)} \quad [12]$$

where Ω represents entire image in spatial domain, the similarity is measured between two images $f_1(x)$ and $f_2(x)$, $S_i(x)$ is the similarity calculated using PC and GM measures with assigned relative importance and $PC_m(x) = \max(PC_1(x), PC_2(x))$.

The BRISQUE is a convenient measure towards naturalness in the image. One advantage of BRISQUE is it does not include any frequency domain transforms like discrete cosine transform or wavelet transform as many other NR IQA techniques. This makes the metric simpler and faster. This metric is based on a generalized Gaussian distribution (GGD) fit of the mean subtracted contrast normalized (MSCN) coefficients applied on the locally normalized luminance of the input image. The scoring mechanism in the metric is based on a regression model where the singular value decomposition features have been subjected to support vector machine regressor (SVR). The lower scores indicate higher degree of naturalness in the image.

The NIQE is a feature based metric where a multivariate Gaussian (MVG) fit of the natural scene statistics (NSS) features are extracted from the test image



Figure 14: The binarized PCQI map of test image 'Girl'; (top row left to right) GHE, BBHE, DSIHE, CLAHE, (middle row left to right) AGCWD, AMSR, LLIEA, DFHE, (bottom row left to right) GAHE, ABCHE and HEBCO

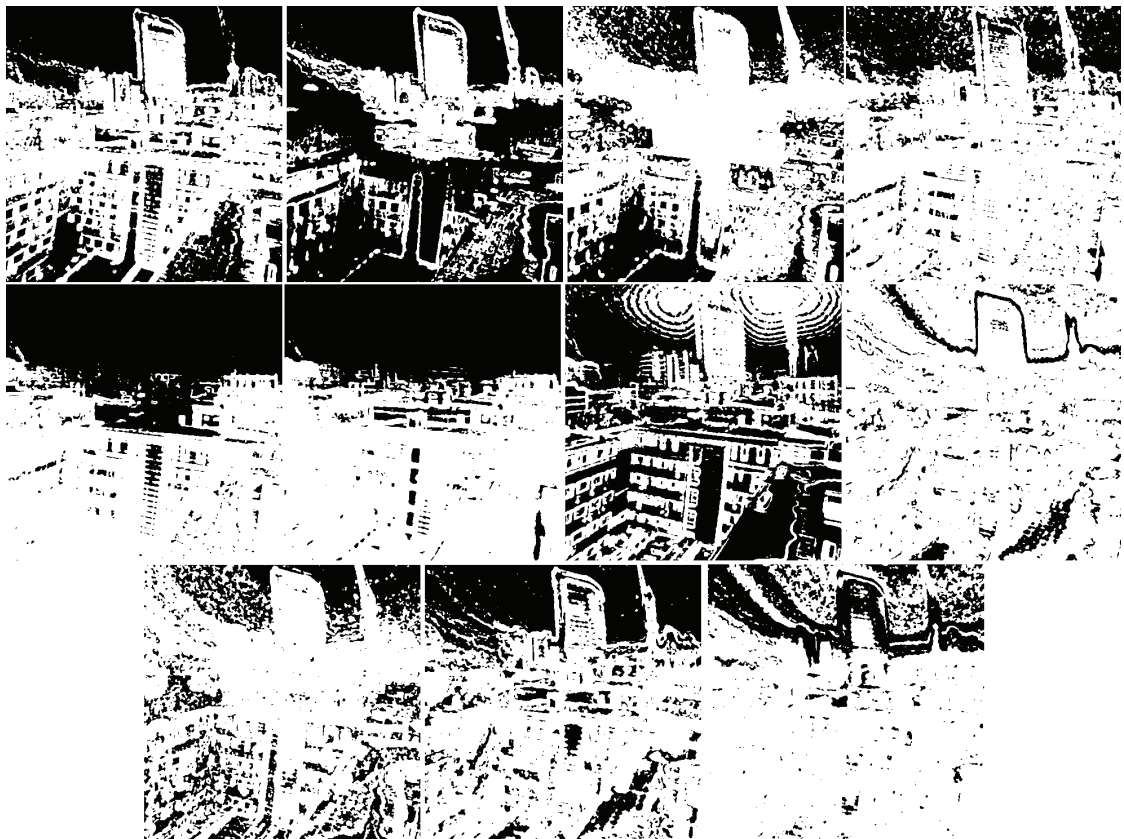


Figure 15: The binarized PCQI map of test image from LIVE database shown in Figure 10; (top row left to right) GHE, BBHE, DSIHE, CLAHE, (middle row left to right) AGCWD, AMSR, LLIEA, DFHE, (bottom row left to right) GAHE, ABCHE and HEBCO

and the quality is assessed as distance between this MVG and a defined MVG of the quality image features extracted from a numbers of natural images. A lower distance as indicated by lower metric value D indicates better result. It is expressed as Equation [13].

$$D(v_1, v_2, \Sigma_1, \Sigma_2) : \\ = \sqrt{\left((v_1 - v_2)^T \cdot \left(\frac{\Sigma_1 + \Sigma_2}{2} \right)^{-1} \cdot (v_1 - v_2) \right)} \quad [13]$$

where v and Σ are mean and covariance matrix, respectively, and T denotes the transpose operation. The natural MVG model and distorted MVG models are indexed as 1 and 2, respectively.

The mean evaluation results against these four metrics for individual databases are consolidated in Table 3 where the top two performers in respect to each metrics and databases have been highlighted. Table 3 shows that in terms of mean PCQI CLAHE performs best among all other techniques, HEBCO is next to CLAHE. But, in case of LIVE database, LLIEA performs better than CLAHE. The conventional techniques, particularly GHE, are also competitively performing for SIPI and TID databases but performance becomes visibly poor in case of LIVE database. This conveys the limitation of conventional techniques for unevenly illuminated images.

The significant downfall in the performance of DFHE is also visible while the CI techniques based HE perform consistently well against all the databases under consideration. Since, PCQI is a measure of patch-wise over- and under-enhancement or distortions in the obtained

image. It can be concluded from Table 3 that HEBCO can result in better contrast enhancement and lesser distortion in variety of images.

The FSIM is an indicator that can show the retention of original image features in resulting image. The LLIEA technique performs best across all the databases in this regard while HEBCO can perform well but could not perform as good as AMSR and DFHE in case of SIPI and TID databases, respectively. Although in case of LIVE database the performance is considerably better than most of the algorithms, which conveys the feature retention capability of HEBCO for unevenly illuminated images. In an overall judgment HEBCO performance is not poor as it can outperform many other techniques in terms of FSIM.

The BRISQUE and NIQE metrics convey the naturalness in resulting image which is very important and can be used to assess the ability of an algorithm to avoid artificial appearance caused due to inappropriate enhancements. In terms of those two metrics HEBCO shows its potential to retain naturalness in the resulting images avoiding under- and over-enhancement.

The conventional algorithms like GHE, BBHE and DSIHE along with some of the advanced algorithms like AMSR also cause loss of naturalness. LLIEA technique performs well against BRISQUE measure and AGCWD performs well in case of NIQE measure. Therefore, inference can be drawn that none of the techniques including HEBCO can perform best against all of the metrics but HEBCO has merits over many of the reported techniques in each aspect considered here. The HEBCO needs to improve its performance in terms of FSIM to secure position in top two best performers.

Table 3: Consolidated evaluation results against mean PCQI, FSIM, BRISQUE and NIQE

Techniques	mean PCQI			FSIM			BRISQUE			NIQE		
	SIPI	TID	LIVE	SIPI	TID	LIVE	SIPI	TID	LIVE	SIPI	TID	LIVE
GHE	1.018	1.156	0.466	0.702	0.608	0.622	33.8	19.16	84.18	6.68	3.6	19.64
BBHE	0.939	1.087	0.461	0.696	0.605	0.620	36.6	25.69	92.75	6.85	4.4	19.75
DSIHE	0.911	1.081	0.457	0.667	0.611	0.621	39.7	28.47	84.55	7.54	4.6	19.67
CLAHE	1.268	1.279	0.489	0.795	0.601	0.619	27.4	16.35	84.04	5.23	3.5	19.83
AGCWD	1.065	1.083	0.472	0.872	0.601	0.620	24.9	14.76	87.16	5.16	3.4	19.21
AMSR	0.977	0.999	0.878	0.928	0.927	0.300	29.7	14.57	94.79	20.20	19.4	22.40
LLIEA	0.999	0.999	0.999	0.929	0.924	0.997	21.9	11.61	86.72	19.90	19.1	19.26
DFHE	0.999	1.024	0.685	0.857	0.927	0.235	30.3	13.26	91.95	5.57	3.7	16.02
GAHE	1.022	1.105	0.973	0.881	0.599	0.978	28.2	14.68	20.37	5.34	3.5	16.17
ABCHE	0.944	1.096	0.907	0.885	0.879	0.976	28.5	8.92	17.63	5.68	3.5	16.33
HEBCO	1.083	1.164	0.974	0.904	0.883	0.978	23.6	11.40	18.02	4.97	3.4	15.23

5. Conclusions

The work has presented application of BCO towards contrast enhancement using HE methodology to obtain enhanced images while preserving the important characteristics of the original image. The frequency domain analysis of contrast enhancement has been used to formulate the fitness function and the optimization is performed in respect of different parameters like image brightness, signal/information fidelity and structural as well as feature information of the original image. The results have been presented visually and objective assessments have been drawn in comparison to the established HE techniques. The comparative analysis shows the competitive potential of HEBCO against the established techniques while overcoming different limitations of conventional HE approaches.

The work can further be extended to the application of other CI algorithms, tuning the fitness function for more robustness, BCO parameter optimization, a predictive model of the optimization framework where the input image can be enhanced based on a set of defined equalized histograms obtained by BCO, model based HE applications and inclusion of more optically derived measure of contrast for objective function formulation. The presented method has been explored considering image appearance in general which provides another important direction towards inclusion of prepress and press parameters in the objective function to obtain improved output quality of different prepress and printing systems. Finally, the paper has presented an important step towards application of BCO algorithms for image characteristics preserving contrast enhancement.

List of Abbreviations

ABC	artificial bee colony
AHE	adaptive histogram equalization
AMBE	absolute mean brightness error
AMSR	adaptive multi scale retinex
BBHE	brightness preserving bi-histogram equalization
BCO	bacteria colony optimization
CI	computational intelligence
CLAHE	contrast limited adaptive histogram equalization
<i>CPDF</i>	cumulative probability density function
DCE-MRI	dynamic contrast enhancement of magnetic resonance imaging
DFHE	dynamic fuzzy histogram equalization
DHE	dynamic histogram equalization
DSIHE	dual sub-image histogram equalization
EHS	exact histogram specification
<i>ENT</i>	entropy
FFT	fast Fourier transform
FLHS	fast local histogram specification
FR	full reference
FSIM	feature similarity index measure
GA	genetic algorithm
GC-CHE	gain-controllable clipped histogram equalization
GGD	generalized Gaussian distribution
GHE	global histogram equalization
GM	gradient magnitude
HE	histogram equalization
HE_{FFT}	binary FFT spectra of histogram equalized image
HSV	Hue, Saturation, Value
IBF	incomplete beta function
I_{FFT}	binary FFT spectra of original image
IQA	image quality assessment
LLIEA	low-light image enhancement algorithm
LTHM	logarithmic transform histogram matching
LTHS	logarithmic transform histogram shifting
LTHSG	logarithmic transform histogram shaping using Gaussian distributions
<i>M</i>	magnitude function
MSCN	mean subtracted contrast normalized coefficient
MSR	multi scale retinex
MVG	multivariate Gaussian
N_c	maximum number of step in a chemotaxis process
NOSHP	overlapped sub-blocks and local histogram projection
NR	no-reference
NSS	natural scene statistics
<i>P</i>	probability
P_b	bacterium parameter
PC	phase congruency
PCQI	patch-based contrast quality index
<i>PDF</i>	probability density function
RSECE	residual spatial entropy-based contrast enhancement
RSECDCT	residual spatial entropy-based contrast enhancement extension to discrete cosine domain
<i>S</i>	shape parameter
S_b	total bacteria number
SECE	spatial entropy-based contrast enhancement
SECDCT	spatial entropy-based contrast enhancement by discrete cosine transform
SMIRANK	spatial mutual information rank
SSIM	structural similarity index metric
SVR	support vector machine regressor
V	Value channel
φ	fitness function

References

- Abdullah-al-Wadud, M., Kabir, M.H., Dewan, M.A.A. and Chae, O., 2007. A dynamic histogram equalization for image contrast enhancement. *IEEE Transactions on Consumer Electronics*, 53(2), pp. 593–600. <https://doi.org/10.1109/TCE.2007.381734>.
- Agaian, S.S., Silver, B. and Panetta, K.A., 2007. Transform coefficient histogram-based image enhancement algorithms using contrast entropy. *IEEE Transactions on Image Processing*, 16(3), pp. 741–758. <https://doi.org/10.1109/tip.2006.888338>.
- Arici, T., Dikbas, S. and Altunbasak, Y., 2009. A histogram modification framework and its application for image contrast enhancement. *IEEE Transactions on Image Processing*, 18(9), pp. 1921–1935. <https://doi.org/10.1109/TIP.2009.2021548>.
- Bovik, A.C., 2009. *The essential guide to image processing*. 2nd ed. Boston, MA, USA: Academic Press.
- Cao, G., Huang, L., Tian, H., Huang, X., Wang, Y. and Zhi, R., 2018. Contrast enhancement of brightness-distorted images by improved adaptive gamma correction. *Computers & Electrical Engineering*, 66, pp. 569–582. <https://doi.org/10.1016/j.compeleceng.2017.09.012>.
- Celik, T., 2014. Spatial entropy-based global and local image contrast enhancement. *IEEE Transactions on Image Processing*, 23(12), pp. 5298–5308. <https://doi.org/10.1109/TIP.2014.2364537>.
- Celik, T., 2016. Spatial mutual information and page rank-based contrast enhancement and quality-aware relative contrast measure. *IEEE Transactions on Image Processing*, 25(10), pp. 4719–4728. <http://doi.org/10.1109/TIP.2016.2599103>.
- Celik, T. and Li, H.-C., 2016. Residual spatial entropy-based image contrast enhancement and gradient-based relative contrast measurement. *Journal of Modern Optics*, 63(16), pp. 1600–1617. <https://doi.org/10.1080/09500340.2016.1163427>.
- Chen, H., Niu, B., Ma, L., Su, W. and Zhu, Y., 2014. Bacterial colony foraging optimization. *Neurocomputing*, 137, pp. 268–284. <https://doi.org/10.1016/j.neucom.2013.04.054>.
- Chen, J., Li, C. and Yu, W., 2016. Adaptive image enhancement based on artificial bee colony algorithm. In: K. Hyunsung and L.-C. Hwang, eds. *Proceedings of the International Conference on Communication and Electronic Information Engineering (CEIE 2016)*. Guangzhou, China, 15–16 October 2016. <https://doi.org/10.2991/ceie-16.2017.88>.
- Chien, C.-L. and Tseng, D.-C., 2011. Color image enhancement with exact HSI color model. *International Journal of Innovative Computing, Innovation and Control*, 7(12), pp. 6691–6710.
- Coltuc, D., Bolon, P. and Chassery, J.-M., 2006. Exact histogram specification. *IEEE Transactions on Image Processing*, 15(5), pp. 1143–1152. <https://doi.org/10.1109/TIP.2005.864170>.
- Ghadiyaram, D. and Bovik, A.-C., 2015. *LIVE In the wild image quality challenge database*. [online] Available at: <<http://live.ece.utexas.edu/research/ChallengeDB/index.html>> [Accessed March 2021].
- Horé, A. and Ziou, D., 2010. Image quality metrics: PSNR vs. SSIM. In: *Proceedings of the 20th International Conference on Pattern Recognition*. Istanbul, Turkey, 23–26 August 2010. IEEE Computer Society. <https://doi.org/10.1109/ICPR.2010.579>.
- Hoseini, P. and Shayesteh, M.G., 2010. Hybrid ant colony optimization, genetic algorithm, and simulated annealing for image contrast enhancement. In: *Proceedings of the IEEE Congress on Evolutionary Computation (CEC)*. Barcelona, Spain, 18–23 July 2010. <https://doi.org/10.1109/CEC.2010.5586542>.
- Jayaraman, S., Esakkirajan, S. and Veerakumar, T., 2011. *Digital image processing*. New Delhi, India: Tata McGraw-Hill Education.
- Jobson, D.J., Rahman, Z. and Woodell, G.A., 1997. Properties and performance of a center/surround retinex. *IEEE Transactions on Image Processing*, 6(3), pp. 451–462. <https://doi.org/10.1109/83.557356>.
- Kim, T. and Paik, J., 2008. Adaptive contrast enhancement using gain-controllable clipped histogram equalization. *IEEE Transactions on Consumer Electronics*, 54(4), pp. 1803–1810. <https://doi.org/10.1109/TCE.2008.4711238>.
- Kim, Y.-T., 1997. Contrast enhancement using brightness preserving bi-histogram equalization. *IEEE Transactions on Consumer Electronics*, 43(1), pp. 1–8. <https://doi.org/10.1109/30.580378>.
- Konar, A., 2006. *Computational intelligence: principles, techniques and applications*. New Delhi, India: Springer Science & Business Media.
- Larson, E.C. and Chandler, D.M., 2010. Most apparent distortion: full-reference image quality assessment and the role of strategy. *Journal of Electronic Imaging*, 19(1): 011006. <https://doi.org/10.1117/1.3267105>.
- Lee, C.-H., Shih, J.-L., Lien, C.-C. and Han, C.-C., 2013. Adaptive multiscale retinex for image contrast enhancement. In: K. Yetongnon, A. Dipanda, R. Chebir, L. Gallo and N. Nain, eds. *SITIS'13: Proceedings of the International Conference on Signal-Image Technology & Internet-Based Systems*. Jaipur, India, 4–7 December 2013. Piscataway, NJ, USA: IEEE. <https://doi.org/10.1109/SITIS.2013.19>.
- Li, S., Jin, W., Li, L. and Li, Y., 2018. An improved contrast enhancement algorithm for infrared images based on adaptive double plateaus histogram equalization. *Infrared Physics & Technology*, 90, pp. 164–174. <https://doi.org/10.1016/j.infrared.2018.03.010>.

- Lin, S.C.F., Wong, C.Y., Rahman, M.A., Jiang, G., Liu, S., Kwok, N., Shi, H., Yu, Y.-H. and Wu, T., 2015. Image enhancement using the averaging histogram equalization (AVHEQ) approach for contrast improvement and brightness preservation. *Computers and Electrical Engineering*, 46(C), pp. 356–370. <https://doi.org/10.1016/j.compeleceng.2015.06.001>.
- Liu, H.-D., Yang, M., Gao, Y. and Cao, L., 2014. Fast local histogram specification. *IEEE Transactions on Circuits Systems for Video Technology*, 24(11), pp. 1833–1843. <https://doi.org/10.1109/TCSVT.2014.2329373>.
- Maini, R. and Aggarwal, H., 2010. A comprehensive review of image enhancement techniques. *Journal of Computing*, 2(3), pp. 8–13.
- Majumder, A., Laha, D. and Suganthan, P.N., 2019. Bacterial foraging optimization algorithm in robotic cells with sequence-dependent setup times. *Knowledge-Based Systems*, 172, pp. 104–122. <https://doi.org/10.1016/j.knosys.2019.02.016>.
- Mittal, A., Moorthy, A.K. and Bovik, A.C., 2011. *BRISQUE software release*. [online] Available at: <http://live.ece.utexas.edu/research/quality/BRISQUE_release.zip> [Accessed March 2021].
- Mittal, A., Soundararajan, R. and Bovik, A.C., 2012a. Making a ‘completely blind’ image quality analyzer. *IEEE Signal Processing Letters*, 20(3), pp. 209–212. <https://doi.org/10.1109/LSP.2012.2227726>.
- Mittal, A., Soundararajan, R. and Bovik, A.C., 2012b. *NIQE software release*. [online] Available at: <<http://live.ece.utexas.edu/research/quality/nique.zip>> [Accessed March 2021].
- Niu, B., Wang, H., Wang, J. and Tan, L., 2013. Multi-objective bacterial foraging optimization. *Neurocomputing*, 116, pp. 336–345. <https://doi.org/10.1016/j.neucom.2012.01.044>.
- Osareh, A., Shadgar, B. and Markham, R., 2009. A computational-intelligence-based approach for detection of exudates in diabetic retinopathy images. *IEEE Transactions on Information Technology in Biomedicine*, 13(4), pp. 535–545. <https://doi.org/10.1109/TITB.2008.2007493>.
- Padhani, A.R., 2002. Dynamic contrast-enhanced MRI in clinical oncology: current status and future directions. *Journal of Magnetic Resonance Imaging*, 16(4), pp. 333–483. <https://doi.org/10.1002/jmri.10176>.
- Passino, K.M., 2010. Bacterial foraging optimization. *International Journal of Swarm Intelligence Research*, 1(1), pp. 1–16.
- Ponomarenko, N., Lukin, V., Zelensky, A., Egiazarian, K., Carli, M. and Battisti, F., 2009. TID2008 – a database for evaluation of full-reference visual quality assessment metrics. *Advances of Modern Radioelectronics*, 10(4), pp. 30–45.
- Raju, A., Dwarakish, G.S. and Reddy, D.V., 2013. A comparative analysis of histogram equalization based techniques for contrast enhancement and brightness preserving. *International Journal of Signal Processing, Image Processing and Pattern Recognition*, 6(5), pp. 353–366. <http://doi.org/10.14257/ijcip.2013.6.5.31>.
- Reza, A.M., 2004. Realization of the contrast limited adaptive histogram equalization (CLAHE) for real-time image enhancement. *Journal of VLSI Signal Processing Systems for Signal, Image and Video Technology*, 38(1), pp. 35–44. <https://doi.org/10.1023/B:VLSI.0000028532.53893.82>.
- Ritika, and Kaur, S., 2013. Contrast enhancement techniques for images – a visual analysis. *International Journal of Computer Applications*, 64(17), pp. 20–25. <http://doi.org/10.5120/10727-5679>.
- Saravanan, G., Yamuna, G. and Nandhini, S., 2016. Real time implementation of RGB to HSV/HSI/HSL and its reverse color space models. In: *Proceedings of the IEEE International Conference on Communication and Signal Processing (ICCSP)*. Melmaruvathur, India, 6–8 April 2016. <http://doi.org/10.1109/ICCSP.2016.7754179>.
- Shakeri, M., Dezfoulian, M.H., Khotanlou, H., Barati, A.H. and Masoumi, Y., 2017. Image contrast enhancement using fuzzy clustering with adaptive cluster parameter and sub-histogram equalization. *Digital Signal Processing*, 62, pp. 224–237. <http://doi.org/10.1016/j.dsp.2016.10.013>.
- Sheet, D., Garud, H., Suveer, A., Mahadevappa, M. and Chatterjee, J., 2010. Brightness preserving dynamic fuzzy histogram equalization. *IEEE Transactions on Consumer Electronics*, 56(4), pp. 2475–2480. <http://doi.org/10.1109/TCE.2010.5681130>.
- SIPI, n.d. *The USC-SIPI image database*. [online] Available at: <<http://sipi.usc.edu/database/>> [Accessed March 2021].
- Tang, L., 2014. Image edge detection based on quantum genetic algorithm. *Computer Modeling & New Technologies*, 18(12B), pp. 517–523.
- Tohl, D. and Li, J.S.J., 2019. Contrast enhancement by multi-level histogram shape segmentation with adaptive detail enhancement for noise suppression. *Signal Processing: Image Communication*, 71, pp. 45–55. <https://doi.org/10.1016/j.image.2018.10.011>.
- Wan, M., Gu, G., Qian, W., Ren, K., Chen, Q. and Maldague, X., 2018. Particle swarm optimization-based local entropy weighted histogram equalization for infrared image enhancement. *Infrared Physics & Technology*, 91, pp. 164–181. <https://doi.org/10.1016/j.infrared.2018.04.003>.
- Wang, C. and Ye, Z., 2005. Brightness preserving histogram equalization with maximum entropy: a variational perspective. *IEEE Transactions on Consumer Electronics*, 51(4), pp. 1326–1334. <https://doi.org/10.1109/TCE.2005.1561863>.
- Wang, S., Kede, M., Yeganeh, H., Wang, Z. and Lin, W., 2015. A patch-structure representation method for quality assessment of contrast changed images. *IEEE Signal Processing Letters*, 22(12), pp. 2387–2390. <https://doi.org/10.1109/LSP.2015.2487369>.

- Wang, Y., Chen, Q. and Zhang, B., 1999. Image enhancement based on equal area dualistic sub-image histogram equalization method. *IEEE Transactions on Consumer Electronics*, 45(1), pp. 68–75. <https://doi.org/10.1109/30.754419>.
- Ying, Z., Li, G., Ren, Y., Wang, R. and Wang, W., 2017. A new low-light image enhancement algorithm using camera response model. In: *Proceedings of 2017 IEEE International Conference on Computer Vision Workshops (ICCVW)*. Venice, Italy, 22–29 October 2017. Piscataway, NJ, USA: IEEE. <https://doi.org/10.1109/ICCVW.2017.356>.
- Zhang, G., Sun, D., Yan, P., Zhao, H. and Li, Z., 2009. A LDCT image contrast enhancement algorithm based on single-scale retinex theory. In: M. Mohammadian, ed. *Proceedings of the IEEE International Conference on Computational Intelligence for Modeling Control & Automation*. Vienna, Austria, 10–12 December 2008. Piscataway, NJ, USA: IEEE. <https://doi.org/10.1109/CIMCA.2008.231>.
- Zhang, L., Zhang, L., Mou, X. and Zhang, D., 2011. FSIM: a feature similarity index for image quality assessment. *IEEE Transactions on Image Processing*, 20(8), pp. 2378–2386. <https://doi.org/10.1109/TIP.2011.2109730>.

JPMTR-2104
DOI 10.14622/JPMTR-2104
UDC 159.925-021.131:004.92

Original scientific paper | 149
Received: 2021-04-09
Accepted: 2021-06-17

Examining the uncanny valley effect in virtual character design for digital games

Ugur Bakan and Ufuk Bakan

Izmir Kâtip Çelebi University,
Balatçik Kampusu 35620 Cigli Izmir, Turkey

ugur.bakan@ikc.edu.tr

Abstract

Today, games, where visuality is at the forefront, have similar features with a cinema project in terms of both the content and the technologies used. When the realistic appearance of robots and digital designs that do not fully resemble humans exceeds a point, the images created leave their place to negative emotions such as disgust, fear, and hate. The feeling of disgust emerges when the level of affinity reaches the highest level. The negative mood status which took its place in the literature as an uncanny valley is an important reference for game designers and researchers. Masahiro Mori's uncanny valley theory about humanoid robots is used by animators and video game designers in the content creation process in video games, every day. In this study, the design evolution of Lara Croft, who has found an important place in the video game world, has been evaluated in terms of exposure to the uncanny valley. This study has used images and videos representing Lara Croft, the strong and smart female icon of the Tomb Raider games. A total of 67 undergraduate students (32 for experiments and 35 as a control group), 34 male (50.7 %), and 33 female (49.3 %), voluntarily participated in this study. In this study, the quasi-experimental design was used with experimental and control groups, since the data collection tool used to compare the experimental and control groups did not allow them to reflect the student's past game experiences. The findings of this study suggest the following design principles: to use a high polygon count to design attractive, ideal faces that are not spooky.

Keywords: computer-generated models, video games, facial expression, human-likeness, emotion design

1. The uncanny valley

The developments in technology have enabled objects in animation movies and video games to look as realistic as possible and characters to act like humans today. The realistic appearance of these computer-generated (CG) imagery visuals created in the computer environment might sometimes have negative effects on users who experience it (Tinwell, 2015). This negative emotion, which is conceptualized and was first introduced by a Japanese roboticist Masahiro Mori in 1970 as the uncanny valley effect (Mori, 1970), is evaluated for realistic characters created in a computer environment as well as robots with humanoid appearance. The origin of the concept of the uncanny valley goes back to the German psychiatrist Ernst Jentsch's explanation of the phenomenon of "uncanniness" in his article. Jentsch (1906) argues that the concept of uncanniness emerges as a result of indecision that occurs when people cannot distinguish whether objects are real and alive. He defined an unknown and unfamiliar phenomenon with

the concept of "unheimlich". In German, "heimlich" expresses the opposite of the word "uncanny" and means familiar, acquaint, native, according to paper of Freud (1919), which is among the pioneering studies on the uncanny concept and explaining the meaning of this concept. Freud identified the uncanny as anything that reminds us of the frightening realm of our unconscious mind, of repressed memories and impulses from childhood that feel unknown but vaguely and threateningly recognizable (Suler, 2016). Today the uncanny valley hypothesis suggested by Mori (1970) has been widely acclaimed in fields involving human–robot interaction throughout the development of increasingly human-like androids (Tung, 2016). In his article, Mori (1970) tried to formulate the emotional effects of beings with artificial appearances such as robots, prosthetic hands, puppets with various features, on humans. These effects were further studied by Bartneck, et al. (2009), and Ho and MacDorman (2010). Mori (1970) assumes that in the relationship of humans with robots, the familiarity with robots will increase as the robots look

more like humans; however, at a certain point, robots will not be able to give what is expected by humans, and this familiarity will be replaced by an extremely uncomfortable feeling (Schwind, et al., 2018). When humanoid robots become too real but do not resemble authentic human beings at the same time, people's perceptions towards the objects turn to negativity (Strait, et al., 2017). Mori (1970) mentioned zombies and puppets as examples to explain the concept of the uncanny valley (Schwind, et al., 2018). Here, the effect of familiarity level on individuals is shown as a deep valley shape on the graph (Figure 1).

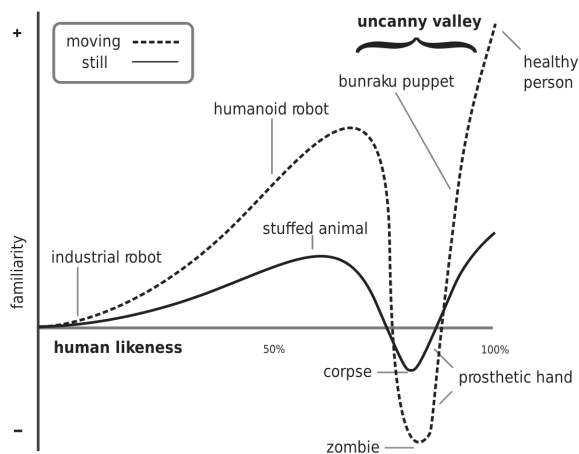


Figure 1: The uncanny valley graph was created by Masahiro Mori (1970)

Mori (1970) has prepared a graph that visualizes the emotional impact of robots resembling humans in terms of physical appearance on individuals. According to Figure 1, the uncanny valley phenomenon divides the characters into two main categories, which are dynamic and static characters (Mohamad Ali and Hamdan, 2017). In this graph, the familiarity level is followed on the vertical plane while the horizontal plane reveals the affinity to humans in terms of percentage. While the dashed line that forms the graph contains human-like products that can move, the continuous line contains products that do not move. When the graph is examined, the starting point of the curve corresponds to industrial robots. Industrial robots, which are completely developed for mass production, do not create a feeling of familiarity because they do not have humanoid features. Robots or prostheses with anthropomorphic features can also be seen on the graph as the first point created by the feeling of familiarity by sliding up the curve. Mori (1970) cites bunraku puppets, toy robots with hands and feet as examples. People continue to be familiar with stimuli such as robots and other artificial devices until they reach a certain point. The sense of familiarity begins to decrease sharply when we perceive that human-

like copies resemble human beings but are not human. The fact that this decrease leaves its place in negative behaviors such as disgust, fear, and hate leads to the formation of the uncanny valley.

1.1 Uncanny valley and game characters

The limited processing capacity of the computer hardware in the early days of video games brought along some issues that video game designers should pay attention to in the preparation process of the games. With the transition from 2D graphics to 3D, the visibility has come to the forefront and the games have become increasingly complex. The characters created in video games, cartoons, caricatures, illustrations, and 3D applications are divided into three groups as stylized, semi-realistic, and realistic in terms of design. Stylized design is a form of design in which the changes in shape, size, and colors come to the fore rather than making the characters look photorealistic. Stylization allows the artist to explore possibilities beyond those found in the real world to enhance the attractiveness or expressiveness of characters, particularly when it comes to cartoons or illustrations (McCloud, 1993; Gooch, Reinhard, and Gooch, 2004). A few common elements found in stylized characters are exaggerated proportions, bold colors, cel-shading, retro effects, and geometric shapes (Lundwall, 2017, p. 8). Such characters are mostly reflected in cartoons, caricatures, and 3D animated movies, with changes in the proportions of the head, hands, feet, and other limbs of the figures.

Semi-realism, in essence, is creating something that we can define as "real" or "close to reality" based on our perceptions, rather than an image of the natural world as it is (Hall, 2016, p. 7). In general, semi-realistic animated movie characters are different from caricatured and exaggerated characters frequently used in traditional animations (Kaba, 2013). Although these concept artists have creative freedom, they have to be close to realism in their designs, especially anatomically. Within the framework of these rules, the elements such as muscles, curves, eyes, etc. are tried to be revealed clearly to show a character more attractively.

In order to create characters with a realistic appearance, it is necessary to reflect the appearance and movements of the character as photorealistically as possible (Wallraven, et al., 2008, p. 23). In this process, artists create a character, starting from basic shape and proportion, adding skin tones, hairstyles, clothes, accessories, basic postures, walk, movement energy, attitude, and facial expressions (Bancroft, 2006). The photorealistic artists who aim to transfer only the photographic image to the work and who are not interested in the original of the object differ from the realistic artists who aim to give life as it is in that sense (Lucie-Smith, 1996, p. 204).

At the same time, this perception of depth provides a perception that the body movements and facial expressions of the characters are close to a real person. The human face is a rich and powerful source full of communicative information about human behavior and emotion (Yong, 2007). Although the face is the primary channel expressing a person's emotions, it forms a meaningful whole in the game only when it combines with the character's posture and body language. Besides the visual features, characters who can think and act like real people can be designed with the possibilities of artificial intelligence technologies in games. While these features bring the character closer to the humanoid appearance, they also increase the tendency to be exposed to the uncanny valley.

For the first time in the digital game market where the main heroes are mostly male, the female character being the main character in a game represents a major transformation in this market. Gender-based game studies have shown that white male characters are generally at the forefront, and female players play a decisive role even in the games that are preferred more than male players, even though white male players are not in the main dominant role (Lynch, et al., 2016). While women generally appear as women in trouble, the male protagonist of the game undertakes the task of rescuing the female character, who is represented as a stereotype as naive and weak.

The first significant change in the way female characters are represented in games over the years was seen in 1996 in the action-adventure digital game *Tomb Raider*, which is about Lara Croft's adventures. Although a series of adventure games offer many female character options, the main protagonist is traditionally male, and female characters appear to be largely in supporting roles. Although Lara represents the success of a heroine, she seems to have done little to change the relationship between female players and the game industry (Cassell and Jenkins, 2000, p. 30). Lara Croft is a powerful figure with incredible gymnastic abilities, able to fight physically like a masculine character. In almost 80 % of the games, there are elements of violence and aggression as a part of the game strategy, and in 28 % of the games where there are female characters, these female characters are featured in their physical appearance or are depicted as sex objects (Dietz, 1998). In contrast to the role of an archaeologist, Lara appears to be represented in an iconic body as men desire, being hyper-sexualized with large breasts, thin waist, curved hips (Mikula, 2003). Therefore, the sociological and psychological dimensions of the game experiences provide important information about the players. Whether or not it has an impact on the attitudes of the people watching or playing this media forum is another topic that researchers investigate.

1.2 Previous research on the uncanny valley in the digital games

The uncanny valley is an assumption that tries to explain the sudden negative reactions we experience when a robot appears and behaves with human-like features, even if not as much as a real human being, such as surprise, fright, disgust, and hate. Many studies examine the different styles of the characters to reveal the uncanny valley effect. Among these studies, participants were asked to classify them as biological or artificial, based on their movements, among a series of examples of point lights, ellipses, robots, aliens, clowns, and running human figures (Chaminade, Hodgins and Kawato, 2007). The participants evaluated that the point lights, which have the simplest appearance among these examples, move more naturally than the other examples. In another study, to examine the relationship between humanoid appearance and visual appeal, they asked participants to react to 75 virtual characters, both from video games and elsewhere (Schneider, Wang, and Yang, 2007). As a result of the study, it was seen that there is a direct relationship between human appearance and attractiveness. It was concluded that characters who have a humanoid appearance but are not completely human-like have a lower rate of attraction. The first experimental research on the uncanny valley was conducted by MacDorman, et al. (2009); they used four empirical studies to reveal the relevance of the effects of motionless images on users with the uncanny valley. They analyzed the examinations of Mori (1970) on the uncanny valley effect by comparing a series of photographs created by combining human and robot faces in two different ways. Hanson (2006) showed that the emergence of the uncanny valley effect on morphed images depends on aesthetic design rather than a realistic appearance of images. Seyama and Nagayama (2007) in the experimental study using the asynchronous morphing technique, where artificial faces gradually turn into real faces, have shown the negative effect of images with abnormal features such as enlarged eyes on people leads to an uncanny valley curve. Another study was carried out to examine whether the character that is visually deficient in facial expressions affects the phenomenon of uncanny (Tinwell, et al., 2011). It was designed to reveal the effects of changes in the facial proportions, skin texture, and detail level of the character designed in a computer environment on perceived strangeness and attractiveness of humanoids, (MacDorman, et al., 2009). In an experimental study using the real robot and human pictures, the effect of anthropomorphism on participants' perceptions has been investigated (Złotowski, et al., 2015). An experimental study has been conducted in order to determine the effects of facial expressions on the real dimension in human perception (Wallraven, et al., 2008).

In four empirical studies (Seyama and Nagayama, 2007; MacDorman, et al., 2009; Złotowski, et al., 2015; Wallraven, et al., 2008), the facial proportions, skin texture, and detail level of the CG human character have been varied. They aimed to reveal whether these changes affect perceived oddness, human resemblance, and attractions. The use of less photo-realistic textures in studies that do not aim to reflect reality is another matter to be considered during the design stage. Chen et al. (2010) conducted an experimental study to determine the changes in perception of human faces of people who have looked at stylized design faces for a certain period. In the same study, cartoon videos with big-eyed characters were shown to the participants, and they were asked to examine human faces in terms of attractiveness during the adaptation process. This study concluded that adapting to cartoon faces with large eyes leads to an orientation in people's preferences towards large-eyed images rather than ordinary human faces (Chen, et al., 2010).

In a study conducted by Flach, et al. (2012), it was evaluated how CG characters in the media are perceived by people and the uncanny valley effect of these characters was examined. In the study, pictures from different media sources were evaluated visually and categorized according to the uncanny valley effect. In another study by McDonnell, Breidt, and Bülthoff (2012), it was tried to determine the uncanny valley effect in video game characters created in the computer environment. In another study on virtual characters that make up the entire visual space of three-dimensional animated movies and designed in a computer environment, the effect of shape and material factors that define how a character looks has been analyzed by Zell, et al. (2015) who observed that the material is a determining factor in reflecting the attractiveness. A study by Mathur and Reichling (2016) was conducted to reveal human responses to 80 android robot faces encountered in real life. The same study constituted another aspect of the study in determining whether a potential uncanny valley effect implicitly influences the social decision-making process of people. In the study conducted by Kätsyri, Mäkäräinen, and Takala (2017), 54 participants were asked to evaluate five movies that included semi-realistic animation, caricatured animation, and human players. It was made in order to reveal whether the semi-realistic animated movie characters affect negative evaluations. As a result of the study, it was seen that movies with semi-realistic characters have higher eeriness scores than those in the other category. While *Beowulf* and *The Polar Express* out of these movies were selected by the participants, it was concluded that *Beowulf* had a higher eeriness rate than all other movies. In another study, 40 participants were asked to evaluate a series of visual images reflecting various happy, neutral, sad, angry, and fearful states of human

and robot faces (Reuten, van Dam, and Naber, 2018). In the same study, the changes in the pupil size of the participants during the appearance of these images were also recorded. It was observed that the uncanny valley effect of humanoid robots was higher than similar visuals, it was scored lower in terms of imaginary interaction, and the pupil showed less change than for other stimuli (Reuten, van Dam, and Naber, 2018).

Emotional expressions were found to be more difficult to notice. Kätsyri, Gelder, and Takala (2019) used both painted and CG faces to test whether CG faces are susceptible to the uncanny valley effect and demonstrate a correlation between large-scale humanity. When the data were evaluated, a linear relationship was found between humanity and affinity. In the same study, it was observed that less realistic faces trigger an eerie sense.

2. Methodology

The purpose of this study is to investigate whether and how playing a realistic game character whose a near-identical resemblance to a human being affects feelings of eeriness and uncanniness compared to a less realistic game character. Perceived both facial attractiveness and distinctiveness was the variable of focus for the character (realistic versus stylized). The case study design was selected because it offered the opportunity to be very descriptive and holistic (Glesne, 2011) and its examination of one or more specific situations and focus on activities as they occur in the real world (Yin, 2009). For this purpose, this study used images and short videos (approx. 30 seconds) representing Lara Croft that is the most iconic character of the Tomb Raider games released by Japanese video game producer Square Enix. Until today, 24 years after the release of the first Tomb Raider game in 1996, Lara Croft still is regarded as one of the most famous video game heroines of all time. And until today, 25 Tomb Raider games, 3 movies, 5 books, and many comic books have been released in total (on all platforms). This study asked participants to compare and rate the proportions of the body and the face of four different Lara Croft characters. Perceived body proportion was the variable of focus for the characters.

To address the primary purpose of this research study, the following research questions (RQ) were investigated:

RQ1 – What is the effect of the realism level and movements of the game characters on falling into the uncanny valley?

RQ2 – Which parts of the faces of the game characters increase the effect of the uncanny valley?

RQ3 – What negative emotions do people who are exposed to the effect of uncanny valley produce?

RQ4 – Which aspect (physical or emotional) of the game characters would increase the uncanny valley effect more?

RQ5 – Is there a significant relationship between the uncanny valley effect and the duration of exposure?

In this study, the quasi-experimental design was used with experimental and control groups, since the data collection tool used to compare the experimental and control groups did not allow them to reflect the participant's past game experiences. Since the uncanny valley effect measured within the scope of the research was not instantaneous and teachable, the pretest and posttest could not be applied. Instead, the experimental group ($n = 32$) played one time TR 13: Rise of the Tomb Raider (2015) before starting the research in connection with the research hypothesis, while the control group ($n = 35$) did not. The reason for choosing this version of the Tomb Raider game is that the haunted valley meat appears more prominently in the characters that are closest to the realistic appearance. In the next step, the differences were measured by applying data collection tools to both groups. The purpose of this activity is to prove that the uncanny valley effect is not permanent, it is experienced instantly, and that the effect is reduced only to a certain level as a result of external intervention.

2.1 Materials and stimuli

This survey included the main character appearing in four editions of the Tomb Raider game series: TR 6: The Angel of Darkness (2003), TR 9: Underworld (2008), TR 13: Rise of the Tomb Raider (2015), and TR 14: Shadow of the Tomb Raider (2018). The first part of the questionnaire was designed with four items that collected participants' demographics information and user preference, and digital game backgrounds. The second part consisted of questions designed to understand the participant's opinions on how the character looked and how attractive was in terms of realism, empathy, and strangeness (Dill, et al., 2012). In the third part, the Subjective Measurement Scale (5 items) was used to determine the type of emotion expressed facially and orally by the human or virtual character such as human-likeness, eeriness, disgust, fear, and attractiveness. The rating scale was developed by Burleigh, Schoenherr, and Lacroix (2013) using 7-point Likert scale. The last part was a 5-item questionnaire that measured the perception of how unrealistic/realistic the characters' body proportions appeared to be (Murphy, 2016). Each character was displayed on a uniform white background with a resolution

of 500×500 pixels. The images for each experiment were presented in random order. After presenting each image and video, the participants were requested to fill a questionnaire.

2.2 Design and procedure

This research centers on the perception of the emotion of CG characters in digital games. Therefore, the problem of the study is to examine the relationship between the impact on attitudes and behavior of undergraduate students that play different editions of the same video game series and their perception of computed graphics characters. According to previous studies' classification criteria the variables perceived strangeness, friendliness, and human-likeness were used as items to measure the uncanny (Bartneck, et al., 2009; Burleigh, Schoenherr and Lacroix, 2013; Schneider, Wang and Yang, 2007; Ho and MacDorman, 2010). The study was carried out as a quasi-experimental with a web-based survey that uses images and videos of game characters and rating questions for each participant. Experimental studies are defined as studies based on testing the differences that occur within the framework of the problem determined by the researcher on the dependent variable. In the quasi-experimental design, just as in the experimental design, it is aimed to compare groups with similar characteristics (Chiang, Jhangiani, and Price, 2015). Quasi-experimental research involves the manipulation of an independent variable without the random assignment of participants to conditions or orders of conditions. The quasi-experimental study is the process of formulating and realizing a series of actions and activities to achieve the desired positive change, evaluating the applications performed through the scientific method, and generating information about the intervention to help practitioners in the field (Proctor and Rosen, 2008).

In the research, the participants were asked to evaluate the visuals of Lara Croft, the main character of the TR 6, TR 9, TR 13, and TR 14 versions of the Tomb Raider game series. In the first phase of the study, the participants were asked to evaluate the character according to only physical appearance features. In the second stage, the emotional states formed in their minds when they look at the character were examined in the "emotional appearance" category.

2.3 Participants

The population for this study was a convenience sample of 67 undergraduate students (32 in experimental and 35 in the control group) selected from different departments at a midsize university in Turkey by appropriate sampling method and determined by random assignment as participants for 30 minutes experiment.

During the 2020–2021 school year, the researchers measured the attitudes of students in a state university in Turkey for two weeks. This limitation was caused by accessibility and convenience of time, location, and availability when conducting this research. To address the aforementioned research questions a between-groups (experiment, and control group) quasi-experimental design with a follow-up study was conducted in the study. All 67 undergraduate students, 34 males (50.7 %) and 33 females (49.3 %), voluntarily participated in this study. Their ages ranged from 17 to 23 years old at the onset of the study. A detailed overview of the scope and goals of the study as well as the link to the survey were posted to the students.

3. Analysis and results

The coded data were entered into a Microsoft Excel spreadsheet. Data were analyzed on the computer by using IBM SPSS Statistics version 24, the margin of error was assumed to be $p < 0.05$. Today, many studies are examining the relationship between game types and addiction level, especially massively multiplayer online role-playing games – MMORPGs. Research results show a significant increase in more time playing computer games when the high image quality and difficulty level of games increase (Wan and Chiou, 2006). All participants were asked: On average, how many hours do you play video games? The response rate was: 50.7 % played for 0–1 hours, 16.4 % for 1–2 hours, 17.9 % for 2–4 hours, and 15 % for 4–6 hours. No significant difference was found according to the t -test result in which the difference was investigated according to the game playing times of the participants and the gender variable ($t = -2.615$; $p = 0.111$).

Today, video games can be played through mobile phones, tablets, or portable consoles anywhere with internet access. As the speed and prevalence of the internet increased, the types and playing times of video games were directly affected by this development. When asked about the platforms they frequently play games with, 65.7 % of them stated that they use mobile phones/tablets, 31.3 % of them use comput-

ers (PC, Mac), and 3 % of them use gaming consoles (Xbox, PlayStation, Nintendo). In this study, when the variance by game types is examined, it was observed that the three most preferred game types are 40.3 % traditional games (Tetris, solitaire, checkers, chess), 16.4 % first-person shooting games (FEAR, Half-Life, Counter-Strike) and 13.4 % simulation and strategy games (Warcraft, Rise of Nations, Age of Empires).

In the section where a different dimension of the physical attributes of the characters was evaluated, the participants were asked to rate the video game characters according to the video images and how realistic the body proportions looked. Also, the sexiness, strength, and attractiveness of the character were scored according to the 5-point Likert scale. In this analysis, the direction of the changes in the development process of the character over the years was determined. According to Table 1, while the participants found the Lara Croft character in TR 9 to have realistic human proportions ($M = 3.84$) they found that TR 6 having the least realistic rates ($M = 3.13$). Based on the analysis made according to the weak/strong appearance of the characters, it was determined that the characters in the TR 13 and TR 9 versions seems stronger than the others. Similar results were observed in the distribution of the average scores according to the characters' aggressive/submissive appearance level with weak/strong and unattractive/attractive levels. On this scale, the TR 9 and TR 14 characters are in the first place at the sexy appearance level of the characters, while the TR 13 version, which is positive in the other items, has the lowest average score in this item.

The RQ1 asks if there was an effect of the realism level and movements of the game characters on falling into the uncanny valley. Questions (items 1 and 2 in Table 2) were asked with the intention to capture the level of human-likeness (how realistic is the character) in the user's perception. Results for the first item (Do you think that the character is real person or CG?) demonstrated: 98.5 % of the mean for all of the participants stated that the Lara Croft character in TR 6 seemed to be created in a remote computer environment (created with CG); in the case of TR 9 it was 64.2 % (see Table 2).

Table 1: Descriptive statistics for character body versions (where M denotes mean value, and SD denotes standard deviation)

Variable	TR 6 M (SD)	TR 9 M (SD)	TR 13 M (SD)	TR 14 M (SD)
Weak/strong	3.49 (1.19)	3.67 (1.05)	4.18 (0.97)	3.19 (1.23)
Submissive/aggressive	3.63 (1.36)	3.91 (1.14)	4.30 (1.07)	3.91 (1.18)
Unrealistical/realistical	3.13 (1.23)	3.84 (1.18)	3.33 (1.31)	3.55 (1.28)
Unattractive/attractive	3.81 (1.25)	4.12 (1.07)	4.24 (1.20)	3.79 (1.31)
Not sexualized/sexualized	3.13 (1.38)	3.93 (1.19)	2.87 (1.46)	3.18 (1.36)

Table 2: Descriptive statistics for a physical appearance in percentage by the experimental (Exp.) and control (Cont.) groups, and mean of the groups (M)

Items	TR 6			TR 9			TR 13			TR 14		
	Exp.	Cont.	M	Exp.	Cont.	M	Exp.	Cont.	M	Exp.	Cont.	M
1. View												
A real person	–	2.9	1.5	40.6	31.4	35.8	81.2	34.3	56.7	78.1	60.0	68.7
Created with CG	100.0	97.1	98.5	59.4	68.6	64.2	18.8	65.7	43.3	21.9	40.0	31.3
2. Degree of realism												
Very realistic	–	–	–	28.1	5.7	16.4	93.8	68.6	80.6	78.1	45.7	61.2
Moderately realistic	43.8	45.7	44.8	56.3	65.7	61.2	–	–	–	6.3	37.1	22.4
Unrealistic	56.2	54.3	55.2	15.6	26.6	22.4	6.2	31.4	19.4	15.6	17.1	16.4
3. Characterization												
Sympathetic	46.9	28.6	37.3	65.6	45.7	55.2	50.0	31.4	40.3	56.2	57.1	56.7
Antipathetic	53.1	71.4	62.7	34.4	54.3	44.8	50.0	68.6	59.7	43.8	42.9	43.3
4. Strangeness												
Yes	59.4	74.3	67.2	37.5	62.9	50.7	43.8	57.1	50.7	37.5	20.0	28.4
No	40.6	25.7	32.8	62.5	37.1	49.3	56.2	42.9	49.3	62.5	80.0	71.6

As the answer to the same question, 68.7 % of the participants said that the character in TR 14 was designed as closest to human. Lara's character in TR 14: Shadow of the Tomb Raider, which was released in 2018, has a 4K resolution at 60 fps but can be clearly distinguished from a real person by the participants. With the implementation of technological developments required to produce realistic graphics, game designers feel freer to create all the features of the character they dream of. In the second question, the reality level of the character created in the computer environment was examined at three levels: 61.2 % of the participants find the TR 14 version and 80.6 % the TR 13 version quite realistic. The last two items, which measure the positive and negative perception felt at first glance to Lara Croft's characters, determine the familiarity in exposure to the uncanny valley. Question 3 was asked to evaluate the perception of the character's personality (characterization). In this context, 56.7 % of the participants find TR 14 sympathetic and 55.2 % of them find TR 9 sympathetic, while 62.7 % of them find TR 6 antipathetic and 59.7 % TR 13 antipathetic. In the last question related to antipathetic thinking, 67.2 % of the participants were uncomfortable with TR 6, while a group of 71.6 % reported that there was no disturbing element in TR 14. As seen in Table 2, when the scores of the experimental group with students who played games for one hour were examined, no significant difference compared to the control group was found in the TR 6 and TR 9 versions, which did not have a realistic appearance in the first question answers. In the TR 13 version where the uncanny valley effect is expected, 81.2 % of the experimental group students ($n = 26$) found the character realistic, while 34.3 % ($n = 12$) of the control group students found the character realistic. For the second question, in which the realistic views of the characters were classified, close results were obtained in the TR 6

and TR 9 versions; 93.8 % ($n = 30$) of the experimental group students and 68.6 % ($n = 24$) of the control group students saw the character in TR 13 version as "very realistic". In the same question, 2 % ($n = 2$) of the experimental group and 31.4 % ($n = 11$) of the control group defined it as "unrealistic". According to these results, it was determined that there was a significant decrease in the level of falling into the uncanny valley of the students in the experimental group where the game was practiced for one hour.

The following section addresses the study's second research question RQ2. The human face is an important indicator of other forms of communication and any facial expression that is the source of this indicator is the visible sign of a person's sensation, attitude, character, and psychological state. When the parts of the disturbing face were examined, the participants were asked to evaluate the eyes, mouth, nose, hair, and other elements in the last question. According to results in 46.3 % of the participants in TR 6 and 29.9 % of the participants in TR 9 find the eyes of the characters disturbing, while 49.3 % of the participants in TR 13 and 71.6 % of the participants in TR 14 stated that they found the other factors disturbing in the first place. Research has shown that the large eyes and skin texture of the highly realistic characters are one of the important factors that increase the uncanny valley effect. This is consistent with what has been found in previous studies (Seyama and Nagayama, 2007) wherein the eyes in the character face plays role in the uncanny valley effect.

The RQ3 tried to determine the emotions that occur when exposed to the uncanny valley effect. To define these emotions, the relationship between positive emotions (human-likeness and attractiveness) and

Table 3: Correlation coefficients *r* for observed variables

Emotions	TR 6				TR 9			
	1	2	3	4	1	2	3	4
1 Human-likeness	1				1			
2 Eeriness	-0.356**	1			-0.246*	1		
3 Fear	-0.297*	0.876**	1		-0.177	0.836**	1	
4 Disgust	-0.489**	0.544**	0.481**	1	-0.427**	0.606**	0.560**	1
5 Attractiveness	0.532**	-0.416**	-0.381**	-0.550**	0.534**	-0.502**	-0.491**	-0.628**

Emotions	TR 13				TR 14			
	1	2	3	4	1	2	3	4
1 Human-likeness	1				1			
2 Eeriness	0.015	1			0.150	1		
3 Fear	-0.060	0.930**	1		-0.157	0.789**	1	
4 Disgust	-0.434**	0.498**	0.589**	1	-0.031	0.375**	0.504**	1
5 Attractiveness	0.476**	-0.310*	-0.329**	-0.537**	0.319**	-0.201	-0.114	-0.411**

p* < 0.05; *p* < 0.01

negative emotions (eeriness, fear, disgust) was examined. Correlational analyses were conducted between familiarity and negative emotions and relationships were computed using bivariate Pearson analysis (see Table 3). When facial expressions were examined according to the familiarity dimension that evoked negative emotions, it was found that emotional appearance was more effective in TR 13 and TR 14 compared to TR 6 and TR 9 versions.

The characters were analyzed through emotions, which is the second determinant in the case of exposure to the uncanny valley. Considering the emotional states of the participants towards the characters, it was seen that there was a significant difference in human-likeness status between the character in TR 6 and the character in TR 9. Similarly, differences were observed in human-likeness status between TR 6, TR 13, and TR 14, while no difference was found in familiarity status. A significant difference was determined between TR 9 and TR 13 as well as between TR 13 and TR 14 in both dimensions.

This correlation analysis aims to define the emotions efficient in the emergence of the uncanny valley effect. For this aim, inverse relationships among the emotions in the correlation have been taken into consideration. According to Table 3 as a result of the correlation analysis, it has been determined that there is an inverse correlation *r* between the variables of human-likeness that represents positive emotions and fear (*r* = -0.297; *p* < 0.05) in version TR 6 that contains the least uncanny valley effect, and between human-likeness and the emotion eeriness (*r* = -0.246; *p* < 0.05) in the version TR 9. It has also been determined that

there is an inverse correlation between attractiveness that represents positive emotions of the characters in the version TR 13 in which the uncanny valley effect was measured at a high level and eeriness (*r* = -0.310; *p* < 0.05). It has been stated that there is no meaningful statistical correlation among the other variables because negative emotions such as eeriness, fear, and disgust may be confused with each other as these kinds of emotions have transitivity at a high rate.

Facial expressions that are the elements of non-verbal communication are the most basic elements of interpersonal communication. Many emotions that cannot be explained through words are transferred by facial expressions. People’s expressing their feelings and thoughts with gestures creates a more realistic effect than words. Especially with the technological developments in the designs of the character, with the higher resolution modeling, the emotions of the characters appear more clearly. According to RQ4, when the physical appearances of the character and emotional appearances are compared (Table 4), no significant difference was observed between the physical appearance average scores according to human-likeness. From the results of the study, it has been concluded that the point averages of physical appearance are higher than the point averages of sensory appearance. It has been found that the value of familiarity of the physical appearance in TR 14 in which the uncanny valley effect has been observed is low as compared to the other versions (*M* = 1.886).

Human-likeness and familiarity, the two variables used to measure the uncanny valley, were calculated separately for the experimental and control groups. In

Table 4: Descriptive statistics for the study variables in experiments 1 and 2 (where M denotes mean value and SD standard deviation)

Variable	Physical appearance				Emotional appearance			
	Human-likeness		Familiarity		Human-likeness		Familiarity	
	M	SD	M	SD	M	SD	M	SD
TR 6	2.597	0.974	2.134	1.065	0.231	0.266	0.351	0.418
TR 9	2.384	0.773	1.955	1.003	0.649	0.477	0.522	0.456
TR 13	2.313	0.859	2.592	1.233	1.090	0.577	0.448	0.453
TR 14	2.511	0.593	1.886	0.953	1.067	0.583	0.642	0.425

Table 5: Comparison between experimental and control groups by One-Way ANOVA (where n denotes number of participants, M is for mean value, SD is for standard deviation, and t and p are statistical values)

Game	Uncanny valley effect	Group	n	M	SD	t	p
TR 6	Human-likeness	Exp.	32	1.703	0.560	17.218	0.554
		Cont.	35	1.419	0.557	15.081	
	Familiarity	Exp.	32	2.042	1.113	10.376	
		Cont.	35	2.219	1.028	12.764	
TR 9	Human-likeness	Exp.	32	2.172	0.624	19.689	0.715
		Cont.	35	1.943	0.688	16.703	
	Familiarity	Exp.	32	1.823	0.927	11.122	
		Cont.	35	2.076	1.066	11.518	
TR 13	Human-likeness	Exp.	32	2.125	0.696	17.273	0.326
		Cont.	35	1.743	0.747	13.813	
	Familiarity	Exp.	32	2.428	1.171	11.723	
		Cont.	35	2.743	1.286	12.617	
TR 14	Human-likeness	Exp.	32	2.375	0.635	21.174	0.756
		Cont.	35	2.157	0.616	20.711	
	Familiarity	Exp.	32	1.823	0.817	12.628	
		Cont.	35	1.943	1.071	10.731	

the calculation of the human-likeness value, the mean scores of the reality level, body proportions, and attractiveness level were taken, while when measuring the familiarity values, the disturbing elements on the character’s face, and emotional appearances (eeriness, fear, disgust) score averages were taken. The following section addresses the study’s fifth research question. The findings obtained on the RQ5 showed that the effect of the uncanny valley is different between those who look at a game character for the first time and those who look at the character again after playing the same game for a certain period. The difference between the opinions of the participants in the experimental group that played games for a length of time and the opinions of the participants in the control group that didn’t play any games has been evaluated according to the analysis of One-Way ANOVA (Table 5).

This analysis was used for dependent groups to reveal the uncanny valley effect of the control group and experimental group students and whether there was any difference before and after the experimental proce-

dure. According to the results of the analysis in Table 5, it was found that the uncanny valley effect scores of the students in the experimental group where the game was applied for one hour and the control group students who did not apply the same procedure differ at a certain level, but not at a statistically significant level ($p < 0.05$).

As seen in Figure 2, it was revealed that the students in the experimental group had a less uncanny valley effect compared to the control group in TR 13 and TR 14 games with more realistic graphics.

As a result, when Figure 2 is examined, it is seen that the data obtained from both groups are consistent with each other and the effect occurs at a certain level in both. Because the uncanny valley is an instant effect, after a certain period of exposure, the effect decreases. The uncanny valley effect is at its highest for participants who see the character for the first time. Eyewear occurs after a player plays the game for a certain period and there is a slight change in the perspective of the character.

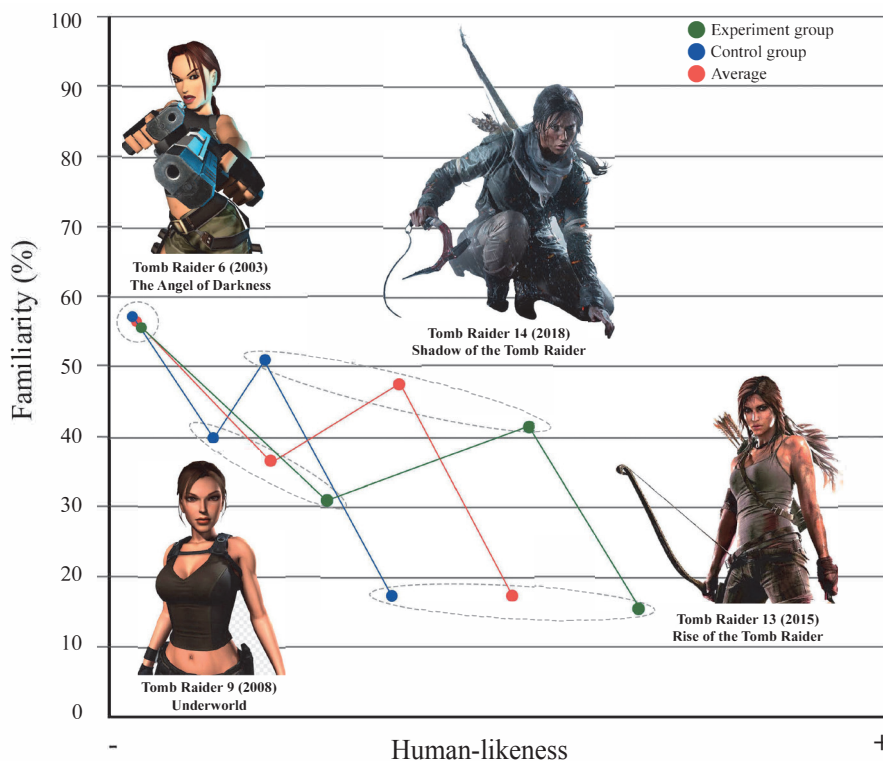


Figure 2: Ratings for the uncanny valley effect by the experimental and control group of students

4. Discussion

As in other media products, digital games need creativity and rationality in the game as well as the fantasy of the game and the characteristics of the characters in order to attract the masses to the game (Walkerdine, 2007, p. 9). The developments in computer technology and the applications developed at the same pace have enabled the creation of virtual images that are hard to distinguish from reality. The ability to reflect the appearance and movements of the characters as real as possible has been made possible by the developments in technology in the last decade. While the characters look humanoid, designers need to take into account the effects of virtual images that can make motor movements similar to facial expressions and human movements. The aim of the figures with a realistic appearance to reflect the reality of all details enriches the visual language and limits the designers to determine their personal preferences in the content creation process. It offers some suggestions regarding the issues that video game designers should pay attention to in the process of making the characters appear realistic to the desired extent.

Lara Croft is recognized as a source of self-empowerment for women, a feminist icon, and a huge step towards gender equality in games. With the transfor-

mation of popular culture into mass culture, digital games have become an important tool in reflecting the identity and cultural values of individuals. In general, players reach satisfaction by reflecting their social and psychological needs in their daily lives to the game content. Today, many types of research are carried out on the effects of digital games on people’s behavior, as in traditional media environments that appeal to millions of people. These researches are used to contribute to the development of the content quality of games, as well as to determine the positive and negative effects on people. It has shown that male characters are at the forefront in gender-based approaches, which have an important place among these studies, and have a determining effect on the outcome of the game even if they are not in the main dominant role. As in all fields of art, it is a pleasure to look at naked women in games, because the female body is one of the most important tools in the formation of admiration and aesthetics. As a symbol of passion and lust in women’s games, it has remained within the framework of this dominant view in patriarchal systems for ages. It is observed that especially the self-expression problem of women is also effective in games. Woman plays an active role in shaping gender-related attitudes under the pressure of men. Nowadays, it is seen that the female body is under the control of men, and roles and duties are given by men in games where mythological subjects are usually

taught. Thus, the powerful and sexy body woman was given a new identity, and this identity was interpreted together with her natural beauty.

In another part of the research, various physical characteristics of the character were evaluated by considering the short videos of the character. It has been determined that the character who appears to be the strongest in this episode is the character with the highest effect of the uncanny valley. Strength is measured by clearly drawing a character's muscular structure. Another factor is the physical reactions of the character in situations that require physical power. With the development of animation technologies such as motion capture, motion elements that are very close to humans have become transferable to the character. While analyzing the aesthetics of many important characters such as Lara Croft, the continuity of the traditional design in previous games and the success of the character in the role in the game are taken into account. Therefore, design analysis should not be considered independent of the character's background. Nowadays, in order to attract the attention of the players, the value perception of the scenario and characters may change according to the user trend. Gender perception sees men as suitable for higher status roles because society considers them to have the qualities necessary for leadership. The character of Lara, who has a free spirit due to her profession, was drawn with a sexy body, especially in the first versions, under the pressure of social morality in the male-dominated order. Generally, the one-piece outfit that covers the whole body emphasizes the operational abilities and sexuality of the characters. With the shirt, covered with armor in the shoulder and neck area, military canvas style trousers, boots, and a blue beret she has a look of a soldier who is ready for duty. This situation is like the projection of an idea in which interest was built on sexuality in the early stages of the game world. The same attitude caused the denial and lockdown of all sexual practices that are the obstructive force of the dominant discourse. The rulership created a detailed template of the sexual act and determined the distribution of all sexual identity roles through the video game character.

5. Conclusion

In this study, the design evolution of Lara Croft, who has found an important place in the video game world, has been evaluated in terms of exposure to the uncanny valley. The game designer, who takes advantage of the opportunities provided by modern technology, tries to adapt the quality and intense data provided by photography and video images to his/her works. The theory is built on the fact that humans empathize with the humanoid features of robots or prostheses with anthro-

pomorphic features. Each of these elements provides important clues for the companies that develop the games and the people researching the games to measure the short- and long-term effects. In this research, participants were asked to evaluate the game character both visually and sensually. In the first evaluation, the realism levels were tried to be determined by examining the character designs only through photographs. The results of this analysis revealed the human-likeness and familiarity position of the characters specified in the uncanny valley methodology. Looking at the designs according to this point, the negative emotions that occur and cannot be defined, that is, the exposure to the uncanny valley can be determined. The concept includes negative emotions such as fear, disgust, hate, and startle, as well as unfamiliarity (alienation), which gives a feeling of discomfort. According to these results, TR 6, which has a more stylized design, appears to be the character with the lowest uncanny valley effect. The TR 13 character, where this effect is at the highest level, has a very realistic design. It is a state of behavior and thought that occurs instantly in a state of antipathy, which includes negativities and negative attitudes in response to a situation. While a person displays this attitude, he/she seeks to produce valid reasons for his/her actions and thoughts. The results showed that semi-realistic characters had a greater impact on players being exposed to the uncanny valley than cartoony or realistic characters (Kätsyri, Mäkäräinen and Takala, 2017). It was also revealed in this work that especially stylized characters have less frightening features for humans. Besides the visual features, characters who can think and act like real people can be designed with the possibilities of artificial intelligence technologies in games. It was found that as the uncertainty of the disturbing elements increased, the tendency to be exposed to the uncanny valley increased as well. In body language, eyes are the most obvious indicator for expressing emotions. It enables the classification and detection of emotional state (emotion) analysis, mental state, and different emotions from eye movements. When asked about the disturbing elements on the faces of the four characters selected from the participants in this study (Figure 1), it was determined that TR 6 and TR 9 characters have certain disturbing elements such as eyes, mouth, and hair. In the characters in TR 13 and TR 14, which have more realistic designs, it was observed that the disturbing elements were more ambiguous. According to these results, it was found that the exposure to the uncanny valley increases in realistic designs where the gruesome elements are uncertain. Many studies in the literature have shown that pupil size changes in size can be noticed during different kinds of emotional stimulation (Kinner, et al., 2017; Chen, et al., 2010; Reuten, van Dam and Naber, 2018). According to the analysis results, the eye features of the TR 13 and TR 14 characters, which have a high tendency to be exposed

to the uncanny valley, were found to be less disturbing by the participants compared to the TR 6 and TR 9 versions. Especially in the recently developed Lara Croft characters such as TR 13 and TR 14, this effect is highly visible. As a result of this research, it was determined that there is a direct relationship between human-like appearance and attractiveness, as in a similar study in the literature (Schneider, Wang and Yang, 2007). Unlike similar research, no link could be established between the level of authenticity and reality. Although especially stylized characters are seen as more sympathetic to people than realistic or semi-realistic characters, sufficient data could not be found to generalize. In the last part of the study, emotional states were examined by revealing the effect of the uncanny valley. A lot of fictional element in the game has a key role in integration between the fictional world and the real world. This section aims to classify the immediate negative emotions that occur in the players' behavior. The sense of attractiveness is evaluated in the human-likeness category and the familiarity category in various emotions such as eeriness, fear, and disgust. In familiarity, where negative emotions are generally determinant, a mix of many emotions is experienced.

In addition to being close concepts in terms of their contents, fear, and disgust, the two most influential emotions in the uncanny valley effect, the situation that reveals the feeling of disgust is not very clear to the person. Naturally, people want to stay away from situations they consider dangerous as much as possible, even if they are in this situation, they want to escape and protect themselves. However, the individual who is afraid or feels the feeling of fear for any reason seeks an authority that will surrender him/herself to. Therefore, emotions such as fear and disgust are universal as well as their severity varies according to individual differences. According to the results of the research, it is seen that the negative effects of the uncanny valley such as fear and disgust increase as the physical power features of the character increase.

Likewise, a negative relationship was found between the character's sexy appearance and fear. When a person encounters or imagines what he is afraid of, the intensity of the fear increases and the feeling of disgust is added. It is almost impossible to determine the dominance level of the fear and disgust situations that cause the uncanny valley effect.

References

- Bancroft, T., 2006. *Creating characters with personality: for film, TV, animation, video games, and graphic novels*. New York, USA: Watson-Guptill Publications.
- Bartneck, C., Kanda, T., Ishiguro, H. and Hagita, N., 2009. My robotic doppelgänger – a critical look at the uncanny valley. In: *RO-MAN 2009: Proceedings of the 18th IEEE International Symposium on Robot and Human Interactive Communication*. Toyama, Japan, 27 September – 2 October 2009. IEEE, pp. 269–276. <https://doi.org/10.1109/ROMAN.2009.5326351>.
- Burleigh, T.J., Schoenherr, J.R. and Lacroix, G.L., 2013. Does the uncanny valley exist? An empirical test of the relationship between eeriness and the human likeness of digitally created faces. *Computers in Human Behavior*, 29(3), pp. 759–771. <https://doi.org/10.1016/j.chb.2012.11.021>.
- Cassell, J. and Jenkins, H. eds., 2000. *From Barbie to Mortal Kombat: gender and computer games*. Massachusetts, USA: MIT Press.
- Chaminade, T., Hodgins, J. and Kawato, M., 2007. Anthropomorphism influences perception of computer-animated characters' actions. *Social Cognitive and Affective Neuroscience*, 2(3), pp. 206–216. <https://doi.org/10.1093/scan/nsm017>.
- Chen, H., Russell, R., Nakayama, K. and Livingstone, M., 2010. Crossing the “Uncanny Valley”: adaptation to cartoon faces can influence perception of human faces. *Perception*, 39(3), pp. 378–386. <https://doi.org/10.1068/p6492>.
- Dietz, T.L., 1998. An examination of violence and gender role portrayals in video games: implications for gender socialization and aggressive behavior. *Sex Roles*, 38(5–6), pp. 425–442. <https://doi.org/10.1023/a:101.870.9905920>.
- Dill, V., Flach, L.M., Hocevar, R., Lykawka, C., Musse, S.R., & Sarroglia Pinho, M., 2012. Evaluation of the uncanny valley in CG characters. In: Y. Nakano, M. Neff, A. Paiva and M. Walker, eds. *Proceedings of the 12th International Conference, IVA 2012*. Santa Cruz, CA, USA, 12–14 September 2012. Springer Verlag, pp. 511–513. https://doi.org/10.1007/978-3-642-33197-8_62.
- Flach, L.M., de Moura, R.H., Musse, S.R., Dill, V., Pinho, M.S. and Lykawka, C., 2012. Evaluation of the uncanny valley in CG characters. In: *SBC Proceedings of SBGames 2012*. Brasília, Brasil, 2–4 November 2012. Sociedade Brasileira de Computação, pp. 108–116.
- Freud, S., 1919. The ‘Uncanny’. In: A. Freud and J. Strachey, eds., 2001. *The standard edition of the complete psychological works of Sigmund Freud: volume 17 (1917–1919): an infantile neurosis and other works*. Translated from German under the general editorship of James Strachey. London, UK: Vintage, pp. 217–256.
- Glesne, C., 2011. *Becoming qualitative researchers: an introduction*. 4th ed. Boston, MA, USA: Pearson.
- Gooch, B., Reinhard, E. and Gooch, A., 2004. Human facial illustrations: creation and psychophysical evaluation. *ACM Transactions on Graphics*, 23(1), pp. 27–44. <https://doi.org/10.1145/966131.966133>.

- Hall, C.D., 2016. *The creation process of a stylized character in comparison to a semi-realistic character*. Undergraduate honors thesis. East Tennessee State University.
- Hanson, D., 2006. Exploring the aesthetic range for humanoid robots. In: *Proceedings of the ICCS/CogSci-2006 Long Symposium: Toward Social Mechanisms of Android Science*, Vancouver, Canada, 26 July 2006. Citeseer, pp. 16–20.
- Ho, C.-C. and MacDorman, K.F., 2010. Revisiting the uncanny valley theory: developing and validating an alternative to the Godspeed indices. *Computers in Human Behavior*, 26(6), pp. 1508–1518. <https://doi.org/10.1016/j.chb.2010.05.015>
- Jentsch, E., 1906. On the psychology of the uncanny. Translated from German by R. Sellars, 1997. *Angelaki*, 2(1), pp. 7–16. <https://doi.org/10.1080/09697259708571910>.
- Kaba, F., 2013. Hyper-realistic characters and the existence of the uncanny valley in animation films. *International Review of Social Sciences and Humanities*, 4(2), pp. 188–195.
- Kätsyri, J., Mäkäräinen, M. and Takala, T., 2017. Testing the ‘uncanny valley’ hypothesis in semirealistic computer-animated film characters: an empirical evaluation of natural film stimuli. *International Journal of Human-Computer Studies*, 97, pp. 149–161. <https://doi.org/10.1016/j.ijhcs.2016.09.010>.
- Kätsyri, J., de Gelder, B. and Takala, T., 2019. Virtual faces evoke only a weak uncanny valley effect: an empirical investigation with controlled virtual face images. *Perception*, 48(10), pp. 968–991. <https://doi.org/10.1177/0301006619869134>.
- Kinner, V.L., Kuchinke, L., Dierolf, A.M., Merz, C.J., Otto, T. and Wolf, O.T., 2017. What our eyes tell us about feelings: tracking pupillary responses during emotion regulation processes. *Psychophysiology*, 54(4), pp. 508–518. <https://doi.org/10.1111/psyp.12816>.
- Lucie-Smith, E., 1996. *Visual arts in the 20th century*. London, UK: Laurence King.
- Lundwall, C., 2017. *Creating guidelines for game character designs*. Bachelor thesis. Luleå University of Technology.
- Lynch, T., Tompkins, J.E., van Driel, I.I. and Fritz, N., 2016. Sexy, strong, and secondary: a content analysis of female characters in digital games across 31 years. *Journal of Communication*, 66(4), pp. 564–584. <https://doi.org/10.1111/jcom.12237>.
- MacDorman, K.F., Green, R.D., Ho, C.-C. and Koch, C.T., 2009. Too real for comfort? Uncanny responses to computer-generated faces. *Computers in Human Behavior*, 25(3), pp. 695–710. <https://doi.org/10.1016/j.chb.2008.12.026>.
- Mathur, M.B. and Reichling, D.B., 2016. Navigating a social world with robot partners: a quantitative cartography of the uncanny valley. *Cognition*, 146, pp. 22–32. <https://doi.org/10.1016/j.cognition.2015.09.008>.
- McCloud, S., 1993. *Understanding comics: the invisible art*. New York, NY, USA: William Morrow Paperbacks.
- McDonnell, R., Breidt, M. and Bühlhoff, H.H., 2012. Render me real?: investigating the effect of render style on the perception of animated virtual humans. *ACM Transactions on Graphics*, 31(4): 91. <https://doi.org/10.1145/2185520.2185587>.
- Mikula, M., 2003. Gender and videogames: the political valency of Lara Croft. *Continuum*, 17(1), pp. 79–87. <https://doi.org/10.1080/1030431022000049038>.
- Mohamad Ali, A.Z. and Hamdan, M.N., 2017. The effects of talking-head with various realism levels on students’ emotions in learning. *Journal of Educational Computing Research*, 55(3), pp. 429–443. <https://doi.org/10.1177/0735633116672057>.
- Mori, M., 1970. The uncanny valley. Translated from Japanese by K.F. Sellars and N. Kageki, 2012. *Energy*, 7(4), pp. 33–35. [online] Available at: <<https://spectrum.ieee.org/automaton/robotics/humanoids/the-uncanny-valley>> [Accessed June 2021].
- Murphy, H., 2016. *Effects of female video game character body-idealization exposure*. Master of Arts thesis. University of Minnesota.
- Chiang, I.-C.A., Jhangiani, R.S. and Price, P.C., 2015. *Research methods in psychology*. 2nd Canadian ed. Victoria, BC, Canada: BCcampus. Available through: BCcampus website: <<https://opentextbc.ca/researchmethods/>> [Accessed June 2021].
- Proctor, E.K. and Rosen, A., 2008. From knowledge production to implementation: research challenges and imperatives. *Research on Social Work Practice*, 18(4), pp. 285–291. <https://doi.org/10.1177/1049731507302263>.
- Reuten, A., van Dam, M. and Naber, M., 2018. Pupillary responses to robotic and human emotions: the uncanny valley and media equation confirmed. *Frontiers in Psychology*, 9: 774. <https://doi.org/10.3389/fpsyg.2018.00774>.
- Schneider, E., Wang, Y. and Yang, S., 2007. Exploring the uncanny valley with Japanese video game characters. In: *Proceedings of DiGRA International Conference: Situated Play*. Tokyo, Japan, Septemeber 2007. DiGRA, pp. 546–549.
- Schwind, V., Leicht, K., Jäger, S., Wolf, K. and Henze, N., 2018. Is there an uncanny valley of virtual animals? A quantitative and qualitative investigation. *International Journal of Human-Computer Studies*, 111, pp. 49–61. <https://doi.org/10.1016/j.ijhcs.2017.11.003>.
- Seyama, J. and Nagayama, R.S., 2007. The uncanny valley: effect of realism on the impression of artificial human faces. *Presence: Teleoperators and Virtual Environments*, 16(4), pp. 337–351. <https://doi.org/10.1162/pres.16.4.337>.
- Strait, M.K., Aguilon, C., Contreras, V. and Garcia, N., 2017. The public’s perception of humanlike robots: online social commentary reflects an appearance-based uncanny valley, a general fear of a “Technology Takeover”, and the unabashed sexualization of female-gendered robots. In: *2017 26th IEEE International Symposium on Robot and Human*

- Interactive Communication (RO-MAN)*. Lisbon, Portugal, 28–31 August 2017. IEEE, pp. 1418–1423.
<https://doi.org/10.1109/ROMAN.2017.8172490>.
- Suler, J., 2016. The uncanny in the digital age. *International Journal of Applied Psychoanalytic Studies*, 13(4), pp. 374–379.
<https://doi.org/10.1002/aps.1479>.
- Tinwell, A., 2015. *The uncanny valley in games and animation*. New York, USA: A K Peters/CRC Press.
<https://doi.org/10.1201/b17830>.
- Tinwell, A., Grimshaw, M., Nabi, D.A. and Williams, A., 2011. Facial expression of emotion and perception of the uncanny valley in virtual characters. *Computers in Human Behavior*, 27(2), pp. 741–749. <https://doi.org/10.1016/j.chb.2010.10.018>.
- Tung, F.-W., 2016. Child perception of humanoid robot appearance and behavior. *International Journal of Human-Computer Interaction*, 32(6), pp. 493–502. <https://doi.org/10.1080/10447318.2016.1172808>.
- Wan, C.-S. and Chiou, W.-B., 2006. Psychological motives and online games addiction: a test of flow theory and humanistic needs theory for Taiwanese adolescents. *CyberPsychology & Behavior*, 9(3), pp. 317–324.
<https://doi.org/10.1089/cpb.2006.9.317>.
- Walkerdine, V., 2007. Introduction. In: V. Walkerdine, ed. *Children, gender, digital games: towards a relational approach to multimedia*. Basingstoke, UK: Palgrave Macmillan, pp. 1–15.
- Wallraven, C., Breidt, M., Cunningham, D.W. and Bülthoff, H.H., 2008. Evaluating the perceptual realism of animated facial expressions. *ACM Transactions on Applied Perception*, 4(4): 4. <https://doi.org/10.1145/1278760.1278764>.
- Yin, R.K., 2009. *Case study research: design and methods*. 4th ed. Los Angeles, CA, USA: Sage.
- Yong, Y., 2007. *Facial expression recognition and tracking based on distributed locally linear embedding and expression motion energy*. Master thesis. National University of Singapore, pp. 1–40.
- Zell, E., Aliaga, C., Jarabo, A., Zibrek, K., Gutierrez, D., McDonnell, R. and Botsch, M., 2015. To stylize or not to stylize?: the effect of shape and material stylization on the perception of computer-generated faces. *ACM Transactions on Graphics*, 34(6): 184. <https://doi.org/10.1145/2816795.2818126>.
- Złotowski, J., Proudfoot, D., Yogeewaran, J. and Bartneck, C., 2015. Anthropomorphism: opportunities and challenges in human–robot interaction. *International Journal of Social Robotics*, 7, pp. 347–360.
<https://doi.org/10.1007/s12369-014-0267-6>.

TOPICALITIES

Edited by Markéta Držková

CONTENTS

News & more	135
Bookshelf	137
Events	143

News & more

Recently completed projects funded under Horizon 2020

Besides the selected projects that are introduced in more detail in the following sections, the Horizon 2020 projects funded till past months include, for example, SILENSE, developing (ultra)sound interfaces and low energy integrated sensors by combining conventional silicon technologies with printed flexible, large-area electronics, HoliFAB (Holistic digital-to-physical prototyping and production pilot for microfluidic MEMS), SmartLine (Smart in-line metrology and control for boosting the yield and quality of high-volume manufacturing of organic electronics), iPES-3DBat (Innovative polymeric batteries by 3D printing), FLUID (Functional low-intensity light upconverting inks for everyday applications), and several bioprinting projects. The projects supporting business innovation, which started in 2018 and have been completed in recent months, include FoodiniPro (The connected 3D food printer appliance for every kitchen), HelpingHAND (A 3D printed, affordable myoelectrical prosthetic hand of personalizable size for optimal comfort and functionality), and TUMOURPRINT (High throughput bioprinting of tumour models for drug development and oncology research).

GrapheneCore2 – Graphene Flagship Core Project 2

This project with a budget of 88 mil. EUR represents the third stage of the EC-funded part of the Graphene Flagship, which is coordinated from Sweden by the Chalmers University of Technology. More than 150 partners are taking part in the core project, and the number of associated members, mostly industrial, has grown over 90. Almost nine hundred peer-reviewed articles published within GrapheneCore2 include an extensive open-access review of 2D materials named 'Production and processing of graphene and related materials', with 70 co-authors and over 1 500 references. Among other outcomes, there are dozens of reports on various technological aspects of graphene and related materials, models for pH and ionic strength graphene charge-neutrality point and for current–voltage characteristics for graphene solution-gated field-effect transistors implemented in MathWorks MATLAB, multianalyte sensing demonstrator, nano-oscillator prototype, textile demonstrator, demonstrators of anti-corrosion coatings and photocatalytic coatings for air or water remediation in real-life conditions and building materials, and the graphene-perovskite solar park in Crete.

In October 2020, the project 2D-EPL – Graphene Flagship 2D Experimental Pilot Line was launched to enable prototype production of electronics, photonics and sensors based on graphene and related layered materials.

INNPAPER – Innovative and smart printed electronics based on multifunctionalized paper: from smart labelling to point of care bioplatfoms

This long-term project being completed this June has been coordinated by the CIDETEC organisation based in Spain. Contributing to the research and innovations towards paper-based electronics, the project involved the design and manufacturing of the platform integrating battery, display and a near-field communication system printed on a multifunctional paper sheet

New Intergraf publications

 Intergraf, the European federation for print and digital communication, has recently released its regular annual reports and also five guidance documents to help printers and other related companies comply with the new legislation and implement the necessary measures.

The 2021 Intergraf Economic Report summarises the available statistical data for the graphic industry in the European Union, United Kingdom, Norway and Switzerland. The first part briefly overviews the current global and European economic situation, provides information on the European graphic industry in terms of its profile, labour costs, production value and trade figures, and reviews the development in print markets and 12 selected countries. Namely, it includes the reports from Belgium, Bulgaria, Denmark, Germany, Italy, Latvia, Lithuania, Luxembourg, The Netherlands, Norway, Portugal, and Sweden. The second part consists of the European print market review for 2020–2025 provided by Smithers and the post-Brexit UK print market review provided by the British Printing Industries Federation.

The documents reflecting recent changes to legislative requirements and best practices relevant to the graphic arts industry include the Guide to the EU Ecolabel for Printed Paper, covering a new set of criteria focusing on the main environmental impacts throughout the lifecycle of the printed paper products that was adopted in November 2020, the Guide to the Authorisation of Chromium Trioxide Use for Gravure Printers, granted by the European Commission in December 2020, the Guide to the EU-UK Trade and Cooperation Agreement, which provides information about the main provisions for trade between EU and UK companies, such as customs, VAT

and the rules of origin requirements, the document named BAT in Heatset: Practical and Legal Guidance, dealing with the best available techniques conclusions as established in the Commission Implementing Decision (EU) 2020/2009 under Directive 2010/75/EU on industrial emissions, which are applicable to heatset plants, and the Guide to Applying Food Contact Materials Legislation, prepared in cooperation with the Flexographic Technical Association Europe. The first three guidance documents published since last December are only available for Intergraf members, while the last two can be downloaded from the Intergraf website, including the Solvent Mass Balance/Solvent Management Plan Template in Excel sheet.

A complete overview of the work carried out during the past year and the future outlook can be found in the Intergraf Activity Report for the period from June 2020 to May 2021.

The winners of the TAGA student awards

This time, the Technical Association of the



Graphic Arts invited the students from the schools worldwide to submit their work to competitions.

While the winners of the student poster and student research journal competitions are yet to be announced, the winners of the individual awards for 2021 are already known.

Based on the scores for relevance, technical content, clarity, discussion, bibliography, and charts/graphs/illustrations, Samantha Stante from Ryerson University (Toronto, Canada)

has won the Harvey Levenson Undergraduate Student Paper Award for her paper 'What Impact do the

Accessibility Features of Colour and Contrast, Text-to-Speech, and Magnification in ePublications Have on Undergraduate Students' Ability to Retain Information?', and Maayane Lugassy from Grenoble INP Pagora (Grenoble, France) has won the Dusty Rhodes Graduate Student Paper

Award for her paper 'Study of the Behavior of Cadmium-Free Quantum Dots in Functional Inks'.

by screen-printing to be used in three use-cases. These comprise smart labels for food packaging that include humidity, temperature and pressure sensors, point-of-care quantitative immunoassays for drug and caffeine detection in saliva and drinks, respectively, and point-of-care genetic assays for rapid diagnosis of infectious diseases (influenza virus and Streptococcus bacteria). Collection, display and cloud storage of the data can be accomplished using a free smartphone application.

NanoTextSurf – Nanotextured surfaces for membranes, protective textiles, friction pads and abrasive materials

This three-year project coordinated by VTT, Technical Research Center of Finland, and completed in November 2020 aimed to upgrade the existing pilot lines for manufacturing and demonstrating nanotextured surfaces with mechanically enhanced properties through the application of cellulose nanomaterials by cast coating, foam coating and screen-printing. Among the studied products, the development of barrier coating based on microfibrillated cellulose and two novel abrasive materials using cellulose nanocrystals as additives and applied on textile and plastic substrates, respectively, continues in three industrial-scale implementation projects.

SeSaMe – Sustainable routes for smart photonic materials

This long-term project started in 2015 and finished this March received the European Research Council Starting Grant and was hosted by The Chancellor, Masters and Scholars of the University of Cambridge. The interdisciplinary research studied the assembly and optical response of natural materials, cellulose and chitin, to allow the production of low-cost, biodegradable photonic materials. The findings were published in almost 40 scientific articles, two book chapters and a doctoral thesis. The outcomes include the successful fabrication of cellulose-only coloured particles that can be used as bio-compatible and edible pigments.

NANOGEN – Polymer-based piezoelectric nanogenerators for energy harvesting

This is another project hosted by The Chancellor, Masters and Scholars of the University of Cambridge and funded by the European Research Council Starting Grant. It was focused on nanoscale piezoelectric energy harvesters based on ferroelectric polymers. During five years from 2015 to 2020, the researchers identified suitable piezoelectric polymers and incorporated them into scalable nanogenerator devices through the use of novel additive manufacturing routes. See also the doctoral thesis 'Aerosol-jet printed nanocomposites for flexible and stretchable thermoelectric generators' presented in the previous issue of JPMTR.

Photomechanics – Photomechanical printing in Europe in the mid-19th century: History, theory, visual culture, science and the international network in the 1840s–1860s

This project coordinated by De Montfort University (UK) illustrates that not all resources are directed towards innovations. One of the outcomes of the research supported through a one-year individual fellowship grant till September 2020 is an open-access online database with visual and textual data about preserved incunabula and other relevant visual and written documents identified in dozens of collections. Some early experiments to reproduce daguerreotypes are introduced by an online exhibition.

Bookshelf

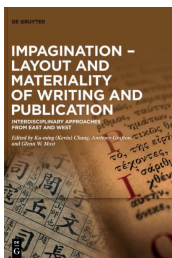
Impagination – Layout and Materiality of Writing and Publication Interdisciplinary Approaches from East and West

This work deals with the placing of text and other content onto a carrier medium, investigating the type of page or another corresponding unit, its written or printed content, and the way the content elements, including graphics, are spatially arranged. That all the authors express by the title word, impagination. The book considers various aspects of local conventions and traditions of impagination, bringing a global comparison of the relations between materials and formats as well as between formats and layouts. It pays attention to the extent of paratextual information and discusses the importance of psychological aspects, social practices, textual genres and other influences for adaptation of existing approaches or invention of the new solutions.

After the introduction, the book includes 13 chapters written by the editors and other 10 authors. The five chapters of the first part describe the impagination before and up to the paged codex format. Namely, the authors examine ancient Greek and Roman layouts from the early ones on papyrus rolls to the late ones on parchment in codices, the development of the form and layout of the Hebrew Bible, early Chinese texts from those on bamboo slips to paper editions, the evolution of the page layout of Tibetan Kanjurs based on the analysis of different loose-leaf editions of the Tibetan Vimalakīrtinirdeśa dating from before 1035 to 1934, and the impagination practices in South Asia, in particular, in the early Hindi manuscripts from the 14th through early 17th centuries.

The second main part, named The Printed World, examines reader's drawings on the margins of early printed pages in Renaissance Europe, Samgangaengsildo, the Korean book on ethics, particularly its version from 1505 with three narratives (two textual, in Chinese and Korean scripts, and one pictorial) and their mutual interaction on the printed page, the evolution of the typical page in the hand-press era till the beginning of the industrial revolution in the Southern Netherlands, the specific layout of some woodblock-printed books in early modern China, two typical layouts for different layers of Chinese texts, i.e. the pages with two or three horizontal sections and the pages with two columns of small characters inserted into the primary text, the ambilingual design in Chinese/Manchu language reference manuals, and the changes in the layout of pages with transformations in media in Japan.

The last part comprises only one chapter that investigates the latest practice of scientific publication, which is going online, beyond the physical page. Today, scientists commonly access periodical publications in digital format on the internet. This shift is connected with various advantages, including the earlier access to the articles prior to their hard-copy publication, instant updates of publication metrics, and multimedia content taking the visual supplements to a new level.



Editors: *Ku-ming (Kevin) Chang, Anthony Grafton, Glenn W. Most*

Publisher: De Gruyter

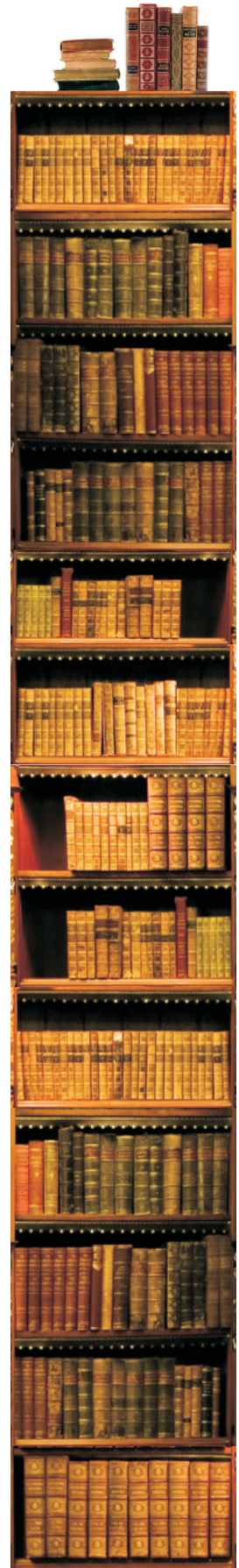
1st ed., January 2021

ISBN: 978-3-11-069846-6

428 pages, 83 images

Hardcover

Available also as an eBook



Coding Art The Four Steps to Creative Programming with the Processing Language

Authors: Yu Zhang, Mathias Funk

Publisher: Apress
1st ed., January 2021
ISBN: 978-1484262634
296 pages, 33 images
Softcover
Also as an eBook



This book published in the Design Thinking series is aimed at artists and designers rather than computer scientists. The first part explains the basics of creative coding – the types and properties of visual elements, canvas transformations, animation and the interactive input, composition and structure, as well as the more advanced options, such as working with noise or using functions, up to the artwork completion, testing and deployment. The second part presents the practical example. The last part is focused on coding practice and advises how to deal with problems, gain advanced skills and improve the creative processes.

Programming Media Art Using Processing A Beginner's Guide

Author: Margaret Noble

Publisher: CRC Press
1st ed., December 2020
ISBN: 978-0367509590
248 pages, 278 images
Hardcover
Also as an eBook



This is another book that introduces visual design using the Processing language. Each of its eight chapters provides the series of lessons with step-by-step examples, starting with the basic overview and then showing how to create responsive environments, automated animations and animated collages, employ conditional interactions and rollovers, develop simple games and work with multilevel architectures and arrays. The project examples are available from the publisher's website.

Principles of Image Printing Technology

Principles of Image Printing Technology written by Yuri Kuznetsov provide a comprehensive overview of the challenges of prepress in the graphic arts industry. The book allows the reader to enter the problematics from a historical point of view up to the current state-of-the-art solutions used in graphic arts. The selected topics are described in-depth both in terms of technical fundamentals and industrial procedures. While some problematics the author explains more in detail, the others are described only superficially. The book is structured into 14 chapters, which cover topics such as image processing, halftoning and related screening techniques, basics of colorimetry, colour management, colour reproduction, basics of optics, film and plate image setters principles, image capturing and sampling, image processing, etc. The book includes quite a large number of images and illustrations, which is helpful for the understanding of the content. On the other hand, it is obvious that the book suffers from insufficient editorial care – not appropriate sorting of the chapters is present, and some information/problematics are spread too much within the whole publication instead of being collected to one chapter. A flaw in the beauty of the book is given by the low quality of some images; some are even distorted, which is not appropriate for such type of publication. The overall high educational value of the book is complemented by the short tests included after every chapter, which are beneficial for the evaluation of the understanding of learned problematics. Overall, the book is for students and readers interested in graphic arts, especially in terms of prepress and related fundamentals.

Book review by Tomáš Syrový, University of Pardubice

Author: Yuri V. Kuznetsov

Publisher: Springer
1st ed., February 2021
ISBN: 978-3-030-60954-2
382 pages, 207 images
Hardcover
Available also as an eBook

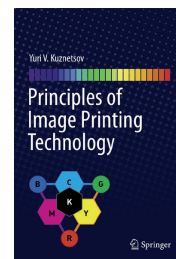


Image and Signal Processing

This volume presents 40 papers selected from submissions to the 9th International Conference on Image and Signal Processing, ICISP 2020, which was cancelled due to COVID-19. The topics include, among others, extraction and recognition of Bangla texts from natural scene images using convolutional neural networks, logo detection using fuzzy clustering algorithm and texture features, and image watermarking based on Fourier-Mellin transform.

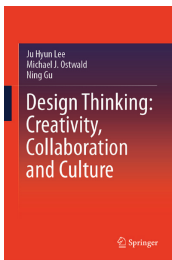
Editors: Abderrahim El Moataz, Driss Mamass, Alamin Mansouri, Fathallah Nouboud

Publisher: Springer
1st ed., July 2020
ISBN: 978-3-030-51934-6
400 pages, 179 images
Softcover
Available also as an eBook



Design Thinking Creativity, Collaboration and Culture

The authors of this book explore the design process supported by digital design environments and provide insight into various strategies of design thinking, which is seen as critical for facing the complex challenges of the present world successfully. The introduction defines the concept of design thinking and presents the research methods employed to gain an understanding of the cognitive operations that occur in design thinking, namely the protocol analysis and expert panel assessment. Three parts then deal in detail with design thinking in terms of creativity, collaboration and culture, as summarised in the fourth, concluding part.

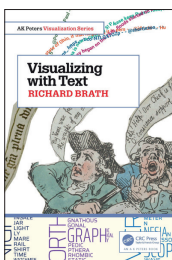


Authors: Ju Hyun Lee, Michael J. Ostwald, Ning Gu

Publisher: Springer
1st ed., August 2020
ISBN: 978-3-030-56557-2
263 pages, 40 images
Hardcover
Available also as an eBook

Visualizing with Text

In this book from the AK Peters Visualization Series, the author builds on the relevant research and literature sources as well as on his long experience in data visualisation and visual analytics. The book presents the text as an integral part of visualisation, beyond the simple support of graphical representation. The content is organised into four parts. The first one documents why to visualise with text, providing the examples from cartography, typography, tables, science classification and notation, code editors, alpha-numeric charts, art and poetry, graphic design and advertising, comics, post-modern text, and also from data visualisation, such as knowledge maps or real-time visualisations. It also defines the design space of visualisation with text and overviews the attributes that can be used. The second part presents the use of text for point labels, in stem-and-leaf distribution plots and as the microtext lines, for example, in the line charts with many series. The third part deals with the applications of text formatting to better discriminate multiple sets and categories, convey information in maps and ordered data visualisations, or visualise ratios and quantitative data. Finally, the last part demonstrates how to treat text layouts to enhance reading, facilitate skimming, help with correct pronunciation, spelling and prosody, use the so-called spark words to encode different kinds of data, and more. The book is illustrated with both historical and present examples from various fields, with more material available on the author website.

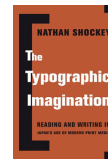


Author: Richard Brath

Publisher: CRC Press
1st ed., November 2020
ISBN: 978-0-367-25930-3
298 pages, 146 images
Hardcover
Available also as an eBook

The Typographic Imagination Reading and Writing in Japan's Age of Modern Print Media

Author: Nathan Shockey



Publisher: Columbia
University Press
1st ed., December 2019
ISBN: 978-0231194280
336 pages, Hardcover
Also as an eBook

This study draws on extensive archival research mapping the commercial print revolution in Japan around the turn of the 19th century into the 20th and through the first decades of the latter when print media, cheap and available, have become a natural part of everyday life. The work examines diverse forms of print and their uses, documents the emergence of new forms of reading, writing and thinking and discusses the related transformation of media and social discourse in modern Japan.

Graphic Design Rules 365 Essential Design Dos and Don'ts

*Authors: Sean Adams, Peter Dawson,
John Foster, Tony Seddon*



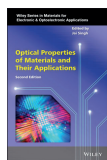
Publisher: Princeton
Architectural Press
2nd ed., April 2020
ISBN: 978-1616898762
384 pages
Softcover

This guide provides practical tips for working with type and typography, layout and design, colour, images and graphics, production and print, and design practice. Each advice is defined on one page and accompanied with the explanatory text as well as the illustration that helps to get the point quickly. This collection might be helpful for both beginners and practitioners – while some of the rules are present in virtually every book on graphic design, some are far less obvious. The revised edition presents the rules in a clear and neat style, abandoning the “thou shall” tone of the original edition, which had discouraged some readers.

Optical Properties of Materials and Their Applications

Editor: *Jai Singh*

Publisher: Wiley
2nd ed., January 2020
ISBN: 978-1119506317
672 pages
Hardcover
Also as an eBook



This comprehensive book overviews the fundamental optical properties of materials in general and then the optical properties of disordered condensed matter and glasses. Further, it explains the concept of excitons and photoluminescence and presents the photoinduced changes in noncrystalline semiconductors and chalcogenide glasses. Next, it deals with photonic crystals and glasses, organic semiconductors, thin films, excitonic processes in quantum wells, and diluted magnetic semiconductor nanostructures. The current edition includes the advances since the original one in 2006 and adds new chapters on transparent white organic light-emitting diodes, quantum dots, perovskites, and characterisation by spectroscopic ellipsometry. Also, it discusses the kinetics of the persistent photoconductivity in crystalline III–V semiconductors.

Biomaterials- and Microfluidics-Based Tissue Engineered 3D Models

Editors: *J. Miguel Oliveira, Rui L. Reis*

Publisher: Springer
1st ed., April 2020
ISBN: 978-3030365875
182 pages, 42 images
Hardcover
Also as an eBook



In 10 chapters, this book covers the microfluidic devices and 3D printing strategies for in vitro models of bone, processing of biomaterials, organs-on-a-chip, patient-on-a-chip models and liver models, and presents the use of microfluidic systems in studies on the central nervous system, angiogenesis and cancer, as well as for drug discovery and testing.

Reactive and Functional Polymers Volume One: Biopolymers, Polyesters, Polyurethanes, Resins and Silicones Volume Two: Modification Reactions, Compatibility and Blends Volume Three: Advanced materials Volume Four: Surface, Interface, Biodegradability, Compostability and Recycling

These four volumes published last year cover a wide range of types and applications of reactive and functional polymers together with their reactions, properties and processing. Among others, the topics include biodegradable and functional synthetic polymers in nanomedicine, reactive modification of fibre polymer materials for textile applications, lignin as a natural antioxidant and as a coating and curing agent, and functional biobased composite polymers for food packaging applications in Volume One, compatibilisation and crosslinking of polymer blends, functional hydrogels, grafting of polymers, and reinforced polymers for electroactive devices in Volume Two, active packaging films based on polyolefins modified by nanoparticles, smart and shape-memory polymers, circularly polarised luminescent polymers as emerging materials for photophysical applications, and polymers for dental applications processed by 3D printing in Volume Three, and surface functionalisation of polymers, polymer interface reactions, switchable and supramolecular polymers for bio-interface applications, recycling of reactive and functional polymers, and the parameters influencing the degradation of reactive polymer-based materials in Volume Four.

Editor: *Tomy J. Gutiérrez*

Publisher: Springer
1st ed., August & October 2020
ISBN: 978-3-030-43402-1 & 978-3-030-45134-9
& 978-3-030-50456-4 & 978-3-030-52051-9
438 & 372 & 217 & 261 pages, 170 & 155 & 135 & 110 images
Hardcover
Available also as an eBook

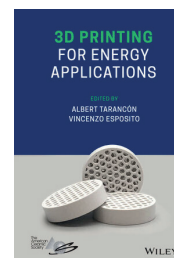


3D Printing for Energy Applications

The first part of this new book presents 3D printing of functional materials, namely metals, ceramics and polymer composites with strain-sensing and self-heating capabilities. The second one discusses the challenges for 3D printing of complex objects, dealing with computational design, multicomponent and multimaterial printing, tailoring component properties and new production concepts. The third part reviews 3D printing of different energy devices, including capacitors, solar cells, fuel cells, electrolyzers, turbomachinery components, thermoelectrics, and possible use for carbon capture.

Editors: *Albert Tarancón, Vincenzo Esposito*

Publisher: Wiley
1st ed., April 2021
ISBN: 978-1-119-56075-3
400 pages
Hardcover
Available also as an eBook



Bookshelf

Academic dissertations

Electromechanical Modelling and Control of Ionic Electroactive Polymer Actuators

This thesis contributes to the research of ionic electroactive polymer materials that can be applied in sensors or actuators. In particular, it addresses their dynamic behaviour by developing an enhanced electromechanical model helping to understand the charge storage kinetics and to predict the bending displacement. It also explores the more straightforward method for the fabrication of soft manipulators and proposes the control techniques for their real-time application. The main content of the dissertation is organised into five chapters. The first of them provides an overview and classification of ionic electroactive polymer actuators and explains the actuation mechanism in the case of carbon-polymer composite and poly(3,4-ethylenedioxythiophene) poly(styrene-sulfonate), PEDOT:PSS. The next one deals with the electro-chemo-mechanical model using the finite element method, which considers the ion transport process, the influence of electrode porosity, the electrochemical kinetics, namely the capacitance of the electric double layer, as well as the redox process for actuators based on conducting polymers, the conditions for charge and material balance, and the mechanical response. This chapter also includes the experimental verification of the electrochemical and electromechanical simulation for actuators from both types of materials. Two chapters then present the development, fabrication and characterisation of a novel soft parallel manipulator utilising four actuators to move the platform with three degrees of freedom. First, the designed manipulator was manually fabricated with the carbon-based electrodes made using spray coating. Then, the manipulator with the PEDOT:PSS electrodes was printed using the syringe-type extrusion system. The performance of both manipulators is compared on the basis of the analysis of their response. Finally, for the printed manipulator, the open-loop application as a four-way optical switch and the closed-loop application as a microscope stage are demonstrated.

Compact Modeling and Physical Design Automation of Inkjet-Printed Electronics Technology

Considering the lack of specific design tools and the resulting gap between technology development and circuit design in the area of printed electronics, the concern of this thesis was to provide the models and tools for the standard design flow and electronic design automation to foster the development of inkjet-printed electronics technology, with a particular focus on the electrolyte-gated transistors with inorganic channel material.

The dissertation provides the background on printed electronics, sources of variability in inkjet-printed electronics, especially the coffee-ring effect, drop coalescence and nozzle issues, the electrolyte-gated transistor technology and the fabrication process employed. Also, it discusses the current design flow challenges. Modelling and physical design are identified as the key design flow components, thus being the focus of the work. The contributions include the models to design and verify the circuits in simulation, technology libraries with the substrate information, standard cell constraints and the layout rules, standard and parameterised cell libraries, as well as

Doctoral thesis – Summary

Author:

S. Sunjai Nakshatharan

Speciality field:

Physical Engineering

Supervisors:

Alvo Aabloo

Barbar Akle

Defended:

26 August 2019, University of Tartu, Faculty of Science and Technology, Institute of Technology Tartu, Estonia

Contact:

sunjainakshatharan@gmail.com

Further reading:

ISBN 978-9949-03-117-7

Doctoral thesis – Summary

Author:

Farhan Rasheed

Speciality field:

Technology Development and Electronic Design Automation

Supervisors:

Mehdi Baradaran Tahoori

Jasmin Aghassi-Hagmann

Defended:

1 July 2020, Karlsruhe Institute of Technology, Department of Informatics Karlsruhe, Germany

Contact:

frasheed.f@gmail.com

Further reading:
DOI: 10.5445/IR/1000121285

Doctoral thesis – Summary

Author:
Chikwesiri Tolu Imediegwu

Speciality field:
Engineering

Supervisors:
Robert Hewson
Matthew Santer

Degree conferral:
1 July 2020, Imperial College London,
Faculty of Engineering, Department
of Aeronautics
London, United Kingdom

Contact:
chikwesiri.imediegwu14@imperial.ac.uk

Further reading:
DOI: 10.25560/81576
DOI: 10.1007/s00158-019-02220-y

the optimisation of cell placement and routing. All these components are combined into the Process Design Kit helping to design, simulate, verify and extract the layout of inkjet-printed circuits. The proposed single-segmented model for printed electrolyte-gated transistors is the extension of the Enz-Krummenacher-Vittoz transistor model and considers all operating regions of output and transfer curves. The work also describes the extraction of model parameters from the data measured for the printed transistors and the estimation of their distribution using a Gaussian Mixture Model. The proposed DC model was experimentally validated for circuit-level simulation, showing higher accuracy when compared with the state-of-the-art models. The developed method of cell placement and routing optimisation employs the evolutionary algorithm and the genetic algorithm, respectively, taking into account the possible issues due to the crossovers insulating the intersections of routing paths in complex inkjet-printed circuits. With this approach, the timing failure paths were significantly reduced through the optimal placement of crossovers. The resulting Process Design Kit for inkjet-printed electronics technology is compatible with the industrial standard computer-aided design and electronic design automation tools.

Multiscale Structural, Thermal and Thermo-Structural Optimization Towards Three-Dimensional Printable Structures

The research in this thesis deals with the optimisation of metamaterials to achieve heterogeneous, spatially varying material properties in the domain of a structure tailored to fulfil functional objectives, with the capacity for their realisation by additive manufacturing. The approach based on the free material optimisation framework employs multiple geometry-based small-scale design parameters for optimisation problems in 3D real space.

The work reviews the methods and approaches used for structural optimisation, namely for the monoscale and multiscale topology optimisation, optimisation of metamaterials and coupled sequential multiscale optimisation. Then, four chapters present the sequential multiscale framework. The development of a microscale model comprises microscale parameterisation, element-based material assignment and homogenisation, which is based on periodic boundary conditions, strain deformation and thermal analyses, and volume averaging. The numerical implementation for a specific microscale model is presented, with the validation of the effective property evaluations, mesh convergence studies, and characterisation of the stress and heat flow. The next step is the generation of the material model, which includes the axis transformation operations, unit cell geometry and material property transformation, property space population and exploration; the performance of lattice parameterisation was checked against Hashin-Shtrikman bounds, with subsequent generation of the response surface model. The last chapter of this part deals with the macroscale problem, presenting the assumptions and mathematical formulations for structural, thermal and thermo-structural optimisation, as well as their numerical implementation with mesh and function space generation, domain initialisation and evaluations. Finally, three chapters describe the systematic application of the framework to seven optimisation problems – namely to compliance minimisation of the top-loaded cantilever beam, engine bracket and goose-neck hinge, structural optimisation considering target deformation for two- and three-prong grippers, thermal optimisation of the cylindrical heat sink, and thermo-structural optimisation of the hollow-pipe section. The proposed approach helped achieve improved optimality of the resulting designs that are physically realisable by additive manufacturing techniques.

Events

SPIE Optics & Photonics 2021



San Diego, California, USA & <https://spie.org>
1–5 August 2021

This year's edition of the event can be joined in person in its traditional venue in North America or participated remotely. It includes three symposia following the advances in Optical Engineering & Applications, Nanoscience & Engineering, and Organic Photonics & Electronics, respectively, featuring altogether more than 50 conferences with over 500 talks to be presented on-site and over 1500 pre-recorded presentations available on demand. For example, the former include the paper describing printing and in-situ investigation of perovskite thin films for printable solar cells and the one demonstrating the approach for accelerating hybrid perovskite research through the use of robotic automation, while the papers dealing with the computer-vision-aided colour correction method for printing content on multiple print media, concepts for inkjet-printed semi-transparent perovskite solar cells for building-integrated photovoltaics, and voxel optimisation in 3D laser nanoprinting to achieve near 100 nm feature sizes can be found among the latter. Also, some speakers chose the option to deliver their lecture remotely to the audience present on site, such as in the case of plenary talks on Coulomb interactions in organic semiconductors and non-radiative voltage losses in organic solar cells. The attendees can also register for the free exhibition on 3–5 August.

SIGGRAPH 2021

The 48th International Conference & Exhibition on Computer Graphics & Interactive Techniques

<https://s2021.siggraph.org>
9–13 August 2021



This established event organised by ACM SIGGRAPH, a special interest group of the Association for Computing Machinery, is held virtually again in 2021. Besides the live events and sessions scheduled throughout the week, the attendees can access the on-demand content from 2 August to 29 October. Scholarly work in computer graphics technology and interactive techniques is presented at the conference during the technical sessions covering a wide range of topics, such as sketching, colour adjustment for graphic designs, face and character animation, character control, and model optimisation for 3D printing, to name a few. All papers submitted to the ACM Student Research Competition are presented in the poster sessions and then the selected ones during the dedicated session.

In addition, the 20th annual Symposium on Computer Animation (SCA 2021) is held in partnership with Eurographics, the European Association for Computer Graphics. While originally planned to take place in Riverside, California, USA from 30 July to 1 August prior to SIGGRAPH 2021, now it is announced as an entirely online event later in summer, 6–9 September 2021.

NANOTECHNOLOGY 2021

Thessaloniki, Greece
& <https://www.nanotexnology.com>
3–10 July 2021



As in 2020, this event combines both on-site and virtual presentations and participation. Keeping the proven concept, it comprises the symposium on flexible organic electronics, conferences on nanosciences and nanotechnologies, 3D printing and bioprinting, digital and additive manufacturing, related summer schools and exposition, business forum and matchmaking event.

AIC 2021

14th Congress of the International Color Association

<https://www.aic2021.org>
30 August to 3 September 2021



This quadrennial multidisciplinary event organised since 1969, and in 2021 for the first time hosted in Italy, is held as an online event due to the ongoing restrictions imposed by the pandemic. It offers five days full of colour-related topics from various fields, including textile design methods for printing with electroluminescent inks, plant transfer printing on cotton and silk, colour gamuts generated by digital printing devices under different conditions, and effects of oxygen on black dye-based inkjet inks fastness.

Online Print Symposium 2021



Munich, Germany
14–15 September 2021

This year the symposium has the theme 'Start Up and Print Online!' and highlights the start-up potentials, mass customisation, e-commerce and digital transformation.

London Imaging Meeting 2021

<http://www.imaging.org>
20–22 September 2021

The second edition of this event organised jointly by the Society for Imaging Sciences and Technology and the Institute of Physics is held online again, with the theme 'Imaging for Deep Learning'. One of the announced topics is 'Image understanding for color constancy and vice versa' discussed by Simone Bianco in his focal talk.



ERA Annual Conference and the Packaging & Decorative Conference 2021

Thessaloniki, Greece
21–23 September 2021

The focus of the presentations scheduled for this year's conference of the European Rotogravure Association is clearly expressed by its title: 'Gravure – the Sustainable Print Process'.



Current information and more events to be found on the Internet

The calendar of events is still provisional, as the pandemic waves come and go and return again. While some events are having luck with venues and dates, some must be postponed or transformed in the online format, or both, such as the 11th International Conference on Flexible and Printed Electronics, at first postponed from 2020 to this year and, in the end, ICFPE 2021 is held online anyway (28 September to 1 October, <https://www.eng.niigata-u.ac.jp/~icfpe>). Some events even had to be cancelled for the second year in a row, such as the fairs Unique 4+1 in Leipzig, Germany, The Print Show in Birmingham, UK, and all events of the Labelexpo Global Series. On the other hand, Tarsus has announced a new event, Label Congress 2021, to take place in Rosemont, Chicago, USA (29 September to 1 October).

Droplets 2021

<https://www.sfb1194.tu-darmstadt.de/droplets21>
16–18 August 2021



The 5th International Conference on Droplets is held online. The programme offers plenary lectures dealing with hydrodynamic quantum analogues, drag reduction and boundary slip at lubricant-infused surfaces, and drop-based energy harvesting. Topics of over 10 keynote lectures include the electrokinetic transport in a sub-nanometric droplet, nanoscale modelling and computing heat flow for evolving films and drops, direct numerical simulation of drop dynamics, an industry perspective on contact angle measurement, and more.

2nd International Circular Packaging Conference

Slovenj Gradec, Slovenia & <https://www.ftpo.eu/CircularPackaging>
9–10 September 2021



This hybrid event features three keynote speakers – Francesca Stevens presenting 'EU policy and regulatory developments on packaging', Duncan Mayes exploring 'Renewable materials and the circular economy – opportunities and challenges', and Samir Kopačić discussing 'Functional barrier coating of packaging materials: application of biopolymers and effects on barrier performance'. Further, the programme offers professional and scientific presentations, including a session on smart and sustainable packaging and printing, and a hands-on workshop.

47th iarigai and 52nd International Circle Conferences

 Athens, Greece
19–23 September 2021

This year, the iarigai conference entitled 'Printing in the Digital Era' and the conference of the International Circle of Educational Institutes for Graphic Arts Technology and Management (IC) entitled 'Print Education – Challenges in an Uncharted World', are jointly organised by HELGRAMED, the Hellenic Union of Graphic Arts and Media Technology Engineers in cooperation with GRAPHMEDLAB, the Hellenic Graphic-Media Research Lab, University of West Attica. The keynotes confirmed so far are 'Defending the competitiveness of the European graphic industry' by Alison Grace, 'Industry 4.0 in printing & converting – The Bobst vision to shape the future of packaging' by François Martin, and 'After the pandemic: printing becomes more sustainable' by Axel Fischer for the iarigai conference, and 'The connected converter' by Konstantinos Spyropoulos, 'From pixel to drop: inkjet innovations for the digital printing industry' by Stelios Manousakis, and 'During the meta pandemic era: learning continues using simulation technology in print education' by Enn Kerner for both conferences. The scientific papers of the iarigai conference deal with the development of Egyptian Blue pigment for screen printing, water-based conductive inks with carbon black and reduced graphene oxide, a fast fabrication workflow for paper embossing tools, the effect of halftoning on the appearance of 3D printed surfaces, wearable art utilising functional inks and electronics, and other topics.

Call for papers

The Journal of Print and Media Technology Research is a peer-reviewed periodical, published quarterly by **iarigai**, the International Association of Research Organizations for the Information, Media and Graphic Arts Industries.

JPMTR is listed in Emerging Sources Citation Index, Scopus, Index Copernicus International, PiraBase (by Smithers Pira), Paperbase (by Innventia and Centre Technique du Papier), NSD – Norwegian Register for Scientific Journals, Series and Publishers.

Authors are invited to prepare and submit complete, previously unpublished and original works, which are not under review in any other journals and/or conferences.

The journal will consider for publication papers on fundamental and applied aspects of at least, but not limited to, the following topics:

- ⊕ **Printing technology and related processes**
Conventional and special printing; Packaging; Fuel cells, batteries, sensors and other printed functionality; Printing on biomaterials; Textile and fabric printing; Printed decorations; 3D printing; Material science; Process control
- ⊕ **Premedia technology and processes**
Colour reproduction and colour management; Image and reproduction quality; Image carriers (physical and virtual); Workflow and management
- ⊕ **Emerging media and future trends**
Media industry developments; Developing media communications value systems; Online and mobile media development; Cross-media publishing
- ⊕ **Social impact**
Environmental issues and sustainability; Consumer perception and media use; Social trends and their impact on media

Submissions for the journal are accepted at any time. If meeting the general criteria and ethic standards of scientific publishing, they will be rapidly forwarded to peer-review by experts of relevant scientific competence, carefully evaluated, selected and edited. Once accepted and edited, the papers will be published as soon as possible.

There is no entry or publishing fee for authors. Authors of accepted contributions will be asked to sign a copyright transfer agreement.

Authors are asked to strictly follow the guidelines for preparation of a paper (see the abbreviated version on inside back cover of the journal).

Complete guidelines can be downloaded from: <http://iarigai.com/publications/journals/guidelines-for-authors/>
Papers not complying with the guidelines will be returned to authors for revision.

Submissions and queries should be directed to: journal@iarigai.org



Vol. 10, 2021

Prices and subscriptions

Since 2016, the journal is published in digital form; current and archive issues are available at:
<<https://iarigai.com/publications/journals/>>.

Since 2020, the journal is published as “open access” publication, available free of charge for **iarigai** members, subscribers, authors, contributors and all other interested public users.

A print version is available on-demand. Please, find below the prices charged for the printed Journal, for four issues per year as well as for a single issue

Regular prices

Four issues, print JPMTR (on-demand)	400 EUR
Single issue, print JPMTR (on-demand)	100 EUR

Subscription prices

Annual subscription, four issues, print JPMTR (on-demand)	400 EUR
---	---------

Prices for **iarigai** members

Four issues, print JPMTR (on-demand)	400 EUR
Single issue, print JPMTR (on-demand)	100 EUR

Place your order online at: <<http://www.iarigai.org/publications/subscriptions-orders/>>
Or send an e-mail order to: office@iarigai.org

Guidelines for authors

Authors are encouraged to submit complete, original and previously unpublished scientific or technical research works, which are not under reviews in any other journals and/or conferences. Significantly expanded and updated versions of conference presentations may also be considered for publication. In addition, the Journal will publish reviews as well as opinions and reflections in a special section.

Submissions for the journal are accepted at any time. If meeting the general criteria and ethical standards of the scientific publication, they will be rapidly forwarded to peer-review by experts of high scientific competence, carefully evaluated, and considered for selection. Once accepted by the Editorial Board, the papers will be edited and published as soon as possible.

When preparing a manuscript for JPMTR, please strictly comply with the journal guidelines. The Editorial Board retains the right to reject without comment or explanation manuscripts that are not prepared in accordance with these guidelines and/or if the appropriate level required for scientific publishing cannot be attained.

A – General

The text should be cohesive, logically organized, and thus easy to follow by someone with common knowledge in the field. Do not include information that is not relevant to your research question(s) stated in the introduction.

Only contributions submitted in English will be considered for publication. If English is not your native language, please arrange for the text to be reviewed by a technical editor with skills in English and scientific communications. Maintain a consistent style with regard to spelling (either UK or US English, but never both), punctuation, nomenclature, symbols etc. Make sure that you are using proper English scientific terms. Literal translations are often wrong. Terms that do not have a commonly known English translation should be explicitly defined in the manuscript. Acronyms and abbreviations used must also be explicitly defined. Generally, sentences should not be very long and their structure should be relatively simple, with the subject located close to its verb. Do not overuse passive constructions.

Do not copy substantial parts of your previous publications and do not submit the same manuscript to more than one journal at a time. Clearly distinguish your original results and ideas from those of other authors and from your earlier publications – provide citations whenever relevant.

For more details on ethics in scientific publication consult Guidelines, published by the Committee on Publication Ethics (COPE): <https://publicationethics.org/resources/guidelines>

If it is necessary to use an illustration, diagram, etc. from an earlier publication, it is the author's responsibility to ensure that permission to reproduce such an illustration, diagram, etc. is obtained from the copyright holder. If a figure is copied, adapted or redrawn, the original source must be acknowledged.

Submitting the contribution to JPMTR, the author(s) confirm that it has not been published previously, that it is not under consideration for publication elsewhere and – once accepted and published – it will not be published under the same title and in the same form, in English or in any other language. The published paper may, however, be republished as part of an academic thesis to be defended by the author. The publisher retains the right to publish the printed paper online in the electronic form and to distribute and market the Journal containing the respective paper without any limitations.

B – Structure of the manuscript Preliminary

Title: Should be concise and unambiguous, and must reflect the contents of the article. Information given in the title does not need to be repeated in the abstract (as they are always published jointly), although some overlap is unavoidable.

List of authors: I.e. all persons who contributed substantially to study planning, experimental work, data collection or interpretation of results and wrote or critically revised the manuscript and approved its final version. Enter full names (first and last), followed by the present address, as well as the E-mail addresses. Separately enter complete details of the corresponding author – full mailing address, telephone number, and E-mail. Editors will communicate only with the corresponding author.

Abstract: Should not exceed 500 words. Briefly explain why you conducted the research (background), what question(s) you answer (objectives), how you performed the research (methods), what you found (results: major data, relationships), and your interpretation and main consequences of your findings (discussion, conclusions). The abstract must reflect the content of the article, including all keywords, as for most readers it will be the major source of information about your research. Make sure that all the information given in the abstract also appears in the main body of the article.

Keywords: Include three to five relevant scientific terms that are not mentioned in the title. Keep the keywords specific. Avoid more general and/or descriptive terms, unless your research has strong interdisciplinary significance.

Scientific content

Introduction and background: Explain why it was necessary to carry out the research and the specific research question(s) you will answer. Start from more general issues and gradually focus on your research question(s). Describe relevant earlier research in the area and how your work is related to this.

Methods: Describe in detail how the research was carried out (e.g. study area, data collection, criteria, origin of analyzed material, sample size, number of measurements, equipment, data analysis, statistical methods and software used). All factors that could have affected the results need to be considered. Make sure that you comply with the ethical standards, with respect to the environmental protection, other authors and their published works, etc.

Results: Present the new results of your research (previously published data should not be included in this section). All tables and figures must be mentioned in the main body of the article, in the order in which they appear. Make sure that the statistical analysis is appropriate. Do not fabricate or distort any data, and do not exclude any important data; similarly, do not manipulate images to make a false impression on readers.

Discussion: Answer your research questions (stated at the end of the introduction) and compare your new results with published data, as objectively as possible. Discuss their limitations and highlight your main findings. At the end of Discussion or in a separate section, emphasize your major conclusions, pointing out scientific contribution and the practical significance of your study.

Conclusions: The main conclusions emerging from the study should be briefly presented or listed in this section, with the reference to the aims of the research and/or questions mentioned in the Introduction and elaborated in the Discussion.

Note: Some papers might require different structure of the scientific content. In such cases, however, it is necessary to clearly name and mark the appropriate sections, or to consult the editors. Sections from Introduction until the end of Conclusions must be numbered. Number the section titles consecutively as 1., 2., 3., ... while subsections should be hierarchically numbered as 2.1, 2.3, 3.4 etc. Only Arabic numerals will be accepted.

Acknowledgments: Place any acknowledgements at the end of your manuscript, after conclusions and before the list of literature references.

References: The list of sources referred to in the text should be collected in alphabetical order on at the end of the paper. Make sure that you have provided sources for all important information extracted from other publications. References should be given only to documents which any reader can reasonably be expected to be able to find in the open literature or on the web, and the reference should be complete, so that it is possible for the reader to locate the source without difficulty. The number of cited works should not be excessive - do not give many similar examples.

Responsibility for the accuracy of bibliographic citations lies entirely with the authors. Please use exclusively the Harvard Referencing System. For more information consult the Guide to Harvard style of Referencing, 6.1.2 Version, 2019, used with consent of Anglia Ruskin University, available at: https://library.aru.ac.uk/referencing/files/Harvard_referencing_201920.pdf

C – Technical requirements for text processing

For technical requirement related to your submission, i.e. page layout, formatting of the text, as well of graphic objects (images, charts, tables etc.) please see detailed instructions at:

<http://iarigai.com/publications/journals/guidelines-for-authors/>

D – Submission of the paper and further procedure

Before sending your paper, check once again that it corresponds to the requirements explicated above, with special regard to the ethical issues, structure of the paper as well as formatting.

Once completed, send your paper as an attachment to: journal@iarigai.org

If necessary, compress the file before sending it. You will be acknowledged on the receipt within 48 hours, along with the code under which your submission will be processed.

The editors will check the manuscript and inform you whether it has to be updated regarding the structure and formatting. The corrected manuscript is expected within 15 days.

Your paper will be forwarded for anonymous evaluation by two experts of international reputation in your specific field. Their comments and remarks will be in due time disclosed to the author(s), with the request for changes, explanations or corrections (if any) as demanded by the referees.

After the updated version is approved by the reviewers, the Editorial Board will decide on the publishing of the paper. However, the Board retains the right to ask for a third independent opinion, or to definitely reject the contribution.

Printing and publishing of papers, once accepted by the Editorial Board, will be carried out at the earliest possible convenience.

2-2021

Journal of Print and Media Technology Research

A PEER-REVIEWED QUARTERLY

The journal is publishing contributions
in the following fields of research

- ⊕ Printing technology and related processes
- ⊕ Premedia technology and processes
- ⊕ Emerging media and future trends
- ⊕ Social impacts

For details see the Mission statement inside

JPMTR is listed in

- ⊕ Emerging Sources Citation Index
- ⊕ Scopus
- ⊕ Index Copernicus International
- ⊕ PiraBase (by Smithers Pira)
- ⊕ Paperbase (by Innventia and Centre Technique du Papier)
- ⊕ NSD – Norwegian Register for Scientific Journals, Series and Publishers

Submissions and inquiries

journal@iarigai.org

Subscriptions

office@iarigai.org

More information at

www.iarigai.org/publications/journal



Publisher

The International Association of Research Organizations
for the Information, Media and Graphic Arts Industries
Magdalenenstrasse 2
D-64288 Darmstadt
Germany

